Characterization of In-Situ Curing PVA-PEG Hydrogels for Nucleus Pulposus Replacement

A Thesis

Submitted to the Faculty

of

Drexel University

by

Kristin Benjamin Kita

in Partial Fulfillment of the

Requirements for the Degree

of

Doctor of Philosophy

December 2010

Acknowledgements

I would like to thank first, my friends, family and colleagues from which I have received a great deal of support. My parents, Ronald and Irene who have provided me with the stable life which has not only facilitated this thesis, but provided me with the mindset to cope with extreme challenges, such as those that are presented with preparing a thesis while having a large number of other obligations, such as full-time employment. My father's enthusiasm and my mother's work ethic have made this thesis possible, and for this I am thankful. I would also like to thank my sister, Veronica for her support. Helena, who has been very patient with my hectic schedule in recent months, also deserves thanks. She has been a source of selfless encouragement that has been invaluable.

I would like to thank my advisor, Dr. Anthony Lowman, who encouraged me to obtain my doctorate. There are few people that a person can meet that can change the way a person actuates their lives. Dr. Lowman has elevated the standards that I aspire to, and for that I am thankful. Dr. Michele Marcolongo has also served as an exemplary role model and mentor, and her guidance is much appreciated. I would also like to thank Drs. Christopher Li and Jonathan Spanier for their help in completing this thesis. I wish to acknowledge the current and graduated students of the Biomaterials and Drug Delivery Lab: Valerie Binetti, Andrew Cheng, Dr. Jennifer Vernengo, Lisa Leone, William Wolf, and many others. The students of Dr. Marcolongo's lab have been very helpful, as well. I am thankful to Sumona Sarkar in particular for being so supportive.

I would like to thank Synthes Spine for making my research possible. This organization, with its numerous talented professionals has refined my skills and shaped my perspective. My abilities have evolved considerably from when I started as a graduate student at the Gelifex startup company eight years ago. Since then I have learned a great deal, and I look forward to my future with Synthes. The labs and personnel from both Synthes Spine and Synthes Biomaterials have been critical to the completion of this thesis, and I have received generous support. The consideration of my managers and directors at Synthes, Michael Keane, Dr. Nigel Smith and Dominique Messerli is also very much appreciated. Dr. Garland Fussell, as both my colleague and committee member has made this gigantic endeavor seem tangible for me. The benefits of his critical analysis and insight are too expansive to describe here, and have helped me daily.

The list of persons who merit acknowledgement for this thesis would stretch for pages, and there is a great deal of encouragement and guidance that I cannot begin to describe in this short section. I wish to extend my sincere thanks to each of the persons mentioned, as well as any of those whom I may have missed.

Table of Contents

List of Tables

List of Figures

Abstract

Characterization of In-Situ Curing PVA-PEG Hydrogels for Nucleus Pulposus Replacement

Kristin Benjamin Kita

Anthony M. Lowman, Ph.D.

Poly(vinyl alcohol) / poly(ethylene glycol) blend formulations are evaluated as an *in situ* forming gel system. The system will provide a minimally invasive approach to nucleus replacement, whereby a cavity formed in the intervertebral disc post-denucleation is filled via an injectable solution that solidifies to function as prosthetic nucleus pulposus tissue, restoring height, and hydration to the disc, as well as correcting the biomechanics of the spine.

PVA/PEG gels have an inherent system incompatibility that results in the formation of a two phase region, where a water rich supernatant and a polymer rich gel phase form. Systems of dense gels have previously had no simple analytical means for separation of the two similar polymers, particularly at the high viscosities required for this specific application. ^{1}H-NMR analytical techniques are developed for preparation of a %w/w phase diagram. Understanding of possible compositional space enables definition of swelling and stability characteristics for the final gel as it relates to composition. Changes in PEG molecular weight are shown to affect swelling and stability in gels. Upon rheological analysis, a change in the resulting system network with the incorporation of varying types of PVA and PEG is evident. Concentrated gels are shown to display a high temperature reduction in viscosity. This effect is shown to be dependent on molecular weight of the PEG component and

gel composition. Similarly, there is a requirement that the system have a low viscosity during the sol stage that shown to be satisfied due to system incompatibility and plasticization effects.

CHAPTER 1: INTRODUCTION

Intervertebral disc degeneration results from a variety of sources. Whether caused by nutritive, genetic, age or systemic sources, the intervertebral disc is often implicated as the source of back pain. The implantation of a prosthetic nucleus pulposus tissue has been proposed as a means to restore the biomechanics of the disc, as well as a treatment to relieve pain resulting from degenerated discs.

Nucleus tissue consists of 70-90% water [1]. The intervertebral disc relies on diffusive and convective processes to transmit nutrients to the area. It is known that the degenerative process results in a reduction in water content local to the area [2]. As diffusion is reduced in degenerated tissues, nutrient supply to discs is similarly reduced. Polyvinyl alcohol hydrogels are commonly chosen for nucleus pulposus implants for their biocompatibility, as well as their ability to retain water [3]. In this manner, hydrophilic materials are currently being investigated as a way to maintain critical swelling pressure within the disc through the retention of water, much in a way similar to nucleus tissue.

Previous research has found that incompatibilities between poly(vinyl alcohol) and poly(ethylene glycol) result in a phase separation that produces a phase concentrated in polymer, as well as a water rich supernatant phase [4]. Further research shows plasticization and interference of vinyl alcohol units from the incorporation of PEG [5].

The production of a gel phase, as concentrated via the phase separation mechanism described by Inamura is evaluated for gelation characteristics using temperature controlled rheometry studies. It has also been shown that a transition exists for poly(vinyl alcohol) in salt solutions as well as low degree of hydrolysis PVA, where viscosity reduction at higher temperatures occurs as a result of reduction in polymer-solvent interactions [6]. It is through these temperature-dependent plasticization phenomena that the material is made flowable at elevated temperature.

The primary objective of this thesis is to address the need for an in situ forming biomaterial that effectively treats disc degeneration via nucleus pulposus replacement with implantation of a biocompatible construct. The construct design is intended to exceed the gelation characteristics of neat PVA gels, via the incorporation of a second polymer component. Crosslinking is obtained via physical means, using the natural hydrogen bonding and crystallization nature of the material to impart stability, in order to avoid any toxic crosslinking compounds. The system provides a minimally invasive approach to nucleus replacement, whereby a cavity formed in the intervertebral disc is filled via an injectable solution that solidifies to function as prosthetic nucleus pulposus tissue, restoring height, and hydration to the disc, as well as correcting the biomechanics of the spine.

The following chapters study the feasibility of the PVA and PEG system through a variety of characteristics necessary for a suitable nucleus replacement. In particular, the thermal gelation profile is described, such as would be observed when cooling to

the gelled state upon delivery and implantation. Effects of swelling and equilibrium water content as a result of the physiologic environment of the cavity created for implantation are described, as well as the resulting stability. Understanding of compositional space is necessary for formulation, and structured via the creation of a ternary phase diagram for a given formulation system. Further, a technique using nuclear magnetic resonance for the chemical separation of PVA and PEG is developed in order to create such a diagram for the target concentrated formulations.

The scientific contribution, through the completion of this work, is as follows:

- Quantification the phase behavior of PVA/PEG gel systems conducive to nucleus replacement
- Characterization of the thermal and time dependent response of gelation behavior across PVA/PEG formulation systems (molecular weight and composition affects on gelation)
- Identification and quantification of the response of different PVA/PEG systems (in particular, molecular weights and relative amounts of components) to a physiologic osmotic environment
- Separation of PVA and PEG via a reliable chemical analytical technique (NMR)
- Relation of PVA/PEG plasticization to melt rheology across formulation systems

CHAPTER 2: BACKGROUND

2.1 Spine Anatomy

The spine is a curved flexible column positioned in the median line at the posterior portion of the trunk (see Figure 2.1) [7]. The spinal column is formed from the junction of thirty-three vertebrae, which are bones situated along the spine. The structural and biomechanical system of the spine is complex, and consists of a variety of elements working in concert, in order to provide the correct function. Intervertebral discs provide joints for the system, the movement and loads also being supported by articulating surfaces on the bones (facets). Viewed laterally, there are four curves in a normal spine. Curves in the cervical and lumbar regions are convex anteriorly, whereas curves in the thoracic and sacral are convex posteriorly. Curvature in the thoracic region is structural, whereas the lumbar and cervical curves result from the wedge shape to the discs. The overall curved shape of the spine is for both flexibility and shock absorption [8].

The regions of the spine are cervical, thoracic, lumbar, sacral and coccygeal, the cervical vertebrae being the smallest, and beginning at the base of the skull and extending seven units to the twelve thoracic vertebrae. Past the thoracic vertebrae, are the five lumbar vertebrae. The sacrum and coccyx make up the caudal, or tail end of the spine [7].

The vertebrae are made up of an anterior solid segment (vertebral body) and a posterior arch. The vertebral body consists of a cortical bone perimeter surrounding a core of cancellous bone. Understanding of the relative percentage of load carrying capacity of either type of bone varies widely in different literature [9]. The posterior arch consists of lamina, pedicles, and several processes. A spinous process is situated along the medial line when viewed posteriorly. Superior and inferior articulating processes face both upward and downward from the posterior arc. Existing for all spinal units, but most visibly in the dorsal and lumbar spine, two transverse processes extend outward at either side of the posterior arch. Facet joints, or articulating processes play a large role in the torsional stiffness of the spine.

There are two functions to the intervertebral disc, to impart flexibility (i.e. flexion, extension, rotation, lateral bending, and intersegmental mobility) as well as to be load bearing. The thickness of discs is greatest in the lumbar and cervical regions, where there is the most vertebral movement [10]. It has been found by Nachemsen, that the loads may be three times the weight of the trunk when the lumbar disc is in the sitting position [8, 11]

The intervertebral disc consists of an outer ring of fibrous tissue (the annulus fibrosus) surrounding a soft, gelatinous core (the nucleus pulposus) (see Figure 2.2). At the boundary of the intervertebral disc and vertebrae are endplates consisting of hyaline cartilage. The annulus fibrosus is made up of 90 layered sheets of collagen fibrils [10]. The fibers are arranged in a helical fashion, running in opposite

directions in adjacent layers[8]. Changes in morphology of the annulus have been known to occur with aging.

The nucleus pulposus consists of thin fibers in a mucoprotein gel [8]. Negatively charged proteoglycans make up 30-50% of the dry weight of the nucleus tissue and function to absorb and retain water [12]. The main proteoglycan is aggrecan, which is made up of many glycosaminoglycan molecules in a brushlike structure [13]. The nucleus is described as having a pseudochondral cellular makeup. The extracellular matrix of nuclear tissue consists primarily of Type I and Type II proteoglycans (keratin sulfate and chondroitin) in fluid [14]. Water content of nuclear material is typically from 70 to 90% and is known to decrease with age. Monitoring of water content can further be performed via MRI. The nucleus pulposus in early life is derived from notochord cells which are no longer present in early adulthood, but replaced by cells similar to load bearing cartilage [1].

The spinal cord runs from the brain down the length of the spine, within the vertebral foramen, which is the region within the posterior arch of the vertebra. The spinal cord ends at the first lumbar segment where it splits into the conus medullaris, a group of nerves which enervate the lower portion of the body. Each vertebral segment has two nerves extending from the spinal cord at either side, which exit to enervate different portions of the body.

Innervation specific to intervertebral discs remains to be fully understood [10]. Whereas no nerves are thought to be in the inner annulus or nucleus, free nerve endings have been identified in the outer annulus. The positions of the exiting nerve roots in a disc are as in Figure 2.2.

There are seven ligaments for the region between C2 and the sacrum: Loads are best carried in the direction of the fibers in these ligaments. Ligaments function as to balance loads applied to the spine and provide tensile resistance. Loads are transferred from bone to bone via these structures. The anterior longitudinal ligament is attached to the anterior surfaces from the atlas to the sacrum. This ligament is attached to vertebrae, but not as tightly to annular fibers. The posterior longitudinal ligament runs down the posterior surface of the spine, covering the dens and transverse ligament. Intertransverse ligaments connect transverse processes of the thoracic spine with muscles in the back. These have little significance mechanically in the lumbar region due to size. Capsular ligaments are attached perpendicular to facets, in particular for allowing flexion and enabling stability in the cervical region. The ligamenta flava connect adjacent vertebrae along the inner portion of the lamina. A tension in the ligamenta flava provides stability for the spine. Adjacent vertebrae are attached at the processes by the interspinous ligaments. Supraspinous ligaments also continue down the tips of the processes [8]. Methods of failure of these ligaments are typically within the ligament or at the point of attachment to bone.

2.1.1 Physiologic Environment of the Nuclear Cavity

The intervertebral disc provides a load-bearing joint for adjacent vertebrae in the spine. The intervertebral disc is avascular, meaning it cannot rely on blood flow to directly provide hydration and nutrients to the nucleus tissue. The tissue remains hydrated via diffusion through the endplate cartilage. The resulting hydration of nucleus material is confined by the relatively impermeable annulus as a swelling force. The disc responds to compressive stress by exuding water from the nucleus, outward through the annulus [15]. In a typical diurnal cycle, nucleus tissue may express approximately 25% of its fluid. Changes in percentage of fluid result in osmolality changes. Swelling and deformation of nucleus tissue occurs as a result of hydraulic permeability at the endplates which changes with loading [14].

Because the intervertebral disc is avascular, cells must derive nutrients via diffusion. The outer annulus is supplied via blood vessels at the disc perimeter. In contrast, the nearby vertebral bodies are very vascular. The annulus, nucleus and transitional zone are each fed by different arteries within the vertebral body. The inner annulus and nucleus are supplied by a capillary bed in the vertebral body which terminates at the cartilaginous endplate [16]. Nutrients are supplied through the endplate via flow-dependent diffusive and flow-independent convective processes for the fluid. Diffusion is also necessary for the removal of the products of cell metabolism.

A major factor in the regulation of the physicochemical environment of nucleus cells is aggrecan concentration [16]. The presence of the negatively charged proteoglycans

within the aggrecan allows for a tight effective pore size in order to entrap water. Positively charged ions, such as sodium thus are found in high concentration within this region, in comparison to plasma [16]. As a result of this network, there is a partitioning in diffusing solutes that occurs [17]. Proteoglycan content strongly affects the size of these pores as well as the osmotic pressure of the nuclear cavity. The proper function of a disc is therefore dependent on proteoglycan content.

Model systems have been developed by Ogston and Wells for estimating hip cartilage osmotic properties. A system developed by Urban using PEG saline solutions is similarly described. Solution concentrations of PEG are related to osmotic pressure using the following equation [18].

$$\pi = RT \left(c/M + Bc^2 + Cc^3 + \dots \right)$$

$$B = 2.59 * 10^{-3}$$

$$C = 13.5 * 10^{-3}$$

M: number average molecular weight

R: 8.314 J mol/°K

2.1.2 Biomechanics of the Spine

The spine has three main functions in biomechanics, to transfer weights and bending moments of the upper portion of the body and head, to allow for the bending motions of these portions, and last to protect the spinal cord [8].

Intervertebral discs in the spine allow for many types of mechanical support, in particular the bending and twisting and support for compressive loads resulting from the weight of the body [19]. The physiologic modes of flexion, extension and lateral bending also produce tensile forces on the disc as well [8]. Direct compressive loading in a neutral position results in compressive stresses in the nucleus and tensile stresses in the annular fibers [8]. See Figure 2.3. Across a vertebral unit, a compressive load is applied axially from one endplate across the nucleus and annulus, to the other endplate. A compressive load applied in a healthy disc results in transmission to the nucleus tissue, which bulges outward pushing the annular ring outward and creating tension in the annular fibers. The helical orientation of the fibers results in axial and circumferential stresses. In a degenerated disc the nucleus is dehydrated, and not capable of generating the required fluid pressure. The load is transmitted in this state primarily through the annulus at the periphery instead, resulting in compressive stresses on inner fibers. As a result of Poisson's effect, there is a bulge to the disc upon compression and a contraction when the disc is in tension.

In bending, the disc is subjected to tension on the side that is convex and compression on the inner, or concave side. Stresses are greatest in compression on the innermost side of bending and are greatest in tension on the outermost side of bending. In axial torsion, the degree of stress has much to do with the degenerate state of the disc, as well as the condition of the posterior elements. Shirazi-Adl et al found that removal

of posterior elements (posterior arch, including lamina and facets) increased annular fiber stresses upon torsion. There was similarly a decrease in stress in torsion, with a decrease in intradiscal pressure [20].

Data from most studies on functional biomechanics has been obtained from cadaver discs. There are few studies measuring in vivo loads [8]. Early work by Nachemson and Morris uses the insertion of transducers into the disc space of cadaveric functional spinal units in order to approximate in vivo loading [11]. Another study by Wilke measures intradiscal pressure, via the insertion of a pressure transducer into the non-degenerated disc of a living subject [21]. Data was compared with Nachemsen and Morris' approximation. Pressures were reported to be highest for flexion while lifting a 20Kg weight, and were measured at 2.3MPa. Other significant pressures included standing flexed forward at 1.1MPa. It was shown from the study that activities had a direct affect on intradiscal pressure. Pressure in the recumbent state has shown to be 0.1 to 0.2MPa. The range of pressures in the spine during normal activity may reach 1-3MPa [13].

Because of changes in water content that occur with loading, loading rate further has been shown to affect structural stiffness of the disc. The disc is described as behaving in a viscoelastic manner. This can be described as a time-dependent response to loading. Load-displacement curves are thus different, when loads are applied over different time-scales [8]. Stiffness will increase with loading rate. The disc expresses fluid upon application of a load. Since fluid outflow is rate dependent, stiffness

increases as fluid outflow becomes more difficult [22]. Pressurization of the disc is necessary for proper uniform distribution of loads between disc and endplate. With degeneration, the ability for discs to support compressive loads is hindered by a condition which decreases fluid flow into nucleus tissue, or increasing flow through the annulus [23].

2.2 Degenerative Disc Disease

Chronic lower back pain affects over 5 million persons in the USA alone [24]. Although the causes of back pain are not currently completely understood, degenerative disc disease is believed to play a significant role [25]. Degeneration in the intervertebral disc often results from mechanical factors as well as nutrition, systemic (cigarette smoking, for example) or genetic sources. Degeneration may begin as early as the first decade of life for males and the second decade for females. Whether or not a degenerated disc is truly the source of back pain remains a subject of controversy. Further, any correlation between degenerated segments and low back pain is yet to be determined. Back pain may be due to mechanical factors, or disease, as in inflammatory disease such as rheumatoid arthritis or ankylosing spondylitis [26]. Degeneration of discs is believed to be the source of stenosis, herniation of the nucleus pulposus, and segmental instability [10].

There is a natural change in the disc with aging. Environmental and genetic causes can accelerate these changes. 8 of 10 adults will experience some form of back pain

in their lives. Along with low back pain, DDD is the greatest source of lost wages annually, and is the third leading cause of disability, which translates to 50-100 billion dollars annually in costs [10, 27]. Most will not require formal treatment [2]. In cases of persistent pain, surgery may be indicated [28].

Based on the vascular configuration local to the disc, inner arteries are affected by immobility or fusion at the vertebral joint. There is a corresponding decrease in blood supply to the central nucleus with age induced degeneration. Calcification of the cartilage endplates also may inhibit diffusion and nutrient flow. A lack of nutrition to the disc may lead to decreased function in cells and ultimately cell death, which is the source of degeneration in the disc [10]. The disease progresses as the proper water flow and nutrients are inhibited, producing dehydration of nucleus material which affects the load distribution. With the resulting loss of motion and disc height, pain is typically experienced, particularly in later stages of degeneration [23].

Age related disc degeneration can be described as follows: There is a decrease in the amount of viable cells in the nucleus which leads to decreased water and proteoglycan content. Nucleus tissue can be observed to become less transparent at this stage. Though cells do not contribute directly to the mechanical properties of the disc they produce extracellular matrix, which does [16]. As a result, a decrease in number of cells forces cells to maintain greater amounts of extracellular matrix [19]. Decreased proteoglycan concentration and water concentration leads to a volume loss

in nucleus pulposus tissue, which in turn leads to a decrease in nuclear pressure. Severely degenerated discs exhibit close to no pressure from the nucleus whatsoever, forcing the annulus, as well as the posterior elements to bear loads [29]. The annulus exhibits degeneration along with this change in nuclear material. There is a further loss in the gelatinous consistency, annular fibers become more coarse, and fissures begin to form on the surface of the disc. When the amount of degeneration is severe, nucleus and annulus material can not be distinguished from each other. Nucleus pulposus herniates at this stage, since degenerated discs can no longer hold the nucleus material [10].

2.2.1 Prolapse of Nucleus Tissue onto Pain Generating Sources

Loads of concern for prolapse of nucleus material from discs are divided into short duration-high amplitude loads and long duration-low amplitude loads. These two classes are significant when taking into account the viscoelastic nature of the disc, in particular, creep and relaxation behavior, and sensitivity of the disc to rate of loading. Structural damage generated by short duration/high amplitude load is often irreparable when the failure stress of the segment is generated, whereas longer duration/low amplitude loads are limited by fatigue characteristics for tear and growth of fissures [8].

It is known that sudden injury may result in disc prolapse. Incidents of bending or lifting are known to precede reports of low back pain and sciatica. Evidence also suggests that prolapse may be slow, as in through a gradual tear and leak of nucleus

material [30]. In vitro testing has further shown that it is difficult to produce herniations of nucleus material from direct compressive loading of a vertebral unit [22]. More complex bending profiles are required. The combination of compression loads with flexion and lateral bend has been proposed as a possible mechanism. In a study by Simunic, evidence suggests that prolapse may be generated by loading in a flexed state. It was similarly observed epidemiologically that persons with occupations which involved repetitive bending and lifting had a 300 to 600% increased risk of herniation [22].

Though acutely prolapsed discs are regarded by most as a definitive source of pain, the sources of all pain remain unproven. A contained disc is much more difficult to diagnose [31]. The intervertebral disc is often implicated in the discussion of pain generating sources in non-prolapsed states, as well. The initial stimulus is described as being from abnormal motion, vibrations, forces and repetitive loading. The result of the stimulus may be inflammation, or infection or structural or material changes that relay the pain sensation to nociceptive sensors [32]. The increase in blood pressure in bone has also been seen to result in pain generation. Pain may be generated by any muscle or tendon structures being strained, sprained or ruptured [8]. Pain receptors are known to be in both the anterior and posterior ligaments, as well as the interspinous ligaments, periosteum, fascia and blood vessels of the vertebrae, posterior annular fibers as well as paravertebral musculature, among other sources [33]. It has been argued that the non-herniated disc is a major source of back pain [8]. As a result of the inconsistencies and difficulties in the diagnosis of pain-

generating degenerative states, the identification of treatment techniques have been equally difficult [34].

2.3 Clinical Treatment Options

2.3.1 Conservative Treatment

Conservative measures remain the treatment for the majority of incidences of back pain [35]. In this case, pain and inflammation is typically mitigated via physical therapy, injections and medications [36]. With time, herniated disc fragments are often seen to reduce in size, coupled with a decrease in symptoms [35]. Apart from conservative care, results which may depend upon severity of the condition of the patient, surgical methods may be necessary. Since spasms have been often thought as pain generating sources, muscle relaxants and massage have similarly frequently been administered to treat these conditions [8].

2.3.2 Surgical Treatment

Surgical procedures are indicated when conservative care fails, or in cases of instability that threatens neural elements. The two current leading surgical treatments are discectomy and disc arthrodesis (fusion) [37]. Fusion requires affixing upper and lower vertebrae via rods and spacers that promote bone to adjoin vertebral segments. The procedure is incredibly destructive and results in loss of motion and a change in stress distribution for fused levels [38].

Certain needle treatments also exist in the form of both pain control injections, as well as IntraDiscal Electrothermal Therapy (IDET, by ORATEC) which is a percutaneous procedure where a catheter with a heated tip is inserted into the disc. Heating continues for 15 minutes, with the intention of removing symptoms of degenerative disc disease in the lower back. IDET is an early stage treatment targeted toward pain generated in the disc, with minimal collapse and corresponding annular tears [34].

2.3.2.1 Microdiscectomy

In cases where conservative care and medication are ineffective in relieving symptoms of low back pain with sciatica, tissue is excised from the disc to clear herniated material impinging on local nerve roots [39]. The procedure typically involves first the removal of a small portion of bony material from the back of the vertebra in order to locate the herniation and nerve impingement. Minimally invasive techniques are often employed for the removal of tissue. The discectomy procedure may be performed using mechanical means or a chemonucleolysis agent, such as chemopapain. Mechanical methods include the use of rongeurs to physically cut and remove tissue (see Figure 2.4). Other methods include the use of the Nucleotome, which has a 2mm diameter probe fitted with a guillotine to slice and remove tissue [39], or Hydrocision which involves use of a high pressure water jet to cut and remove material. Techniques useful for nucleus pulposus removal for discectomy procedures are further useful for the creation of a cavity for nucleus replacement.

This removal of the nucleus tissue, such as in a discectomy results in a gradual decrease in disc height [2] which may result in further complications.

Removal of nucleus tissue further alters the biomechanics of the disc. Motion of the annular fibers is changed to become more disjointed. For an intact nucleus, motion results in bulging outward in both the inward and outward regions [40], in contrast, for a denucleated annulus there is a bulging of the annular material that pushes the outward annulus further out and the inward annulus further inward leading to degeneration. Additional stress on the facets from degeneration may lead to further progression of degeneration.

There is an increase in mobility with nucleotomy. In a study by Eysel, the removal of 5-6 grams of nucleus tissue resulted in 38-100% increase in mobility for the cadaveric spinal segment being tested. It has been suggested that instability due to nucleotomy is better defined as abnormal mobility, i.e. a greater range of motion when compared with adjacent vertebrae [41].

There is a significant reherniation rate associated with discectomy. It has further been shown that even removal of a portion of the nucleus may increase the rate of further degeneration. It has further been shown in an animal study that the reinsertion of a spacer will delay further disc degeneration, including the nucleus, annulus, and end plate [10].

2.3.2.2 Fusion

The current most important surgical procedure in spine care is the technique of spinal fusion. The procedure was first introduced in 1911 by Albee and Hibbs [8]. Hibbs was reported to have removed spinous processes and achieved fusion through the construction of a bridge of bone, once this piece of bone was inserted caudally to contact the inferior vertebral processes and sutured into position [42]. By such methods, fusion limits impingement on pain generating structures by fixing vertebrae into position via arthrodesis, where bone is induced to grow across the disc space, forming an immobile union between the two bones. Reasons for fusion include to provide support and stability, to prevent the progression of deformity, and to alleviate or eliminate pain [8].

Early treatments reported by Cloward in 1952 used ilium bone graft in order to achieve fusion through insertion between vertebrae. From years of study, Cloward also reported the effectiveness of using auto and allograft material for these spacers [42]. Current technologies for spacers include synthetic materials (PEEK, titanium, and others) as well as allograft and autograft (in particular from the iliac crest of the hip) and are typically inserted between vertebrae as part of this procedure, as support for the fusion and for bone to grow in and around, in particular in conjunction with anterior plates and also with posterior fixation. Spacers also have been packed with bone growth protein to further promote fusion. In situ polymerizing methyl methacrylate has also been considered for use as a portion of a fusion construct.

In the early 1980s Steffee popularized the use of screws through the pedicle portion of the vertebra, by employing titanium cancellous bone screws in conjunction with a standard AO plate. Good results (clinical rating of 4 out of 5) were reported from from 89% of the 120 patients that received the system [42]. Currently, rods and screws typically are employed as a means to immobilize and stabilize vertebrae, until fusion can occur (see Figure 2.5). In addition to pedicle screws and rods, which are common for posterior and some lateral approaches, typical methods for securing this fixation for lumbar procedures are the use of plates (Synthes Antegra T, Anterior Thoracolumbar Locking Plate – ATLP) and/or bone graft containing cages (Synthes Zero-P, Medtronic LT-CAGE) from the anterior. Attention by surgeons is typically paid to indications for surgery and anatomic procedural aspects, as well as to postoperative care, for the choice of a surgical construct [8].

Current procedures of fusion vary based on type and direction of access to the spine, as well as the methods for achieving the fusion. Lumbar fusion is the most common, since the greatest amount of weight is on the lumbar segments, causing more frequent degeneration. In lumbar fusion, access routes are posterior (Posterior Lumbar Interbody Fusion, or PLIF), anterior through the abdomen (Anterior Lumbar Interbody Fusion or ALIF), as well as Direct Lateral (DLIF) and Transforaminal Lumbar Interbody Fusion (TLIF), which is an oblique posterior access through the foramen.

Bone morphogenetic protein (BMP) occurs naturally in bone and is responsible for bone regeneration. Early studies performed by Urist showed that demineralized cancellous bone induced bone growth in rats. Work by Urist ultimately allowed to identify the protein. BMPs are now known to induce the differentiation of mesenchymal stem cells (preosteoblasts) into osteoblasts. Demineralized bone matrix (DBM) is similarly used for the small quantities of BMPs present. The production of DBM is through the acid treatment of bone in order to remove the minerals. In order to improve handling of the material, DBM is often mixed with other materials such as carboxymethylcellulose, glycerol, hyaluronic acid or gelatin [43]. Hydroxyapatite (HA) is a family of calcium orthophosphates. It constitutes the inorganic component of bone and is subsequently very biocompatible. Hydroxyapatite structures such as coral and converted forms of coral, as well as tricalcium phosphate, a less crystalline form of hydroxyapatite have been used in fusions since the 1980s [43].

Segments adjacent to fused levels experience increased stress, excessive motion, stenosis as well as even fracture dislocation. Degenerative changes are also common in adjacent segments [8].

There is an argument that persists for advancements in alternatives to fusion procedures. It is believed that treatment with a fusion is only desirable over the short-term, because of the development of problems in adjacent levels [27]. The proper motion of the disc is not preserved [10] and biomechanical studies have shown that more rigid fusion devices accelerate degeneration [28]. Further, in recent history,

arthrodesis for synovial joints has reduced considerably in favor of the motion sparing joint replacement techniques [10].

Fusion is understood to lead to degeneration of adjacent levels, as they attempt to compensate for the loss in biomechanics [37]. Discectomy, also results in a destabilization of the intervertebral disc which may lead to further degeneration [23]. Upon review of the current treatment options, it is apparent that early stage procedures currently do not exist to halt the degenerative process. Current developments of treating diseased levels of the spine look to replacement of a total disc via a prosthetic joint (e.g. Prodisc or Charité) [44], or the potentially less invasive route of replacement of nucleus tissue, to rebuild a disc with a competent annulus.

2.3.2.3 Total Disc Replacement

The concept of an artificial disc is well over 40 years old [34, 45]. Artificial disc replacement involves replacement of the entire disc or a portion using an apparatus that provides a joint often coupled with a means for fixing that joint to the vertebral body. Replacement of only the nucleus tissue is described in the following section. Other proposed options for disc replacement are the implantation of allograft discs, including endplates, nucleus and annulus. Only artificial devices have currently reached clinical trials however [10].

Early devices included one by Fernstrom which consisted of a ball bearing introduced to the disc space from the anterior. Results for patients varied, some were hypermobile, while others resulted in fusion. Migration of the implant out of the disc space as well as settling into the spongiosa were further complications with the device for the period where it was in use [28].

A Total Disc Replacement that consists of two plates attached by a central joint has been developed, as shown in Figure 2.6. Two plates with a posterior hinge & two pairs of springs which provided the basis for Marnay's design. Marnay designed a ball joint which enabled three rotations, however since the center of rotation was not mobilized no translation was possible, resulting in shear stress for each of three translations. Charite III (Depuy) had a two segment nucleus with a double joint but had a number of clinical complications. Depuy had similarly developed Acroflex (see Figure 2.7), a total disc with titanium endplates and a rubber nucleus. Acroflex was implanted into six patients. Four patients reported satisfactory results with the device, whereas one patient did not experience pain relief and another patient needed the implant removed and the vertebrae fused due to device failure. Potential problems with toxicity in the rubber led to a redesign [28].

NuVasive is currently running clinical studies on its XL TDR, lateral access total disc replacement. The lateral access technique for implantation is intended to provide for a minimally disruptive procedure, restoring disc height and maintaining motion. Some potential benefits of the lateral approach are the avoidance of vascular,

intestinal, and ureteral injury, as well as the avoidance of major bleeding risks of the other approaches. Insertion of a total disc replacement is not without its complications, particularly in the lumbar spine, where positioning of a relatively sharp metal device must be done in the immediate vicinity of blood vessels [41].

2.3.2.4 Regeneration

The alternative to disc replacement is disc regeneration, which may include regeneration of nucleus tissue, annulus tissue or both [10]. Nuvasive has considered chymopapain, a chemonucleolysis agent as a means to initiate nucleus pulposus regeneration.

2.3.3 Nucleus Replacement Technologies

Current technologies for total disc replacement require excision of the majority of the disc, whereas an alternative approach that has been in development in recent years involves removal of the soft inner nucleus pulposus tissue central to the disc and replacement with a device for restoring the physiologic, viscoelastic, and biomechanical characteristics [34]. Implantation is geared toward slowing the degenerative cascade, with the intention of postponing or eliminating the need for a spinal fusion surgery [2]. Materials which form in situ within the body have been considered to fill the space that has been created within the disc. Nucleus replacement exists as a potential treatment where, by delivering a prosthetic nucleus,

the length and tension of annular fibers are restored, providing stability and restoring height to the disc, subsequently mitigating the degenerative process [3, 34, 37].

A potential indication for nucleus pulposus replacement is severe lumbar degenerative disc disease which has not improved based on a six month nonoperative care. Disc degeneration is indicated with 10-50% loss of disc height, without fissuring. MRI should show an early stage of degeneration without severe modic changes or facet arthrosis [2].

Current technologies for nucleus replacement similarly have undesirable aspects. Many require invasive procedures or toxic crosslinking agents. The earliest nucleus replacement techniques (late 1950's/early 1960's) involved the injection of polymethylmethacrylate into the space formed from a nucleotomy. Keeping the material confined proved to be difficult, however. As a result the method gained little acceptance [46].

Other in situ forming nucleus replacements include silicon injected by Nachemson and Silicon Dacron injected into primate models by Urbaniak, bone resorption and aberrant bone formation in the latter study is believed to have led to the overall implantation of preformed devices [46]. Biodisc, by Cryolife is an injectable hydrogel that is protein based. It was developed based on the company's Bioglue product. The material polymerizes over short time scales and has been proven to pass fatigue tests, though a 10% immediate loss in height occurred that slowly restored to

the original when the sample was subjected to 10 million cycles. Further materials include the IDN (Injectable Disc Nucleus), by Spinewave, which is an injectable that is based on a silk-elastin copolymer, and DASCOR, by Disc Dynamics, Inc., a polyurethane that injects into a balloon and solidifies [47, 48]. Materials such as DASCOR have been proven to restore kinematics of the disc [49]. A thermoplastic nucleus replacement was also developed by Disc Augmentation Technology that injects and hardens at 66°C within the disc space [46].

2.3.3.1 Historical Development

In 1934, Mixter and Barr identified the disc as the source of pain. 1950's motion sparing technologies arose for replacing nucleus pulposus. In 1955 David Cleveland injected methyl acrylic into the disc. In 1959 Hamby and Glaser reported injecting the same material and were unsuccessful due to troubles with controlling the flow before the reaction had completed. Spheres of cobalt chrome alloy were also implanted in a retroperitoneal approach after discectomy. 1962 Nachemson showed that spacers made of silicone rubber were incapable of withstanding physiologic loads, and in 1966 the Fernstrom stainless steel ball led to subsidence and extravazation [2].

In a 1981 study, Edeland suggested the flow of fluid in and out of the disc tissue could be the source of their viscoelastic response under biomechanical loading [46]. The resulting fluid nature of the disc led to the selection of hydrogels. The use of synthetic hydrogels in the field of nucleus replacement is intended by researchers to

mimic the behavior of soft tissue and such gels been in development since the late 1980's. Hydrogel implants have been designed with the intention of either not swelling (remaining constrained to a fixed volume), or swelling, in order to completely fill the nuclear cavity. Early work involving hydrogels include a device designed by Ray in 1988, as an injectable *in situ* forming gel that swells with the disc [50]. Hydrogels' ability to swell as they imbibe water as well as their ability to contract and deform may result in a reherniation through the defect in the annulus created when the implant is delivered. This defect can be considered to be the direction of least resistance in a disc with an otherwise competent annulus [27]. The design of Ray was later adapted for this reason to encase the gel within a mesh for manufacturability (see Figure 2.8). The resulting product from this effort was entitled the PDN (Prosthetic Disc Nucleus).

Indications for the PDN did not include greater than Grade I spondylolisthesis, an incompetent annulus, low disc height (<5mm) or symptomatic degenerated or fractured facets [28]. These indications were restricted to degenerative disc disease with back pain (leg pain may or may not have been present since discectomy is capable of relieving leg pain, but often not back pain). Low disc heights are not indicated because the device requires a competent annulus placed in tension [51].

Concerns with implanting a preformed device such as the PDN include difficulties with creation of a cavity that matches the size and shape of the device. Implantation also potentially requires a larger annulotomy [2]. Methods used for decreasing the

size of the annulotomy include, in addition to implantation of a swellable implant, the incorporation of two separate units. An anterior tapered unit and a posterior rectangular unit were both implanted. The anterior unit is delivered first, and the posterior unit is delivered second. Both units are sutured together once in position [51].

PDN was further shown in a cadaveric study to restore mobility of a 5-6 gram denucleated disc. Eysel evaluated PDN in 11 cadaveric functional spinal units. A 38-100% increase in mobility for the denucleated specimen was restored to intact state with no statistically significant difference [41]. Biomechanics testing for the device withstood up to 50 million cycles and maintained function of the implant, including disc height and viscoelasticity (loads were 200N and 800N). Testing was performed for intact discs, as well as the 5-6 gram denucleated discs with and without PDN implantation. Implantation proved stabilization was equivalent to pre-nucleotomy [2].

The first PDN clinical trials were conducted in 1996 with two implanted PDN devices. Early clinical studies were effective, however trials from ‘97-‘98 showed a 38% migration rate. Migration was mitigated via revisions to surgical procedure and device shape [51]. A 10% reoperation rate was reported for the device due to migration [14].

Hypan was chosen as the swellable hydrogel. The grade was switched during phase II trials (’97-98) to one that absorbs a greater amount of water, in order to provide a softer device, to avoid concerns of subsidence through the cartilaginous endplate that separates the disc from the vertebrae [51]. Hypan is a polyacrylonitrile based hydrogel copolymer that has seen other uses for implantation, in particular as a therapeutic bulking agent for the bladder [52]. A proprietary hydrolyzed polyacrylonitrile has been similarly used by Replication Medical in their NeuDisc nucleus replacement, where a dehydrated disc is inserted into the denucleated cavity and allowed to swell axially in order to restore disc height [27]. Replication has also marketed Gelstix™, a nucleus augmentation device, where a rod of hydrolyzed polyacrylonitrile is inserted into the disc and allowed to swell, as well as Gelfix™, a hydrolyzed polyacrylonitrile interspinous spacer.

By 2002, 480 implantations of PDN had been performed [46]. Between March and December 2002, a second study was performed with a single unit. In this second study, a range of levels in the lumbar of 45 patients were implanted with the device (26 men / 19 women: ranging 33-47yrs; average age of 35.6yrs). Symptoms had lasted on average 12 months prior to surgery. Disc gained 19.7% in height in comparison to the height before surgery. Disc height was measured on X-rays. Results from the follow-up showed a statistically significant improvement in every measurement, over the preoperative state. 26/30 patients reported much improvement and 4/30 reported little improvement. 3 patients had back pain recurrence [28].

No migration was reported in the study, but four had markers not on a straight line with the disc. No pain was reported in these patients and no measures were taken to correct this orientation. Disc height increased to 10.3 over 8.6 on average preoperatively (19.7%). Improvements in pain, leg pain in particular. 51 patients implanted with the PDN were followed for 4 years. Initial success in these patients was reported at 91% at 3 months post-implantation. Failures within the trial are attributed to inappropriate patient selection, failure to remove all herniated nucleus in order to implant, and strenuous activity by patients soon after the procedure. Oswestry scores for the 51 patients decreased from 52 to 8.3 % after the 4 year period. Mean disc height increased from 8.7 to 10.5mm over this period as well. Modification of the technique included rotation of the device 90° into a transverse position to avoid protrusion into the spinal canal [28].

In addition to the standard posterior approach for implantation, a new surgical approach was introduced. The ALPA, or Anterior Lateral transPsoatic Approach developed by Dr. Rudolph Bertagnoli allows the disc to be accessed from the side by way of the peritoneum, through the psoas muscle [51]. This approach allows the device to be inserted without the rotation required using the posterior approach. In a clinical study by Schonmayr et al (10 patients) eight of ten of the procedures yielded results considered excellent. Migration was observed in three patients, with one reoperation [2].

Polyurethane has been considered for use as a nucleus replacement by Fassio and Ginestie, Edeland, Froening, and Schulmann. Polyurethane was chosen based on its mechanical properties, in particular compressive and tensile strength, as well as elongation at break. The glass transition was identified to be at 1.1°C and degradation at 100°C. Catalysts were chosen to minimize the exotherm produced from polymerization, as well as the rate of polymerization [53] DASCOR, an implant by Disc Dynamics, Inc was an *in situ* forming polyurethane nucleus replacement designed to cure within a polyurethane bag.

2.4 Poly(vinyl alcohol)

Poly(vinyl alcohol) (PVA) is a aliphatic polymer hydrocarbon chain with one hydroxyl per repeat unit (see Figure 2.9). PVA is used as an emulsifier, as well as in the stabilization of colloid suspensions. The material is used in water soluble coatings, textile sizing, and as an adhesive. It is also spun into fibers [6, 54]. It is of particular interest as an implantable biomaterial due to its biocompatibility .

The hydroxyl moieties on poly(vinyl alcohol) interact via hydrogen bonding. Hydrogen bonding is a strong dipole to dipole interaction mechanism where hydrogen is attracted to non-bonding electrons in adjacent chemical structures. This mechanism, though a strong form of interaction, is weaker than typical bonds, with 20kJ/mol required to break a hydrogen bond, in contrast to approximately 400kJ/mol required to break an O-H bond. Hydrogen bonding has an effect on intermolecular interactions, producing substantial increases in boiling points of lower molecular

weight substances, and interactions between molecules which increase the apparent viscosity of hydrophilic materials when in an aqueous or polar medium [55]. Hydrogen bonding is observed to occur between PVA and water, as well as between PVA chains or within the same chain.

The water solubility of the polymer increases with percentage of hydroxyl units. The solubility of the polymer reaches a maximum at 88% hydrolysis, beyond which point the interchain interactions take over, decreasing the solubility, requiring heating above 85°C to dissolve the material. Due to the intermolecular hydrogen bonding of PVA, the crystalline melting point is high. Fully hydrolyzed grades have melting temperatures above 230°C. Further, the material can not be easily directly melted without significant degradation. Processing of the polymer must therefore be performed in the solution state, or via plasticization [54].

Due to the presence of a keto-tautomer in the vinyl alcohol molecule, the majority of synthesis of the polymer is carried out indirectly through the initial production of polyvinyl acetate (PVAc) [54, 56], which is then hydrolyzed, as acetate groups are replaced with the hydroxyl by treating with an aqueous acid or alkali in alcohol solution, however due to resulting impurities, the method has been adapted to alcoholysis of polyvinyl acetate in the presence of sodium methoxide. The conversion of the polymer is typically carried out in the solution or suspension state. The resulting gel from the process is chopped up and the reaction is stopped by the addition of acetic acid. The remaining solid material is washed and dried. PVA has

little branching. Much of the branching in PVAc is cleaved off in the hydrolysis reaction [54]. The majority of polyvinyl alcohol in bulk grades is produced via the PVAc method and is largely atactic with 52-54% syndiotactic dyads [56]. PVA with a greater concentration of syndiotactic material has also been produced via poly(vinyl pivalate).

Control over the portion of syndiotactic dyads is desirable, since hydrogen bonding is believed to be increased with greater percentage of syndiotactic material. Increases in hydrogen bonding in PVA typically result in increased solution viscosity and gel mechanical properties. Further, crystallization is believed to incorporate mostly syndiotactic dyads, in particular during the freeze-thaw physical crosslinking process. Despite this understanding, little has been reported on the complex rheological solution behavior of PVA [56].

Grades of polyvinyl alcohol are described based on their degree of hydrolysis, which is the percentage conversion of the acetate to hydroxyl groups. The presence of hydroxyl groups increases the ability of the PVA to associate, via hydrogen bonding, with water, as well as with itself, often forming crystalline regions (see Figure 2.10). Crystallites are useful in distributing applied mechanical stress on the PVA network [57]. PVA has been shown to have good mechanical strength and elasticity, which make it suitable for the application of a load bearing tissue replacement [58]. Degree of crystallinity via infrared spectroscopy of PVA networks annealed at varying temperatures has been reported in pre- and post-swelling states by Peppas [59].

Crystallites forming in PVA are of the fringed micelle variety. The formation of full crystalline spherulites is not typically observed. The formation of crystals also depends on crosslink density. Densely crosslinked polymers with a small molecular weight between crosslinks (M_c) will not crystallize [57]. Orientation of PVA has been evaluated using birefringence, and degrees of crystallinity are reported using calorimetric methods as well as density upon immersion [60].

The rheological responses of PVA in DMSO solution have been studied by Lee et al. In the study, thermal and shear histories were noted to be kept constant for prepared samples, via developing a standard dissolution technique. Samples were analyzed using 50mm sized parallel plates and a 1mm gap. Tests were performed at 30°C. Samples were fully relaxed for 20 minutes prior to testing. Specific and complex viscosity across a range of frequencies was reported, as well as the dynamic mechanical properties of storage and loss modulus. The test was not performed across a range of temperatures, however, so the temperature dependent gelation behavior was not reported. Instead, the relation of PVA concentration to solution properties was described. It was determined that molecular weight had less of an effect on solution characteristics than the concentration, which suggested that polar effects from the hydrogen bonding of the hydroxyls played a significant role in solution viscosity [56].

2.5 PVA Hydrogels

The fact that PVA sets to a gel upon standing is well known [6]. The resultant gel is tacky and of low modulus, however [61]. Typically, high water content results in poor mechanical properties for PVA gels and higher mechanical strengths limit gel water content [61].

Considering nucleus tissue is the source of hydration in the intervertebral disc, it is believed by many that a tissue replacement should similarly be hydrophilic. Polyvinyl alcohol hydrogels are commonly chosen for nucleus pulposus implants for their biocompatibility, as well as their ability to retain water [3]. Hydrophilic materials are currently being investigated as a way to maintain the swelling pressure within the disc through the retention of water. Hydrogels have multiple states of water that are bound to different extents to the polymer network. The most polar hydrophilic groups bind water the tightest and this state is described as primary bound water. Secondary bound water is defined as the remaining water that interacts with hydrophobic groups as the molecule is swollen by the primary type "total bound water" is the sum of the two. An understanding of water states is useful as it relates to the permeation of nutrients and cells in and out of an implanted gel [62].

Polyvinylalcohol hydrogels may be crosslinked by a variety of methods. Many are prepared via chemical methods using a polyfunctional reagent that forms linkages between portions of adjacent polymer chains. An example of this reaction is the use of glutaraldehyde, a bifunctional aldehyde that reacts with hydroxyl groups on PVA

[63]. N-hydroxysuccinimide (NHS) esters form ester linkages through reaction with hydroxyls, though the ester bonds formed can be subject to hydrolysis in aqueous solution [64]. Boric acid and Congo red have also been used as chemical crosslinkers.

Radiation is another method, where electron beam, ultra-violet light or gamma irradiation are used to create chemical linkages [57] Irradiation below the Tg of the polymer has shown to result in degradation, where radical pairs are incapable of coupling [65]. In contrast, mobility of the polymer above Tg allows for crosslink formation upon irradiation. The nature of the PVA solution is viewed to be analogous to the above-Tg state, with respect to crosslink formation [57].

Methods exploiting the network forming capabilities of the PVA gels in order to form a physically crosslinked network have been similarly developed. Particular benefits to the formation of a network via physical crosslinks, as opposed to chemical, is the absence of toxic materials that could potentially leach from the gel [58]. As a result of this technique, the formation of crystallites provides crosslinks for the formation of a three dimensional network. One common example of physical crosslinking subjects a PVA solution to successive freeze-thaw cycles. Relatively dilute solutions of PVA can form into elastic constructs, using this technique.

Crystallization in PVA hydrogels plays a large role in network formation for physical crosslinking [66]. It has been suggested that crystallization forms the basis of the

freeze-thawed network. There is some debate over the exact process of this method of crosslinking, however it has been hypothesized that freezing water forces a phase separation of the PVA into domains that crystallize [67].

A semi-hydrated preformed poly(vinyl alcohol) implant ("*Aquarelle")* was developed by Stryker. The implant was 80% water. The device was capable of being injected via a 4-5 mm tapered cannula through a disc having a small annulotomy. The implant was delivered via a semi-open access technique, using a pressurized trocar [3, 17, 47]. A preclinical trial reported extrusion in baboons. The defect in the annulus resulting from access was further believed to accelerate disc degeneration, since accelerated degeneration was observed for the control group which received discectomy alone. It was further believed as a result of this outcome that defect size must be decreased in order to reduce this consequence [14].

In a related study by Allen, baboons were implanted with a PVA implant via an anterior approach that resulted in a 33% rate of herniation. The implant consisted of 98.5% hydrolyzed PVA which was crosslinked via freeze-thawing. The implant was confirmed to maintain disc height upon application of load in cadaver segments. Implants were terminally sterilized using gamma irradiation. Implantation followed denucleation using rongeurs. As a result, the implantation technique was modified to anterolateral, which still resulted in 20% rate of herniation. Four of the six extrusions were in the posterior direction, with two in the spinal canal extradurally or intradurally. Implants were well tolerated over the 24 month implantation, in

particular, extruded implants into both the soft tissue and the spinal canal were similarly well tolerated. Implants further showed no signs of local or systemic toxicity. As a result of histological analysis, tissues in animals having damaged implants displayed an inflammatory response. Particles from broken implants were encapsulated via a mechanism similar to a foreign body response. Hyperplasia was observed via microscopy in the lymph nodes of three test specimens and one control, however no PVA particles could be found local to the site of analysis. Endplate damage was reported as a result of the study despite efforts to maintain the integrity of endplates during denucleation. Harvested implants were observed to have flattened in the superior-to-inferior direction, which was expected since implants were reported to be intentionally designed to contour to the cavity, as well as to swell post-implantation. The baboon model was also noted to have a higher intradiscal pressure than humans which would result in lower equilibrium water content upon swelling after implantation [23].

Viscosity was found to increase significantly with time. In a study by Briscoe, 15% gels were measured for viscosity at t=0 and after 20 days. When solution concentration was increased from 10-15%, the relationship of apparent viscosity with respect to time increased. Greater concentrations produced greater increases in apparent viscosity over time. Shear thinning behavior also became more pronounced at greater lengths of time, for concentrated solutions [6]. It has similarly been shown that this time-dependent gelation is not observed for degree of hydrolysis of 88% or lower. This is explained that the relative affinity for the polymer to bind tightly to

itself is disrupted by the smaller number of hydroxyls to bind, along the chain. Apparent viscosity is similarly decreased with decreased hydrolysis. There is a corresponding increase in viscosity for very low degrees of hydrolysis, however, due to a decrease in polymer/solvent interaction resulting from an increase in the acetate group concentration[6].

Studies similarly exist, exploring the suitability of the mechanical properties of freeze-thawed PVA for use as tissue replacements. In addition to nucleus replacement, the replacement of diseased or damaged cartilage in joints via implantation of PVA hydrogels in freeze thawed form has been considered [68].

2.6 Poly(ethylene glycol)

Polyethylene glycol (PEG) is described as a linear polyether because of its structure, which contains oxygen in its carbon backbone (see Figure 2.11). Typically molecular weights above 20kDa are described as polyethylene oxide, however there is little difference and the terms are often used interchangeably.

It has been shown by Fabula that the addition of a small amount of polyethylene oxide to water results in a friction reduction that reduces the pressure drop at a specified flow rate to as low as one fourth [69]. Typical melting temperatures for moderate molecular weight (10-35kDa) commercially available PEG are in the range of 60-70°C, with lower molecular weight material (0.4kDa) being in liquid form at room temperature. PEG is known to crystallize readily forming spherulites [70].

PEG binds to two or three water molecules for each ethylene oxide repeat unit in its structure. The viscosity in the solution state is believed to be related not only to the molecular weight, but to the degree of hydrogen bonding. The viscosity of the solution has been shown to decrease as temperature or pressure increases, as well as with the presence of electrolytes [6]. The presence of electrolytes has been shown also to reduce the solvent quality for PEG and other hydrogen bonded polymers, such as PVA. Unlike PEG, however, PVA has strong interchain hydrogen bonding which affects solution rheology.

It is believed that the flexible chain on the PEG molecule as well as its ability to bind water molecules causes it to swell to 5-10 times larger than a soluble protein of comparable molecular weight. PEG also acts by the same mechanism to exclude cells and proteins from surfaces. Protein absorption has been decreased through the incorporation of PEO onto quartz surfaces in a study by Gregonis et al. [71, 72]. The increased hydrophilicity of PEO has also led to applications for interface/surface coatings.

2.7 Polymer Solution Thermodynamics

A representation of the miscibility of polymer systems has been prepared by Flory and Huggins. The resulting expression describes the free energy of mixing of a system as it relates to the entropy and enthalpy [73]:

$$\Delta G_m = RT(n_1 \ln\varphi_1 + n_2 \ln\varphi_2 + n_1\varphi_2\chi_{12})$$

R: gas constant;

T: absolute temperature (°K);

φ : volume fraction;

n: # of moles;

χ: Flory Chi parameter.

A value of χ of zero indicates miscibility in the system and a value of $\chi > 0.5$ indicates phase separation. The equation described above is prepared for a single polymer (subscript "1") in a single solvent (subscript "2"). The equation has been evaluated for greater than binary systems by adding greater numbers of terms for each component. The Chi parameter must be evaluated for the interactions of the polymers with each other and the solvent.

It should be noted that for the production of a phase diagram that %v/v yields the volume fraction term necessary for evaluation of the χ term. In contrast, evaluation using %w/w is useful for establishing the compositional space for formulation.

2.8 Hydrogel Swelling Thermodynamics

A number of theoretical models exist for predicting swelling properties in hydrogels for physiologic environments. Current models lack application to the in vivo environment due to the deviation from ideality for the case of polymer networks in electrolyte solutions [74]. A reasonable approximation, however is the Flory-Rehner analysis, where gel networks of crosslinked polymers are considered, consisting of a

Gaussian distribution of polymer chain lengths. The spontaneous process of swelling becomes favored thermodynamically when the polymer network is contacted by solvent. The decrease in free energy of mixing resulting from mixing of polymer and solvent is balanced by the elastic energy of the chains. A retractive force resulting from the crosslinks of the network is created to balance the pressure generated as a result of the swelling of the system. A balance of the two forces describes swelling equilibrium. The combination of the rubber elasticity theory and mixing thermodynamics generate the following equation [65] for a swollen system crosslinked in the absence of solvent:

$$\frac{1}{M_c} = \frac{2}{\overline{M_n}} - \frac{\frac{\bar{\upsilon}}{V_1}[\ln(1-\upsilon_{2,s}) + \upsilon_{2,s} + \chi_1 \upsilon^2{}_{2,s}]}{\left[\upsilon^{1/3}{}_{2,s} - \frac{\upsilon_{2,s}}{2}\right]}$$

$\upsilon_{2,s}$: swollen equilibrium polymer volume fraction;

V_1: molar volume of solvent (18cm^3/mol);

$\bar{\upsilon}$: specific volume of the amorphous bulk polymer;

$\overline{M_n}$: number average molecular weight of the polymer; and

χ_1: Flory polymer-solvent interaction parameter.

The expression was adapted for crosslinking of a polymer in the solution state. The $\upsilon_{2,r}$ term was introduced as the volume fraction after crosslinking. The equation is as follows[65]:

$$\frac{1}{M_c} = \frac{2}{\overline{M_n}} - \frac{\frac{\bar{\upsilon}}{V_1}[\ln(1-\upsilon_{2,s}) + \upsilon_{2,s} + \chi_1 \upsilon^2{}_{2,s}]}{\upsilon_{2,r}\left[\left(\frac{\upsilon_{2,s}}{\upsilon_{2,r}}\right)^{1/3} - \frac{1}{2}\left(\frac{\upsilon_{2,s}}{\upsilon_{2,r}}\right)\right]}$$

Crosslinking density is important since it has an effect on mechanical properties. Crosslink density (ρ) is inversely related to molecular weight between crosslinks (M_c) by the following relation [65]:

$$\rho = 1/\upsilon M_c$$

where υ is the specific volume of the polymer. Network mesh size is the distance between crosslinks. Crosslinking and ionic strength of the swelling medium will affect equilibrium swelling. Swelling has been evaluated using the results from tensile experiments [65].

Mc, or the molecular weight between crosslinks can be evaluated through equilibrium swelling experiments, since mesh size is related inversely to Q (equilibrium swelling ratio):

$$Q^{-1} = \frac{V_p}{V_{gel}} = \upsilon_{2,s}$$

Characteristic correlation length, or average distance between consecutive crosslinks can be determined from M_c:

$$(r_0^{-2})^{1/2} = l\left(2\frac{M_c}{M_r}\right)^{1/2} C_n^{1/2}$$

l: bond length;

C_n: polymer characteristic ratio

M_r: polymer molecular weight

Finally, mesh size (ξ) is calculated by:

$$\xi = (r_0^{-2})^{1/2} \upsilon_{2,s}^{-1/3}$$

2.9 Phase Behavior of PVA/PEG

Ethylene glycol has been described as a solvent for PVA [54]. Increasing molecular weight leads to an incompatibility between the two polymers. According to early research, over a given concentration range for PVA/PEG aqueous solutions, there is a phase separation that occurs, yielding a concentrated aqueous PVA phase and a dilute aqueous phase of PEG. The first evidence of the study of this phase separation was in 1968, when Toyoshima et al reported the binodal for low degree of hydrolysis PVA (88%) and 4kDa PEG. In the case of this study, a highly hydrolyzed material was not found to produce a phase separation [75, 76]. Further, more comprehensive work was done by Inamura et al in the 80's, including greater degrees of hydrolysis as well as a variety of molecular weights of both polymer components.

The ternary diagram is related to a polymer-solvent-nonsolvent system in Tompa.et al (see Figure 2.12). Three component systems for incompatible materials have been described by Flory in detail [73]. Particular attention was paid to polymer/solvent/non-solvent systems. Inamura states that for high molecular weight PVA, the system is best approximated in this manner, due to the increased incompatibility with PEG [76].

The ternary diagram for an incompatible system such as will be described is constructed of a binodal curved line representing the phase boundary separating the immiscible region (having two or greater phases) from the miscible (one-phase) region. Typical representations of ternary systems consist of a triangle with each vertex corresponding to 100% of one of three components. The composition of three-component systems is defined in the space by orthogonal distance to each of the three vertices. Formulations prepared in the two-phase space separate to two different compositions on either side of the parabolic binodal curve. For example, a composition prepared that would fall in the two-phase region would separate into a lower layer of one composition and an upper layer of another composition. These two layers will have composition points on the binodal curve, and the line connecting these two points is called a “tie line”. Tie lines yield information about the behavior of a system.

Research on PVA/PEG phase diagrams by Inamura came primarily in two separate papers, the first (1984) discusses the phase separation that occurs for dilute

formulations (less than ~30% total polymer) [76]. These papers describe the formation of the concentrated PVA-rich phase and the dilute PEG-rich phase [76]. Inamura prepares a ternary diagram for this small region of concentrations. PEG is added volumetrically in a systematic manner and the concentrations where turbidity occurs in the solution is determined to be the position of the onset of phase separation, and the subsequent location of the binodal. Phase separation data is shown for systems with PVA = 93kDa and PEG = 7.2-668kDa. The binodal for this system is defined and the curves are shown to move upward on the ternary diagram with PEG molecular weight (see Figure 2.13a). A wide range of molecular weights was also chosen for this study for both polymers (PVA: 37-730kDa; & PEG: 7.2-668KDa), and a similar behavior is observed with respect to PEG molecular weight (see Figure 2.13b). Findings from this research have shown that the binodal for each system moved upward, producing a much greater region of phase separation, as the molecular weight of either PEG or PVA increased. On a ternary diagram, this is represented by the apex of the binodal moving closer to the corner representing 100% H_2O. Higher molecular weights produced phase separation at increasingly more dilute solutions. This agrees with the thermodynamic understanding that a larger molecule will be less entropically favored to mix. As PEG molecular weight increased, the binodal inclined toward the H_2O - PVA axis up to 2000kDa, after which the binodal moved toward the PVA - PEG axis. It was also observed that low molecular weights of PEG (<0.6kDa) did not produce a phase separation.

The Flory χ parameter can be expected to vary based on the system. For ternary systems of polymers with the same molecular weight, χ_{12} is greater than χ_{13} when there is an incline toward the axis of components 1 and 2. In other words, an incline toward the PVA-water axis for a PVA/PEG system of the same molecular weight would mean the formation of a dilute PEG phase and concentrated PVA phase. Through this observation it was determined by Inamura that water is a better solvent for PEG than PVA in the PVA/PEG/H_2O system. The binodal curve can also be expected to be symmetric and tie lines can be expected to be approximately parallel to the polymer/polymer axis for polymers of the same molecular weight [76].

More concentrated solutions of PVA were explored in the later Inamura publication (Figure 2.14). Concentration approached 50% for PVA and PEG for this study, however PVA molecular weight in this case was low (38kDa), in comparison to the molecular weights to be considered for a load bearing material. A ternary diagram and binodal for the PVA/PEG/H_2O system were also determined in this study. This work stated a molecular repulsion for the two polymers as reason for the phase separation.

Work by Lim has been performed on the plasticization of $BaTiO_3$ sheets with poly(vinyl butyral) as the binding agent. It was found that the incorporation of PEG resulted in a decreased viscosity and plasticization behavior, as hydrogen bonding decreased. Hydroxyl peaks in FTIR were shown to decrease with the addition of PEG [5].

Recent work suggests that a specific phenomenon has been identified for the phase separation of similar incompatible systems. For instance, it has been observed that the incorporation of an electrolyte in solution, has the effect of decreasing the viscosity of a solution, through interference of hydrogen bonding. Similarly, the presence of the electrolyte is capable of reducing the interaction between PVA chains and the solvent [6], while solute (electrolyte) and solvent (water) interactions are increased. The resulting effect is a temperature-related jump in solution viscosity that occurs at a critical concentration of salt in solution.

Incorporation of low degree of hydrolysis material has shown to produce solution effects where upon incorporation of lower degree hydrolysis PVA, the PVA becomes increasingly more likely to phase separate at higher temperatures. The reason for this effect is explained as the incorporation of greater amounts of hydrophobic material in the low degree of hydrolysis PVA. In other words, since low degree of hydrolysis PVA has such a large amount of acetate groups remaining, the hydrophobic character of these groups results in a disruption of the behavior in solution. The Viscosity measurements vs. temperature show a transition for low degree of hydrolysis PVA (see Figure 2.15). Observed as a result of this solubility change is a transition in viscosity, where PVA no longer hydrogen bonds with the solution to the same extent, above a given temperature. The resulting change in hydrogen bonding properties reduces the apparent viscosity of the solution.

Similarly, when NaCl solution is added in varying amounts there is a similar viscosity reduction behavior, as greater amounts of NaCl reduce the hydrogen bonding between polymer and solvent, this reducing the apparent viscosity. In the study by Briscoe, poly(vinyl alcohol) was observed to precipitate out at temperatures above the transition temperature, suggesting that the affinity for water had been decreased. Low degrees of hydrolysis are shown to result in a high temperature phase separation that results in a viscosity decrease. See Figure 2.15. The phenomenon observed by Briscoe is an interference in hydrogen bonding association of PVA with water that results in a solubility transition that is manifested in a viscosity transition.

Theta-gels have been proposed by Ruberti et al [77], where through manipulation of the solubility characteristics of PVA (via reduction of solvent quality and the inclusion of a theta solvent), a physically associated gel network is formed. In Ruberti, the theta solvent is thought to force PVA chains in solution into concentrated domains that resist dissolution. Further, Ruberti describes the addition of a theta solvent to PVA as resulting in a spinodal decomposition, which occurs in unstable supersaturated solutions, where spontaneous clustering is thermodynamically favored. The combination of solutions such as NaCl/water, and methanol/water with PVA, are also described to create the theta gelled state. Ruberti et al states without citing a particular theory, that crystalline physical crosslinks are formed, in contrast to the random associations of normal concentrated aqueous PVA gels. Calorimetry experiments later in this thesis will be performed to probe for ordered crystalline structure, such as that shown by a physically crosslinked freeze-thawed gel. Oral et al

describes low molecular weight PEG (0.4kDa) incorporated into PVA gels, which has been shown by Inamura to not produce the supernatant phase [76, 78]. Potential nucleus replacement technologies are described using similar systems [77]. Work by Choi et al further describes the creep behavior of such gels as it relates to equilibrium water content. Creep is seen to decrease with the dehydration of the theta-gels. Dehydration via isopropyl alcohol is shown to reduce equilibrium water content, and increase creep resistance the most.

Though similar, the differences and improvements of the system of this thesis are described throughout the following pages. To be specific, the system described is a polymer blend with higher molecular weight PEG or PEO which exhibits an enhanced gelation transition. The incorporation of the PEG into the network produces a reduced interaction between PVA and water as described by Lim [5] which in turn results in the viscosity transition as described in Briscoe [6]. The production of the viscosity transition occurs spontaneously with interacting polymer functional groups within the network (i.e. without the inclusion of a theta solvent) that produce the high temperature vinyl alcohol/water interference that is the source of the high temperature plasticization. The incorporation of higher molecular weight PEG into the PVA network results in a viscosity transition, in the manner observed at high temperatures by Briscoe et al, as hydrogen bonding between PVA and water is disrupted resulting in a decrease in apparent viscosity. This viscosity decrease allows for flowability at increased temperatures where concentration and network effects

would otherwise prohibit flow. This high temperature phenomenon is in contrast to a low temperature spinodal decomposition suggested in Ruberti et al [6, 77].

PEG has also been used in conjunction with PVA in order to decrease protein absorption and cell deposition to reduce thrombogenicity in cardiovascular biomaterials [79]. PEG was oxidized to yield aldehyde groups. It was also functionalized with isocyanate end groups, both mechanisms with the intention of reacting PEG to PVA [80].

In 1995, Lozinsky studied the effects of polyols on the structure and properties of cryogels. Polyols have been known to be cryoprotectants, that is, to depress freezing temperatures of aqueous solutions. Polyols also are used to reduce ice crystal size, and have been shown to inhibit crystallization enough to allow for glass formation of water. Polyethylene glycol was incorporated into gels (at 400 and 1000 molecular weight) and was shown to increase strength and thermostability of PVA cryogels. Lozinsky mentions formation of gels by pooring the mixed solvent quality. Gels produced using this technique of reducing the quality of the solvent are then freeze-thawed, resulting in increased mechanical properties, and have been suggested as a means for fabrication of soft contact lenses [61].

In recent years, PVA and PEG blend gels have been developed that are physically crosslinked via a freeze-thaw process in order to produce a double network, which results in high mechanical strength [66]. Mechanical strength has been found to be a

factor of composition for these gels. Both fracture strength and strain have been shown to vary with crosslinking for poly(2-acrylamido-2-methyl-1-propane-sulfonic acid / polyacrylamide gels [81]. It has further been shown that dynamic storage modulus increases with increasing amount of PEG in the hydrogels, suggesting that the elastic nature of the gels is increased with PEG content, from 2 to 6 wt. %.

A study in the journal of radiation research and radiation processing regarding the biocompatibility of PVA/PEO gels stated that blend hydrogels made up of these two components exhibited no acute general toxic effects on mice [82].

PVA/PEO gels have found use as adhesion barriers and wound dressings, due to their unique surface properties. The use of the PVA/PEO hydrogels in wound dressings has a number of distinct advantages, including faster wound healing, as well as no sticking of material to the wound, and further, no material remains behind after the dressing is removed. In a study by Yoshii et al., PVA was added to PEO hydrogel wound dressings crosslinked via electron beam in order to impart toughness to the material [83]. Also, a PVA/PVP/polyethylene oxide hydrogel burn and wound dressing under the name of Woundragel has been under development in Vietnam. Similar hydrogels have been evaluated for treatments of a variety of wound dressings for lesions due to leprosy in India. A PVA agar PEG gel has been similarly developed in Bangladesh. Other materials, such as plant starches have been used in combination with PVA in eastern countries, in order to keep production costs low.

2.10 Biocompatibility

A. Hoffman [71] defines biocompatibility as success of the device in fulfilling it's intended function. Hoffman states that only complete devices and never just materials gain FDA "approval". Instead, bioreactions (reactions between materials and biological systems) are a simpler phenomena to understand than biocompatibility. Hoffman mentions that toxicology assays are commonly inappropriately referred to as an assessment of biocompatibility. The tests are concerned with substances leaching from a material. It is these leachables that will elicit a bioreaction in cells and tissues. For materials that do not leach substances, bioreactions are strongly affected by surface properties. Other characteristics potentially affecting bioreactions include porosity, location of implant, hardness and shape. Swelling character is also a consideration for hydrogels. Bioreactions are predicted through the determinations of correlations that arise between material properties and the resultant bioreactions. Fluids with a given critical surface tension exhibit a minimum in biointeraction. Further, correlations between cell adhesion and surface energy have also been investigated in nonproteinaceous media. It was further stated that correlations of bioreactions with material properties are rare. Problems referenced were difficulties in assembling a large enough experimental population, as well as the complexities of the human biology and of the biomaterials themselves.

PVA is known to be well tolerated as an implantable biomaterial [23] producing no systemic or local toxic effects. This material has been evaluated for implantation in physically crosslinked hydrogels, such as the *Aquarelle* and *Hydrafil* nucleus

replacements and is currently being evaluated as an embolic therapy where microspheres are implanted via a catheter (*Biocure*), in order to block blood flow to a tumor.

Polyethylene glycol is similarly widely used as a biomaterial, due to its inherent biocompatibility. PEG has gained FDA approval for use in drug formulations [84], and intramuscular injectables [85]. The biocompatibility of the material is based on its nonimmunogenicity, nonantigenicity and protein rejection properties

.

Further, surfaces of materials have been coated with PEG for expressly improving their biocompatibility. Nonionic PEO hydrogels and have been used in blood contact applications. PEO surfaces have been described as less thrombogenic, which leads to less protein absorption. Surface induced thrombosis and device failure is minimized by the incorporation of PEO onto surfaces [71]. Interactions between cells and macrophages, which are understood to a key element in the foreign body response, are determined by observing protein adhesion and morphology of cells, post-implantation. Protein resistance is an important aspect of biocompatibility.

Protein absorption is related to molecular weight in that the amount of protein absorption has been seen to be a strong function of molecular weight for low molecular weights (700-1900 Daltons) [86]. The reason is cited as that lower molecular weights are incapable of folding into a hydrated coil. This coil excludes

higher molecular weight solutes from the surface. These effects can be seen to level off at increasingly higher molecular weights.

Interactions at a biomaterial surface are considered to be of high importance. Materials are known to be modified with PEO in order to reduce surface-induced thrombosis. The process resulting from initial exposure of a foreign substance to the blood, begins with protein absorption onto the surface, and then leads through a complicated series of steps before ultimate blood biocompatibility is determined. The correlation between surface induced thrombosis and blood compatibility has not yet been established, however.

For drug delivery using PEO functionalized heparin, as a result of the increasing hydrophilicity and dynamic motion of PEO, the adhesion of platelets and absorption may be decreased. Spacers of PEO were used to immobilize heparin. The PEO showed an increased bioactivity over a hydrophobic spacer. PEO is indicated for drug delivery because of its unlimited solubility in water, high mobility in water due to its chain conformation, as well as an excluded volume that is large enough to repel cell and protein interactions [71].

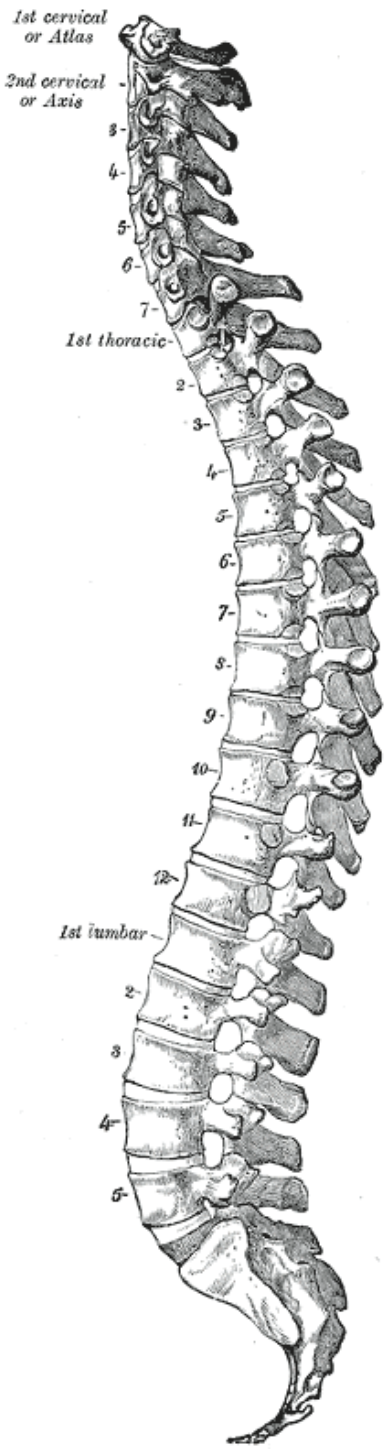

Figure 2.1 The spine, viewed laterally [7]

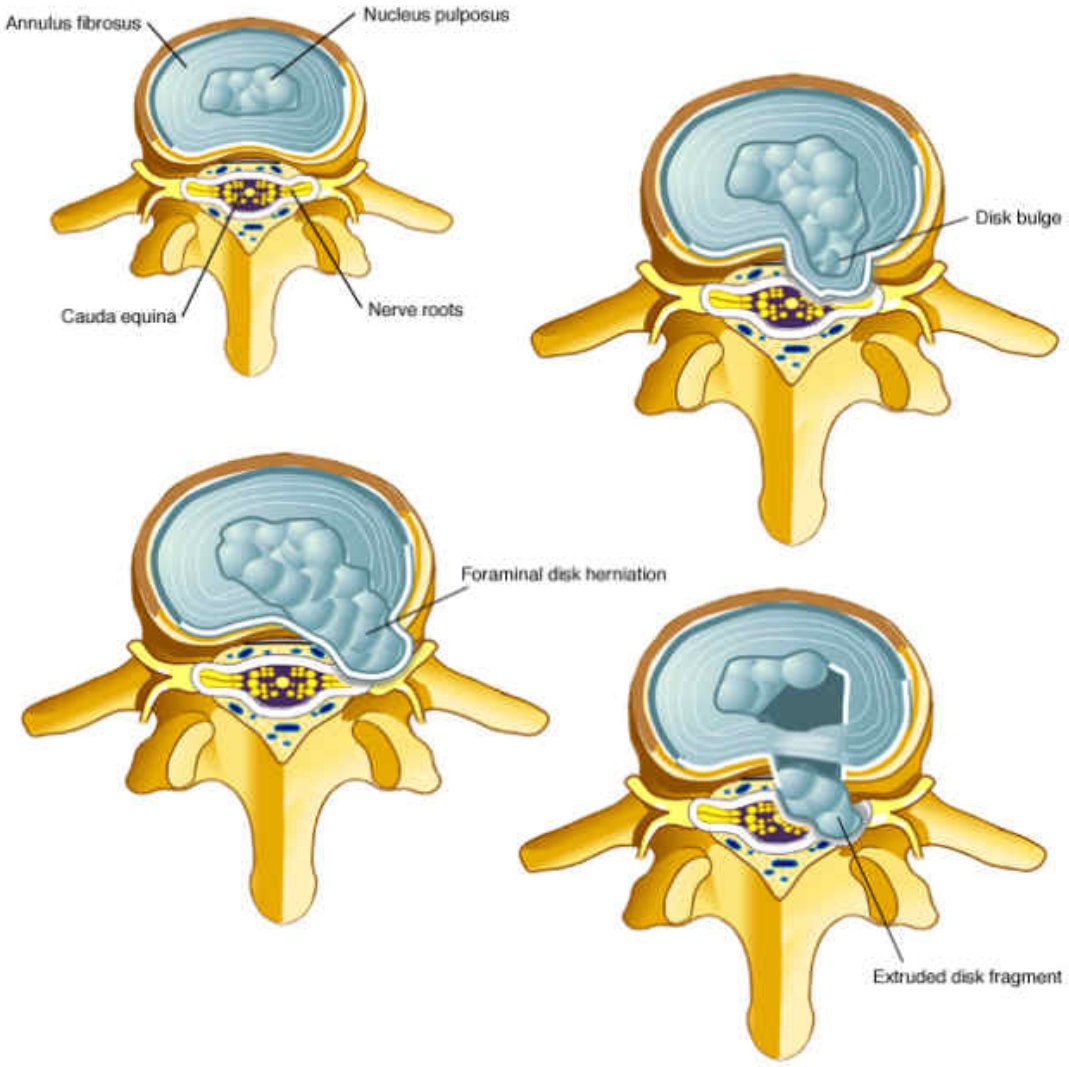

Figure 2.2 An intact disc and states of nucleus pulposus prolapse [87]

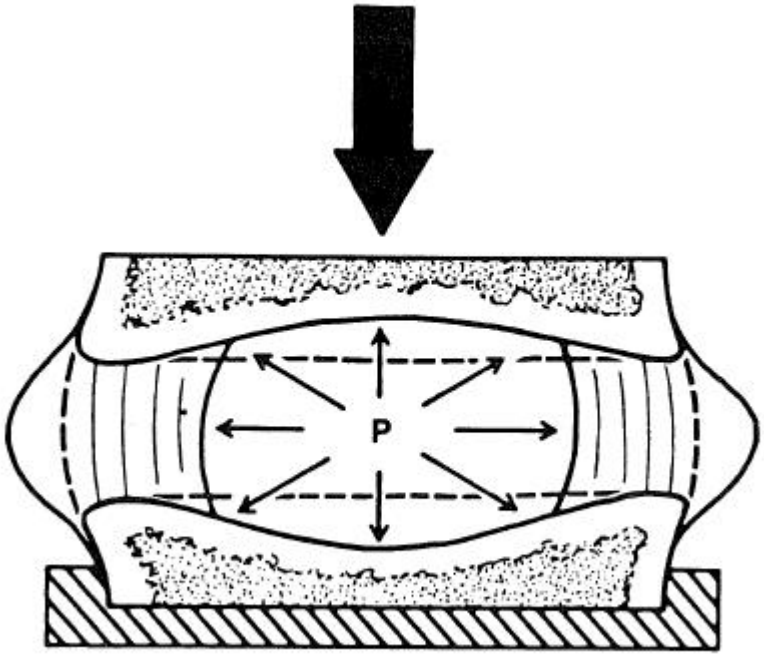

Figure 2.3 Axial compressive loading of an intact intervertebral disc. Pressure of nucleus tissue puts annular fibers in tension [8].

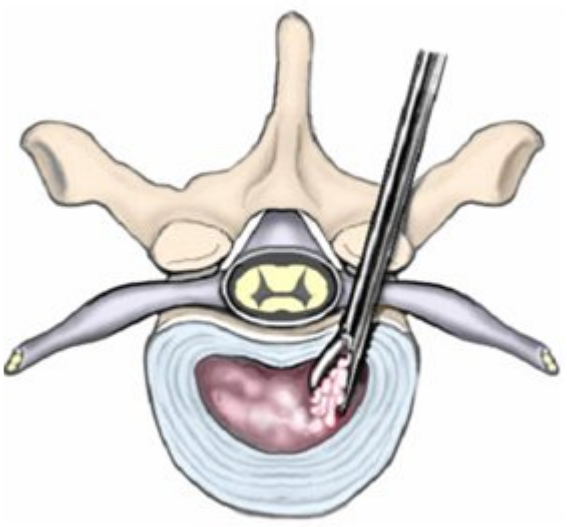

Figure 2.4 Posterolateral thoracic discectomy procedure using rongeurs **[88]**

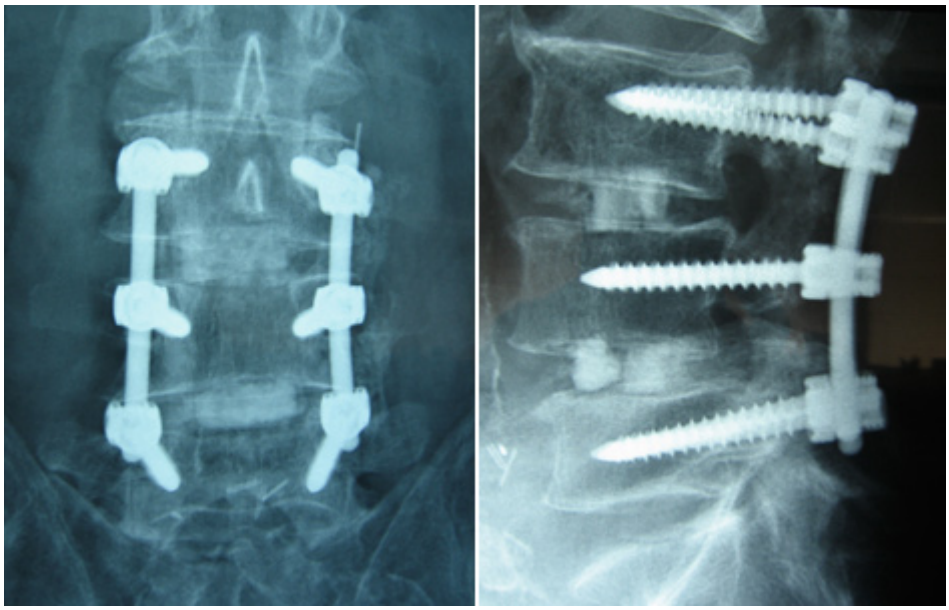

Figure 2.5 Posterior Lumbar Interbody Fusion (PLIF) **[89]**

Figure 2.6 Prodisc-L - Lumbar total disc replacement [90]

Figure 2.7 Acroflex total disc [91]

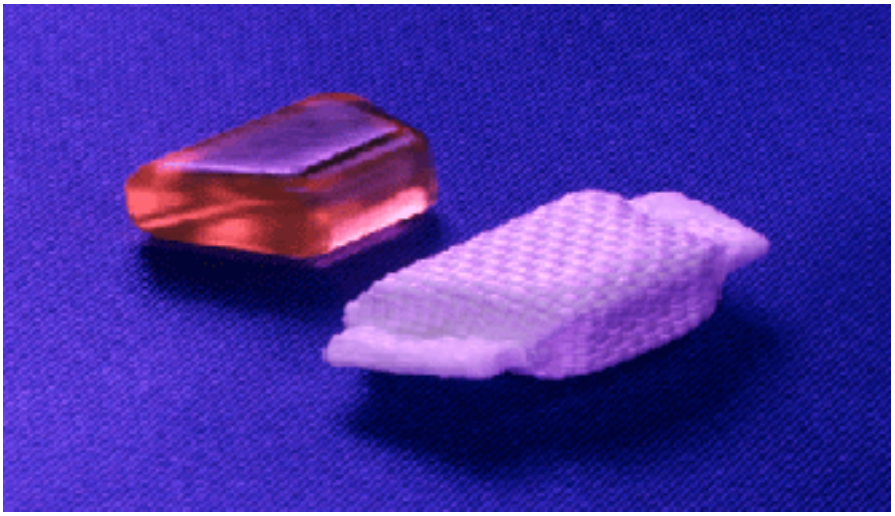

Figure 2.8 Prosthetic Disc Nucleus (PDN) [92]

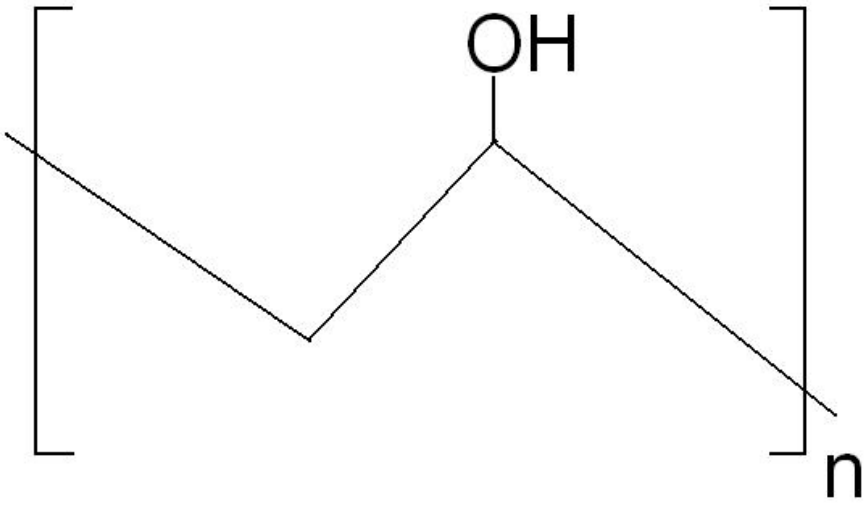

Figure 2.9 Poly(vinyl alcohol)

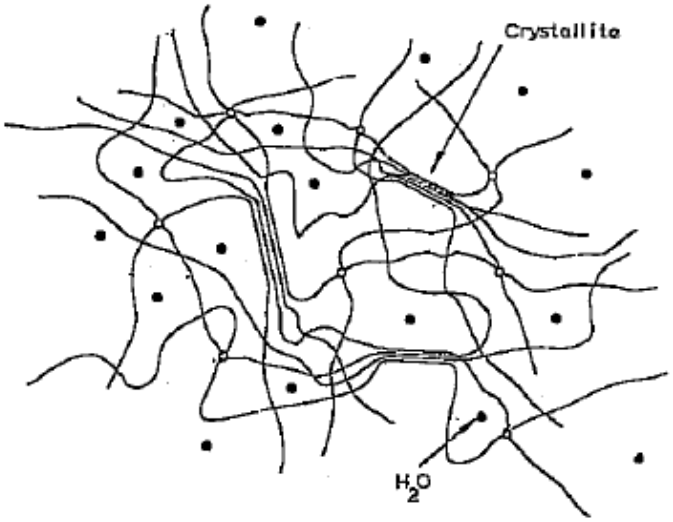

Figure 2.10 Physically crosslinked network via crystallites [57]

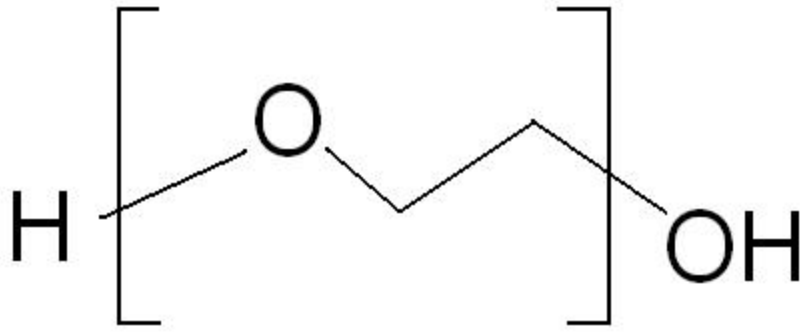

Figure 2.11 Poly(ethylene glycol)

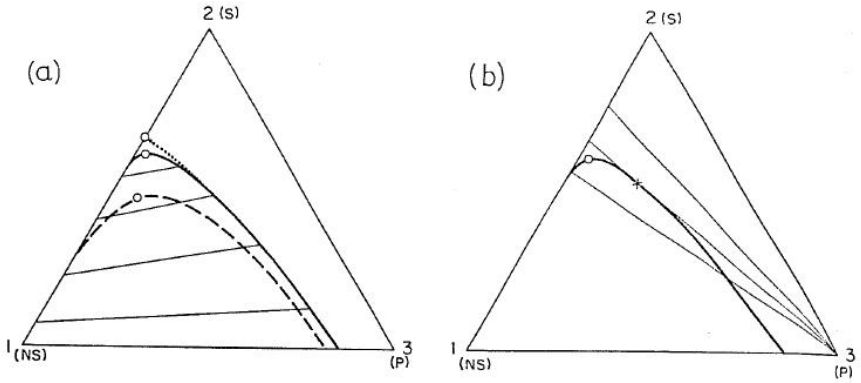

Figure 2.12 Above is shown ternary diagrams for solvent (S) / non-solvent (NS) / polymer (P) systems. Tie lines are represented as well [93, 94].

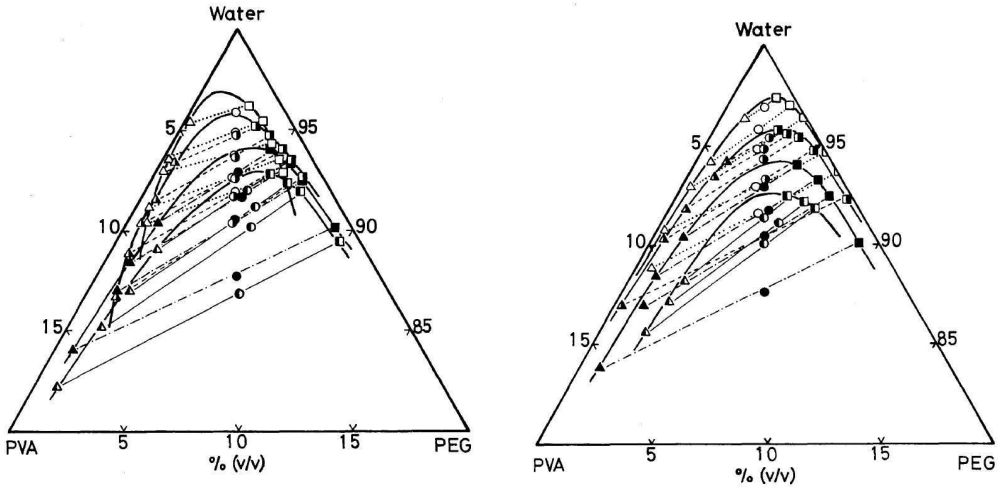

Figure 2.13 PVA/PEG ternary diagrams dilute formulations of a) PVA= 93kDa /PEG = 72-668kDa (at left) and b) PVA= 37-730kDa /PEG =20kDa [76]

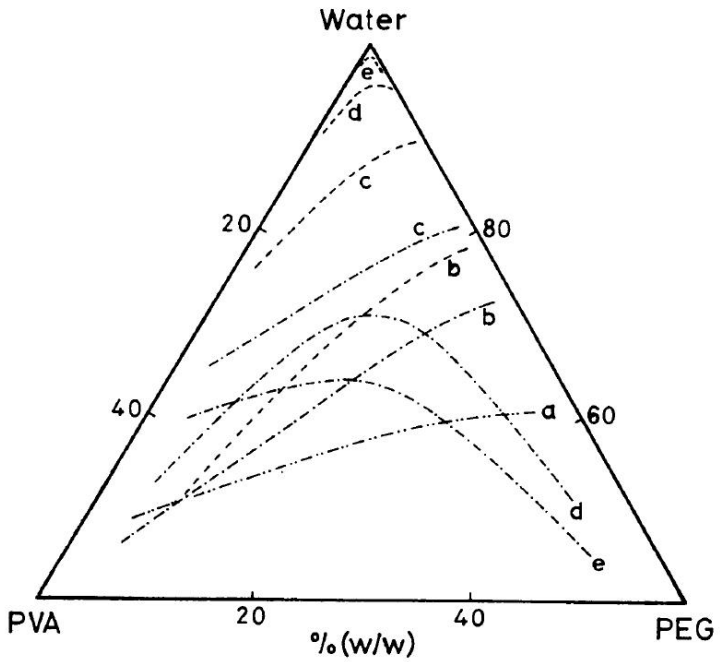

Figure 2.14 PVA/PEG ternary diagram for 38kDa PVA and varying PEG molecular weight (0.6-594 kDa). "a" shows no phase separation of low molecular weight PEG. "b-e" (depicted as ----) show increasing PEG molecular weight. Phase separation line moves upward with PEG molecular weight [4].

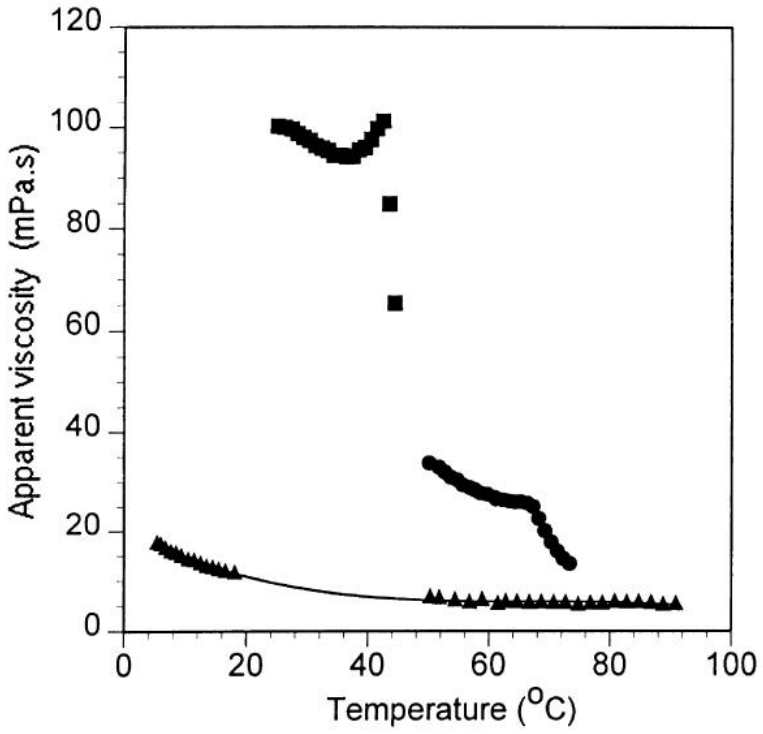

Figure 2.15 Viscosity vs. temperature transition at varying degrees of hydrolysis from Briscoe. ■ represents the lowest degree of hydrolysis, which show the greatest transition; ● represents the next lowest degree of hydrolysis (78%) and ▲represents the highest (83%) [6].

CHAPTER 3: RESEARCH GOALS

The primary goal of this research is to prepare and characterize an injectable in situ forming nucleus replacement with adequate gelation and stability characteristics. Gels are designed in order to support biomechanical loads of the spine, as well as to withstand the physiologic osmotic environment of the intervertebral disc. Systems are developed as blend hydrogels, lacking the presence of potentially toxic crosslinking agents. Poly(vinyl alcohol) will be blended with poly(ethylene imine), poly(vinyl pyrrolidone) and poly(ethylene glycol). An understanding of the resulting systems due to the combination of the incompatible PVA and PEG components will be obtained via phase diagram. An understanding of changes the gel might incur as a result of implantation of a given formulation must be known, such as the potential to imbibe water and lose stability. Improvements over neat PVA hydrogels in setting characteristics are necessary, and the resulting temperature-dependent gelation profile will be evaluated in order to describe short-term setting and gelation characteristics of the systems.

Specific Aim 1. Prepare and characterize an injectable in-situ solidifying PVA-based hydrogel system.

Specific Aim 2. Characterize PVA/PEG phase behavior

Specific Aim 3. Characterize swelling and stability of the PVA/PEG system

Specific Aim 4. Characterize gelation of the PVA/PEG system

CHAPTER 4: SELECTION OF A MATERIAL SYSTEM

4.1 Introduction

A range of systems was considered for combining polyvinyl alcohol with a material that will impart a quick forming nature. In the systems of interest, a supersaturated aqueous PVA solution was combined with a second component, either polyethyleneimine, polyethylene glycol, polyvinyl pyrrolidone, or polyvinyl alcohol of a lower molecular weight. Molecular weights as well as component B content were varied. Solutions of the materials were prepared at elevated temperatures and then allowed to cool to 37°C. The percentages of components are given in Table 4.1.

4.2 Experimental

PVA solutions were prepared by autoclaving a 28% w/w concentration aqueous solution in an autoclave at 121°C for 30 minutes. Each of the four components described in Table 4.1 were then mixed into solution. Control samples of 28% PVA (Mowiol 28-99) without addition of a Component B material were similarly prepared, for comparison. The resulting gels were immediately loaded into Viceroy screw syringes (manufactured by Merit Medical Inc.) and injected into cylindrical molds via a trocar and allowed to cool to 37°C overnight. Gels on the following day were removed from molds and observations of their physical and mechanical properties were recorded.

4.3 Results/Discussion

Qualitative observations were obtained for samples of blends (PVA/PVA, PVA/PVP, PVA/PEI, PVA/PEG) as listed in the experimental section. Samples are compared below by being grouped by concentration of component B.

In none of the samples from the set containing 5% of component B (PVA, PVP or PEI, with the exception of the PEG) was there a noticeable improvement in stiffness over the control. Each sample bowed under its own weight when removed from the mold and could be shaped or deformed easily with handling. Samples containing 5% PEG were malleable and deformed easily. Modulus may have increased over the control but was not measured.

For samples containing 10% of PVA, as component B, none showed a dramatic improvement. Slight improvement was observed with incorporation of 10% 9-10kDa PVA with low degree of hydrolysis as component B. These preliminary results were later attributed to crystallization effects for lower molecular weight PVA, as described in the swelling and stability section of this thesis. 10% PVP samples exhibited a slight noticeable increase in stiffness with molecular weight. 10% PEI samples were of moderate stiffness. PEG samples exhibited an increase in stiffness over other samples. PEG samples also seemed to increase slightly in stiffness with molecular weight. PEG samples appeared homogeneous For 10% of the highest molecular weight PEG as component B, samples recovered well when compressed manually to ~50% of their original height.

For the sample set with 20% 9-10kDa low degree of hydrolysis PVA as component B, gels had a relatively high modulus. This was not observed for 13-23k (sample was soft). 31-50 had solidified a bit, but not as much as the 9-10 sample. Results for low molecular weight material were later attributed to the same reason described previously for 10% 9-10kDa PVA samples

The remaining samples with 20% of component B were observed to have the following properties. PVP samples showed an increased viscosity and were difficult to mold. PEI samples at this concentration retained their shape. Modulus was slightly higher. PEG samples formed a rigid, high modulus gel with an expelled supernatant remaining in the mold. The presence of supernatant accounted for the strange shape of the sample.

Generalized observations for the sample set were as follows. In general, modulus was observed to increase with molecular weight for each component B polymer type. Low molecular weight PVA was an exception. The effects of low molecular weight PVA are better described in the swelling section of this thesis, as the physical properties of the gels are observed to change with incorporation of this component. Modulus increased with component B percentage for each polymer type, which was to be expected since polymer concentration was increasing and water content was decreasing. PVP samples exhibited an increased modulus and injection viscosity at higher concentrations. Further, at any given concentration of component B, PEG

samples showed the greatest stiffness. For this reason, the most attention was paid to the PVA/PEG formulations. Samples containing PEG were viewed to be the best candidates to meet the requirements that the material be biocompatible, injectable and capable of quickly gelling to an elastic solid.

Results varied for each of the systems evaluated. Polyethyleneimine at higher concentrations produced samples that were physically difficult to tear apart, modulus increased for 9-10kDa PVA with lower degree of hydrolysis. Not a large enough effect was observed for low molecular weight PVA.

Compressive modulus data was obtained for PVP 40kDa samples. Results indicated that modulus had increased significantly for test samples when compared to a control sample consisting of only 28% PVA 28-99 (see Figure 4.1). Samples retained a tacky character, however. Injection viscosity became too great for samples containing 360kDa to be considered.

Observations of samples prepared in this initial study showed that samples containing PEG in lesser amounts (5-10% of total mass) produced a swollen hydrogel of noticeably higher modulus. Adding a progressively larger amount of PEG (20% of total mass) to the PVA solution yielded samples that were considerably more rigid. A relatively large percentage of fluid also was observed to have expelled from gel (See Figure 4.2). It was determined that a gel with the appropriate elastic response

would likely be between the values of 10 & 20%. As a next step, 15% samples were prepared to evaluate their properties.

In the process of preparing 15% samples, expelled supernatant was decanted and removed, thereby increasing the polymer content of the samples. Solids needed to be autoclaved in order to restore a flowable state.

Compressive mechanical testing was also performed for PVA/PEG test cylinders made in similar molds. Modulus at 15% strain was determined to be greater at shorter times for test samples, in comparison to formulations without PEG. Preliminary data yielded a mean compressive modulus of 74.8kPa at 30 minutes, which is above the data for PVP previously shown in Figure 4.1 (max. of 54kPa) which was taken at 18 hours. PEG was chosen for its quick setting response as a result of these tests.

A portion of a PVA/PEG 15% sample had been freeze-dried and was analyzed using FTIR in Attenuated Total Reflectance mode. The spectrogram obtained for the material indicated that PVA and PEG were present, however any understanding of network formation could not be obtained from the data. It was suspected that interactions of the complex solution were creating a physical network, since heating solutions to high temperature would restore flow to solid material, suggesting a melting out of physical associations.

The results of physical crosslinking will be explored, as part of this thesis, using differential scanning calorimetry, in order to search for evidence of crystalline physical crosslinking, as a result of the "melting out" that has been observed to result as the gels transition to a lower viscosity flowable state, as temperatures are elevated. The presence of crystalline physical crosslinking would be expected to be observable as an endotherm produced by melting crystallites, as has been observed for freeze-thawed PVA gels. Due to the resulting formation of freeze-thawed networks due to selective crystallization via phase separation as described previously (Section 2.5 PVA Hydrogels [95]), it is understandable that the incorporation of another material (i.e. PEG) may result in the formation of dense PVA domains which are capable of crystallization. The formation of crystallites is doubtful however, as the complex process occurring during freeze-thawing is not transferrable to the simple phase separation of the PVA/PEG system.

4.4 Formulation Naming Method and Component Descriptions

Due to the large number of possible formulations that will be explored, for the purposes of this thesis percentage of components will be named using the following format:

FA-B/C

F indicating that it is a formulation. **A** refers to a chronological numbering system describing percentages of each component, the percentages of each is described in Table 4.2. The system being explored will primarily consist of the PVA/PEG/H_2O gel, The terms **B** and **C** refer to the molecular weights (in kiloDaltons) of PVA and

PEG, respectively. For example F1-145/10, would have the percentages in Table 4.2 with 145kDa PVA and 10kDa PEG. 99:1 polyvinyl pyrrolidone is added as a stabilizing agent[96]. Barium sulfate is added to produce a gel that is visible under fluoroscopy, for the purposes of visualization upon implantation. The percentage of barium sulfate will be set at 7% w/w where possible, since it is believed to be the lower limit of visualization for the implant. Varying levels of phase separation and dehydration will produce gels with greater concentration of these dry components. The grade of PVP will be unchanged at 58kDa (Plasdone C-30, ISP Corp.), unless otherwise noted. The barium sulfate used for all studies is manufactured by J.T. Baker (USP Grade, Cat#:1040). All percentages used will be weight-per-weight (%w/w), unless otherwise noted. Note that water is added by weight in these formulations.

4.5 Sample Preparation, Storage, Handling and Delivery Methods

The steps for preparation are shown in Figure 4.3. It was observed, early on, that the hot PVA solutions mixed with PEG would maintain their flowability. Early gels stored in the 75°C water bath would remain flowable until use. Brief processing steps using the water bath maintained at 75°C were still employed for handling gel since higher temperatures were considered to be dangerous. Concentrated PVA solutions were created in an autoclave (121°C/30min). Once removed from the autoclave, solutions were allowed to cool slightly in the 75°C bath before use. Barium Sulfate and PEG was added and mixed into the hot solution while the bottle was in the heating bath. The bottle was allowed to cool to room temperature for three hours to

allow for supernatant to form. Supernatant was decanted, the solution was autoclaved again to make it flowable. After a final decant, the material was ready to be molded . The material was molded, while hot, into stainless steel cylinders, and the ends were fitted with rubber caps, forming flat-ended cylinders of 18mm diameter and 100mm length. These cylinders were stored in resealable plastic bags at room temperature, filled with ~3ml of DI water to prevent drying until use. In some cases, cylinders were sealed with ~3ml of water inside foil pouches. Cylinders were inserted into a delivery gun capable of heating the gel and extruding it through a luer fitting at its aperture. The luer fitting is capable of attaching to a cannula for delivery. The gun operates via a trigger ratcheting mechanism to deliver heated gel through the cannula to the intended implantation site.

Table 4.1 Component Options for Material Systems

	Component A (wt. %)	**Component B (wt. %)**		
Set 1	**PVA 28% Soln(145kDa)**	**PVA(9-10k)**	**PVA(13-23k)**	**PVA(31-50k)**
	80	20	20	20
	90	10	10	10
	95	5	5	5
Set 2	**PVA 28% Soln(145k)**	**PVP(~10kDa)**	**PVP(~40k)**	**PVP(~360k)**
	80	20	20	20
	90	10	10	10
	95	5	5	5
Set 3	**PVA 28% Soln(145k)**	**PEG(~1k)**	**PEG(~10k)**	**PEG(~35k)**
	80	20	20	20
	90	10	10	10
	95	5	5	5
Set 4	**PVA 28% Soln(145k)**	**PEI(~10k)**	**PEI(~60k)**	
	80	20	20	
	90	10	10	
	95	5	5	

Table 4.2 Formulations

Formln #	**F1**	**F2**	**F3**	**F4**	**F5**	**F6**
PVA	20.2%	9.1%	20.2%	22.4%	10.2%	20.2%
PVP	0.2%	0.1%	0.2%	0.2%	0.1%	0.2%
H2O	55.0%	55.0%	45.0%	38.8%	50.0%	50.0%
BaSO4	7.0%	7.0%	7.0%	7.8%	7.0%	7.0%
PEG	17.7%	27.5%	27.7%	30.7%	32.7%	22.7%
Notes:		+10% PEG	+10% PEG	+13% PEG	+15% PEG	+5% PEG
		-10% PVA	-10% H2O	+20% PVA	-10% PVA	-5% H2O
				-16% H2O	-5% H2O	

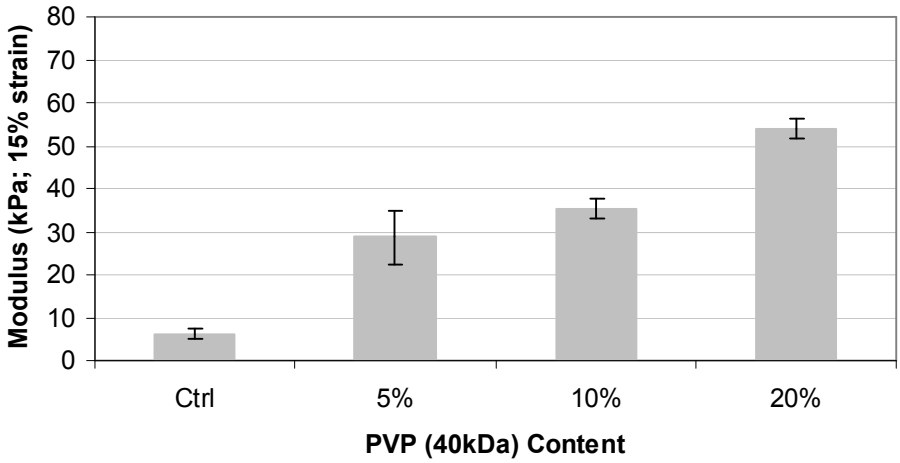

Figure 4.1 Modulus data for poly(vinyl pyrrolidinone) / polyvinylalcohol gels at varying PVP content

Figure 4.2 Resultant gel from a component B of 20% PEG was stiff and dehydrated.

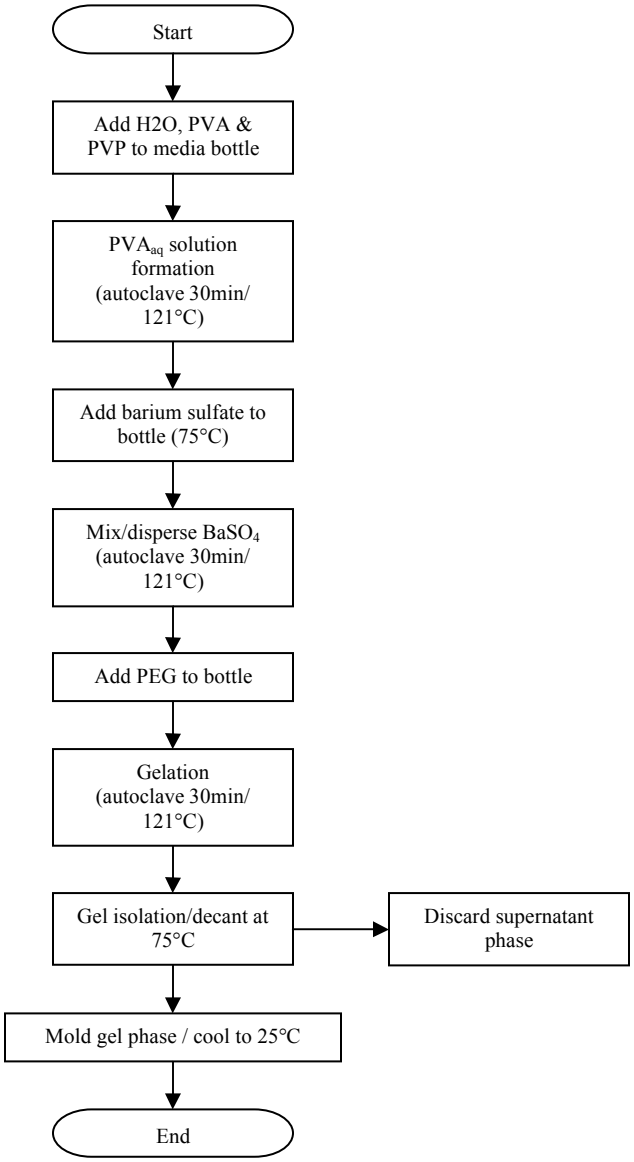

Figure 4.3 Sample preparation steps for PVA/PEG gels

CHAPTER 5: PHASE BEHAVIOR AND COMPOSITION

5.1 Introduction

A phase separation that occurs due to the incompatibility of these two polymers allows for products that could not be developed otherwise. Concentrated PVA solutions are capable of being further concentrated past the point that would be directly processable. For example, for certain concentrated formulations, without utilizing the phase separation technique via PEG addition to the PVA gel, there is not enough water in the formulation to solubilize the PVA granules. The gel that is formed has a high setting viscosity due to the concentration, as well as a willingness to flow at high temperatures that is attributed to the incorporation of the PEG plasticizer.

When an attempt is made to produce the same final formulation of gel that results from the phase separation technique there was not enough water available to bring the PVA granules into solution. The method chosen for homogeneously solubilizing PVA at these high concentrations is autoclaving at 121°C / 30 psi for 30 minutes while sealed in Pyrex media bottles. Even under these aggressive conditions, when test formulations were attempted to be prepared directly they resulted in PVA that was not solubilized to a great extent. In this case the production of the gel relies on the method used to produce the gel. At this particular formulation, the production of a homogenous gel is not possible without dehydration of a more dilute gel because of the solubility limit of the PVA that is being used. The gel that is produced is in a

supersaturated state as a result of the dehydration that occurs via the PEG addition stage. The phase separation is useful, in part, because it allows one to produce hydrogels of an increased concentration, as supernatant removes water from the gel (see Figure 5.1). Phase separation has further been shown to occur in PVA/PEG systems at greater than 0.6kDa PEG, for these reasons systems will be limited to higher molecular weight PEG [76]. The following sections describe the means necessary for the definition of the allowable compositional space, as dictated by this phase separation mechanism. A phase diagram is prepared for the range of concentrated formulations required for a load bearing hydrogel, such as that required for nucleus replacement. Methods for separating the similar PVA and PEG polymers comprising the resultant concentrated samples in order to produce this phase diagram are also developed.

5.2 Theory of the Phase Separation of Aqueous PVA/PEG

As described earlier in this thesis, incompatibilities are known between PVA and PEG. The incorporation of PEG into aqueous PVA solution results in a phase separation which produces a polymer-rich gel phase and a dilute water-rich supernatant phase [76]. PEG is well known as a plasticizer for polymers [85], in particular for PVA [5]. A reduction in hydrogen-bonding in vinyl alcohol units was observed by Lim through the use of PEG. This reduction in H-bonding was identified using FT-IR. Lim further found that molecular weight of PEG affected plasticization effect. In an earlier paper [5], Lim describes PEG affecting crystallite formation in

PVA films. The mechanism that is suggested is the introduction of defects into the PVA crystal lattice.

PVA/PEG phase diagrams prepared by Inamura use a stepwise addition of and mixing of PEG at elevated temperature (100°C), followed by a cooling to 25°C. The point of visible turbidity in the solution was determined to be the point where phase separation was occurring, in a method similar to cloud point determination [76]. Studies by Inamura are limited to more dilute polymer concentrations by the limitations of this method. Concentrations prepared as a result of this study need to be dilute enough to be easily stirred, as well as transparent enough to ascertain whether turbidity is occurring. Subsequently, formulations described by Inamura are limited to less than 30% total polymer for most molecular weights. Inamura goes higher in concentration only for considerably lower molecular weights. These results are not useful for the compositional determination of the phase limits for the preparation of a rigid construct for load bearing applications, however. The following studies describe an understanding of the limits of composition for this incompatible system, using ^{1}H-NMR methods for the separation of the PVA from the PEG component, in order to both understand the limit for formulation within the single phase region, as well as to understand the composition.

5.3 Initial Dehydration Studies

Initial studies for determining the extent of dehydration that occurred as a result of incorporation of PEG into PVA solution began with a fixed water content of 60%.

The remaining two components (PVA and PEG) were varied around this water content to check for the extent of dehydration and the gels that were subsequently produced. Early studies focused on dehydrating from an initial water content of 60%, since water contents greater than 60% seemed to produce gels weaker than was ideal for a nucleus replacement, from experience. Unless otherwise noted, PVA refers to Mowiol 28-99; M_w=145kDa, manufactured by Kuraray Specialties Europe and PEG refers to M_w=10kDa manufactured by Fluka, Inc. 145kDa PVA is used for the majority of the early studies due to the elastic character that the gels exhibit from the high molecular weight network.

5.3.1 Experimental

PVA solutions were prepared in 500ml media bottles by autoclaving (50 minute cycle; 30minutes @ 121°C). If solutions were non-homogeneous after autoclaving, samples were mixed again, using a spatula, and autoclaved again. Mixing had to be performed by hand since automated mixers could not handle the viscosity. At the point of complete solution formation, PEG was added and the mixture was allowed to cool to room temperature. A first decant was performed, and weight of supernatant was obtained. The mixture was autoclaved again, then equilibrated to 75°C, at which point more supernatant was poured off into the beaker with the material from the first pour. Gels were then cooled to room temperature for 16 hours, overnight. Gels were blotted and portions were cut using a razor blade. Mass loss on drying (16hours/105°C) was used to obtain water content (%w/w) for gel and supernatant.

Four formulations were prepared, with the intention of obtaining a full compositional analysis for each. With a fixed water content of 60%, PVA:PEG amounts for the four compositions was 25:15, 22.5:17.5, 20:20 and 10:30, where respectively, the amounts correspond to 25%PVA/15% PEG (formulation 1), 22.5%PVA/17.5%PEG (formulation 3), 20%PVA/20%PEG (formulation 2), and 10%PVA/30%PEG (formulation 4), so that one could obtain an understanding of the effects of either component on the dehydration process.

5.3.2 Results/Discussion

Data for phase separation is shown in Figure 5.2. For this case, a greater percentage of gel was seen with a smaller amount of PEG and a greater amount of PVA. Gels at the left end of the graph were noted to be of a lower modulus, while gels at the right were noticeably more rigid and appeared to have lower water contents. Mass loss on drying produced water contents for gels as in Table 5.1. The remaining percentage for each formulation is PVA+PEG in an undetermined ratio. Water content in gels can be seen to decrease with addition of greater amounts of PEG. Water content in the supernatant also is seen to decrease with addition of PEG. This is believed to be attributable to the fact that more supernatant is removed, as there is less PVA in the system to bind the water.

As previously described, PEG binds with two to three water molecules per repeat unit. When the increased solubility and affinity of PEG for water is considered [4,

76], the amount of water retained by the concentrated PVA-rich phase is considered to be that which is more closely bound to this phase, a large percentage of which is dictated by the interactions and binding of PVA and water. The relative binding potential of the PVA and water in the gel phase is described in the following sections, and is a function of the binding of both the PVA and PEG in the gel phase. Future work describing the interaction of both PVA and PEG with water would be necessary in order to develop a model for the prediction of composition merely due to the binding potential of the two types of hydrophilic polymers, without the subsequent experimental production of a phase diagram.

NMR was proposed as a method for separating PVA and PEG in the solids, and the development of the understanding and methods necessary for the separation by mass of the PVA and PEG polymer components in the dried gel is described in the next section.

5.4 Characterization of PVA/PEG Hydrogels via ^{1}H-NMR

Poly(vinyl alcohol) (PVA) and poly(ethylene glycol) (PEG) have similar chemical structures, enough to inhibit simple means for separation of the two polymers. For instance, once in solid form either can not easily be separated by solubility (since each is soluble in similar solvents), and the separation by melting point, would be very difficult. Though early studies by Inamura et al [76] use separation via precipitation of PVA in a non-solvent (methanol), in order to separate the two polymers, the resulting ternary phase diagram is limited to relatively dilute solutions,

when compared to the formulations necessary to prepare a dense hydrogel. A later study [4] describes the use of higher concentrations, but is limited to a lower molecular weight of PVA. Similarly, a visual test for turbidity is used to determine the point where the phase separation occurs. PVA solutions for the intended application must have a concentration sufficient in order to solidify in the gelled state into a material capable of supporting loads. Whereas chemical crosslinking by methods such as combination with aldehydes and physical crosslinking by freeze-thawing methods are capable of forming gels from more dilute solutions that will not deform under load, gel formation by the hydrogen bonded association of PVA gels occurs at relatively higher concentrations. Since the solutions prepared are very concentrated and behave as semisolids, it was useful to develop an analytical chemical method for the separation of PVA and PEG, in order to obtain a correct compositional analysis of the product, as well as to obtain the full understanding of the phase separation that occurs. Differences between the work of Inamura et al and the present work lie in both the concentrations evaluated (highly concentrated solutions were used in order to produce a modulus necessary for a load bearing biomaterial), as well as the establishment of a method of NMR analysis that allows for the relative quantification of each PVA or PEG polymer component after the gel phase has entered a state of rigid solidification.

Proton nuclear magnetic resonance (^{1}H-NMR), uses the alignment of protons within a magnetic field to probe the molecular structure of a sample [55]. By such techniques, the relative amount of two hydrogen containing functional groups may be discerned,

provided the correct understanding of the chemistry in relation to the spectra can be obtained. Since PVA and PEG need to be separated in order to understand the quantities of each in a given phase, it was necessary to be able to obtain the percentage of each in a sample. This would enable the analysis of trends between the initially mixed feed formulations and the resultant polymer gels and supernatants. In short, a means for complete compositional analysis is necessary for determining the amount of PEG that becomes incorporated within the PVA gel, and the subsequent production of a phase diagram.

5.4.1 Experimental

A number of formulations are prepared for the initial mixture, or "feed". Samples were prepared as follows: PVA solutions were prepared by combining PVA (Mowiol 28-99 from Kuraray, Inc.; M_w=145kDa) and water in a 100ml media bottle and placing in an autoclave for a total cycle of 50 minutes, with 30 minutes at 121°C. After the cycle, solutions were mixed by hand, using a spatula. Solutions were then re-autoclaved if they did not appear homogeneous. After complete formation of solution, bottles were transferred to a temperature bath at 75°C where PEG (in flake form, from Sigma-Aldrich; M_w=10kDa) was added. PEG was stirred in over two minutes using a spatula. After PEG was added, the mixture was allowed to cool to room temperature. A first decant was performed, and weight of supernatant was obtained. The mixture was autoclaved again, then equilibrated to 75°C, at which point more supernatant was poured off into the beaker with the material from the first pour. Gel was allowed to cool to room temperature. Gels were blotted using a

Kimwipe at the time of being harvested, in order to remove supernatant, which would alter PVA/PEG ratio of the analyte. Portions were cut using a razor blade. Mass loss on drying (overnight @ 16hours/105°C) was used to obtain water content (%w/w) for gel and supernatant. A portion of the dried samples was then dissolved in deuterated DMSO (DMSO-d6) at a target concentration of 3mg/ml and analyzed via ^{1}H-NMR.

5.4.2 Results/Discussion

Chemistry of the ^{1}H-NMR analysis was determined by selecting hydrogen-containing functional groups from molecules [97] similar to the ones being analyzed. Peaks representative of hydrogens on both PVA and PEG were obtained. Performing a few preliminary ^{1}H-NMR runs for both PVA (Figure 5.3) and PEG (Figure 5.4) allowed for identification of possible peaks that are characteristic of each polymer. The peaks that were observed to vary with composition of samples were compared with the peak positions from the literature (Figure 5.5).

Hydrogens which are adjacent to a hydroxyl along the carbon chain match the molecule shown in the NMR Band Handbook reference [97] in Figure 5.6. The bracket over the molecule depicted indicates the hydrogens which are identified as “a complex series of lines at 1.33ppm over a medium ppm range.” This matches the positions of the paired hydrogens along the PVA backbone. Since the PVA that is chosen has a molecular weight of 145kDa, the number of these hydrogens per molecule is determined as follows:

A molecular weight (M_w) of 145,000 g/mol with a repeat unit (M_0) of 44g/mol has an average degree of polymerization of: $X_w = M_w / M_0 = 3291.6$ [98]. This means that neglecting the effects of branching and endgroups, there are:

3291.6 repeat units * 2 = 6583.2 of the hydrogens specified above.

Similarly, for PEG 10kDa, NMR spectra were obtained and peaks corresponding to selected hydrogens were identified by comparison with molecules in the same NMR Band Handbook [97]. Figure 5.4 shows a representative spectrum with the peak indicated. The positions of the hydrogens on a similar molecule are indicated in brackets in Figure 5.7.

These hydrogens are described as forming "a doublet at ~3.68ppm", which is seen as a singlet in Figure 5.4, as splitting does not occur due to the similar environments of the two pairs on the PEG. This is missing from the above chemistry due to the presence of the hydroxyl.

Since PEG has a molecular weight of 10,000 Daltons and a repeat unit of also 44g/mol, the degree of polymerization is 10,000 g/mol / 44 g/mol = 227.2727. This number is multiplied by four, since there are four in similar environments. Using "molecules / gram","number of hydrogens / gram" is obtained for each. Ratio of PVA/PEG hydrogens is then obtained.

When samples were prepared containing both PVA and PEG, both peaks were visible simultaneously. The peak identified as PVA as well as the peak identified as PEG were seen to grow or shrink based on relative amounts in the material tested (See Figure 5.5). This enabled calculations for the quantities of PVA or PEG in the final material.

5.4.3 Comparison of Actual Against Theoretical

In order to check the validity of the preceding interpretation of the NMR spectra, samples of known PVA and PEG amounts were analyzed and the outputted ratios of PEG and PVA peak areas were compared against the theoretical, calculated based on the concentration of functional groups present on a per weight basis. Sample preparation was as follows: Three check runs were performed where known amounts of PEG and PVA were weighed into scintillation vials. Material was added to an approximate 6mg of total mass. The relative masses of PEG and PVA that made up the 6mg were made to vary across three values for PEG/PVA as in Table 5.3. Into each vial was added 2000µl (2ml) of DMSO-d6 via micropipette for a target concentration of 3mg/ml. Material was dissolved by sealing the vials and heating to 95°C in a laboratory oven for 15 minute intervals at which point the vials were removed and material was stirred. This was repeated until the material appeared to be fully dissolved. Samples were then transferred to NMR tubes manufactured by Sigma-Aldrich and tested using a 300MHz NMR.

Figure 5.9 also shows the results of ^{1}H-NMR data for three separate, but identical batches. ^{1}H-NMR data was shown to produce similar peak area ratios for each batch. The corresponding PEG/PVA ratio was determined through correlation with the proposed chemistry. Though the points fall outside of the range of the theoretical and check runs, the basis for relating the peak areas to the PEG to PVA ratio is based on the same understanding of the chemistry, and can be inferred. The curve can only be taken as proof of the understanding of the chemistry, and the fact that the PEG/PVA ratios correspond with the peak height ratios in a linear manner is only a result of the calculation method. In other words, the positions of the three points on the curve corresponding to the samples are based on the chemistry and not simply an extrapolation of the graph. Positions of check runs were chosen based on accuracy for weighing of each sample. Upon analysis, the chemistry resulting from the peak area ratio that was obtained for these samples matched closely, the theoretical prediction (Figure 5.8).

Finally, supernatant eluted from the system as a result of equilibration was similarly analyzed for presence of peaks attributable to PEG or PVA. Spectra for supernatant showed no signs of PVA, indicating that any PVA eluting from the gel at this composition would be below the NMR detectable limit. A representative ^{1}H-NMR spectrum for supernatant is seen in Figure 5.9, below. When the dried supernatant was analyzed via FT-IR, the spectrum closely matched PEG, with the exception of a peak at 1730cm^{-1}, that is possibly due to degradation from the drying process (Figure 5.10).

As a result of the compositional analysis of formulations via the methods described in the previous sections, final compositions were capable of being determined. NMR allowed for calculation of PEG/PVA ratio using the method described (Figure 5.11). Lastly, formulations were adjusted to account for PVA vs. PEG content to produce the following full compositions in Figure 5.12. Supernatant NMR was not performed in this case since it is a waste stream from the process.

5.4.4 Conclusions

A method for the separation of poly(vinyl alcohol) from poly(ethylene glycol) was established. ^{1}H-NMR spectra for both PEG and PVA were determined to have representative peaks with areas that could be evaluated to determine the relative mass of either component in a sample. Final composition was established for four feed compositions, enabling the production of a weight-per-weight ternary graphical representation of the 145kDa PVA and 10kDa PEG system to be contructed in the following section. Amount of supernatant was observed to increase with addition of PEG to the system, whereas the water content of gels was concurrently observed to decrease.

5.5 PVA/PEG Phase Characterization in a Range of Interest

Development of the NMR technique of the previous section allowed for compositional analysis of the dry polymer. Separation of PVA and PEG on a mass

basis was possible and set the groundwork for initial attempts at understanding phase behavior of the material system.

Five formulations were prepared, The F1 formulation was chosen to be close to the 20:20 formulation of the previous section. With an understanding that PEG would dehydrate the system, to a varying extent, the relative amounts of PVA and PEG were varied, keeping the water content in the initial ("feed") formulation constant. Keeping samples at a constant water content allowed for processing samples at a higher water content allowing for homogeneous composition, and allowing PEG to dehydrate to varying extents. Samples include PVP as a stabilizer in 99:1 ratio, as well as barium sulfate, as would be added to make the gels radiopaque for visualization under fluoroscopy upon implantation.

5.5.1 Experimental

Hydrogels were prepared with initial compositions according to Table 5.3. Mass loss on drying (%w/w) was performed over 16 hours at 105°C in order to obtain water content. A portion of dried samples was then dissolved in deuterated DMSO (DMSO-d_6) and analyzed via ^{1}H-NMR to yield PEG/PVA ratio for the sample (n=3). Once mass loss on ignition (%w/w) was completed for samples at 650°C for 2 hours, barium sulfate content could be determined. Knowing barium sulfate, and water content enabled total polymer mass to be calculated. PEG and PVA percentages were determined from total polymer mass and PEG/PVA ratio from NMR.

5.5.2 Results/Discussion

Final compositions of gels were obtained using the method described above and are reported in Table 5.4.

All formulations prepared as part of this study passed an injection test from the heated delivery gun using a 2.5mm ID cannula using the current method of internally heating the device to 95°C for 5 minutes. Formulations ranged in viscosity, however. Viscosity behavior in relation to temperature will be discussed in the chapter on gelation in this thesis. Trends observed between initial and final composition in the previous section were similarly observed. With an increase in PEG in the feed, there is a corresponding increase in the amount of supernatant. There is also a decrease in water in the final gel (see Table 5.4). The water content for the supernatant is seen to remain within the same range for the samples in question. For an increase in PEG in the feed formulation, water content in the final gel decreases, total solids content increases, PVA content remains within the 30-40% of the gel for all formulations, and $BaSO_4$ remains at 10-12% for most formulations.

The decrease in water content for samples with PEG addition is as to be expected with the increased affinity of PEG for water, however this trend is not observed across the last two samples in Table 5.4. It is believed that the water content for the +3% samples is artificially low, due to water loss possibly from autoclaving. Compositional analysis for the formulations of this section are evaluated and compared in the rheometry section of this thesis.

5.6 PVA/PEG Phase Diagram

One method for the representation of formulations in a ternary system is the placement of points on a triangular diagram, where each of the three corners corresponds to 100% of each of the three substances. In this section, a similar approach as in Tompa et al [93] will be taken for the representation of a phase separating system consisting of a polymer (PVA 145kDa), a solvent (water) and a non-solvent, which is being considered to be PEG 10kDa, for the purposes of this study.

5.6.1 Experimental

A number of formulations are prepared for the initial mixture, or "feed". PVA solutions were prepared by combining PVA (Mowiol 28-99; M_w=145kDa) and water in a 100ml media bottle and placing in an autoclave for a total cycle of 50 minutes, with 30 minutes at 121°C. After the cycle, solutions were mixed by hand, using a spatula. Solutions were then re-autoclaved if they did not appear homogeneous. After complete formation of solution, bottles were transferred to a temperature bath at 75°C where Polyethylene Glycol (M_w=10kDa) was added. PEG was stirred in over two minutes using a spatula. Samples were allowed to cool to room termpature. After three hours of equilibration, supernatant was poured off into a beaker on a tared balance to obtain the mass of the supernatant. Supernatant and gel were dried overnight for 16 hours at 105C, in order to obtain the water content of samples.

Samples of the same material were dried at room temperature over a longer period of time, for determining PEG/PVA content by NMR. Gels had to be blotted using a Kimwipe at the time of being harvested, in order to remove supernatant, which would alter PVA/PEG ratio of the analyte. Methods for preparation of samples for NMR were identical to in previous sections. A target concentration of 3mg/ml was used. Samples were dissolved in DMSO-d_6.

Each formulation prepared is shown in Table 5.6 and corresponds to a point on the diagram in Figure 5.13. These particular formulations were chosen based on the fact that there is a solubility limit for PVA in water. Sets 1 through 9 in Table 5.6 each have a fixed water content. It is important to note that due to the rules of phase separation that a gel composition for a point on the binodal could theoretically be reached by fixing the PVA/PEG ratio, and varying only water content, thus traveling in a straight line down the ternary diagram and tracing out the binodal with gels of compositions of varying water contents, while this is possible, from a theoretical standpoint, preparing PVA solutions of such a high concentration allows us to effectively dehydrate the system farther by choosing formulations with relatively more PEG over PVA. For example, preparing a homogeneous PVA gel over 50% in concentration is made easier if more PEG is added to dehydrate more and result in lower water content for the gel.

5.6.2 Results/Discussion

When the formulations described in Table 5.6 were prepared, gel formulations clearly defined a binodal at the right of the ternary diagram, as described in Figure 5.14.

Supernatant formulations were seen to form the binodal at the left axis. Samples up to 90% water proved to have no detectable amount of PVA, via ^{1}H-NMR, meaning the gel maintains the majority of its PVA throughout this dehydration process.

As a result of this diagram, the understanding of the phase behavior of dense gels which can not easily be separated via precipitation in non-solvent was established, and methods translating to the characterization of similar systems are enabled.

5.7 Flory Chi Interaction Parameter

Though preparation of a ternary phase diagram through use of %w/w is useful for an understanding from a formulations standpoint, the understanding of solution theory as developed by Flory & Huggins as it relates to phase behavior is best described when an understanding of volume fraction of each polymer can be assessed. Thus, in order to relate this understanding of the position of the binodal to the Flory-Huggins equation for ternary polymer systems, a conversion must be performed. Density for each of the three components as described in Inamura [76] is used to relate w/w to v/v. Weight percent is divided by density to yield volume percent. The densities given by Inamura are PVA: 1.27, H2O: 1.00 & PEG: 1.13. Using this method, a v/v ternary diagram is constructed in Figure 5.15. The position of the binodal can be seen to shift upward slightly with conversion to v/v. Considering the binodal is close to the solvent apex, a large value for χ can be expected. χ for the polymer-polymer interactions can further be expected to be positive for the most concentrated values, as

evidenced by phase separation in the dry state [76]. As the binodal moves toward the water apex, χ is expected to decrease. Increasing PEG molecular weight similarly results in a decrease in χ, as shown by the movement of binodals toward the water apex in Inamura [76]. The proximity of the binodal to the water apex is predicted by the relatively large PVA molecular weight, as predicted by Inamura.

Table 5.1 Water content of phases for selected formulations

Formulation	Water Content in Gel (%)		Water Content in Supernatant (%)	
	Average (n=3)	**Std. Dev.**	**Average (n=3)**	**Std. Dev.**
25:15	55.8%	2.5%	73.4%	1.0%
22.5:17.5	56.1%	4.5%	74.2%	2.6%
20:20	55.2%	2.0%	69.5%	0.4%
10:30	53.4%	2.6%	63.8%	0.2%

Table 5.2 Weighed amounts for check runs and corresponding peak areas

Weighed amounts for Check Runs (mg)			**Peak Area Ratio**	
PEG	**PVA**	**PEG/PVA**	**Theoretical**	**Actual**
2.3	4	0.58	1.15	1.32
3.8	2.8	1.36	2.71	2.90
4.2	1.9	2.21	4.42	4.26

Table 5.3 Initial composition (feed solution)

	Sample Type (% PEG in Feed)				
	-5% PEG	**-3% PEG**	**F1-145/10**	**+3% PEG**	**+5% PEG**
PEG (10kDa)	12.73%	14.73%	17.73%	20.73%	22.73%
PVA (Mowiol 28-99)	25.06%	23.06%	20.06%	17.06%	15.06%
PVP (Plasdone C-30)	0.20%	0.20%	0.20%	0.20%	0.20%
DI Water	55.00%	55.00%	55.00%	55.00%	55.00%
Barium Sulfate	7.00%	7.00%	7.00%	7.00%	7.00%

Table 5.4 Final gel composition

	Sample Type (% PEG in Feed)				
	-5% PEG	**-3% PEG**	**F1-145/10**	**+3% PEG**	**+5% PEG**
PEG	9.1%	8.5%	6.5%	7.7%	10.6%
PVA	31.8%	29.2%	33.5%	40.5%	33.8%
PVP	0.3%	0.3%	0.3%	0.4%	0.3%
DI Water	52.2%	51.9%	47.9%	40.7%	43.4%
Barium Sulfate	6.7%	10.1%	11.5%	10.7%	11.9%
% Solids	47.8%	48.1%	52.1%	59.3%	56.6%
% Polymer	41.1%	38.0%	40.6%	48.6%	44.7%

Table 5.5 Water content of varying formulations

	% Water (Gel)	% Water (Supern)	Supernatant (% of total)
- 5% PEG	52.20%	62.80%	18.0%
- 3% PEG	51.90%	59.40%	18.9%
F1-145/10	47.90%	62.20%	33.3%
+ 3% PEG	40.70%	62.10%	38.0%
+ 5% PEG	43.40%	63.70%	47.7%

Table 5.6 Formulation sets for ternary diagram. All values are in %w/w. 60% water sample data ("Set 6") was taken from a previous study.

Set 1	**Variables**				
	A	**B**	**C**	**D**	**E**
PEG (10kDa)	0.79	0.775	0.75	0.7	0.65
PVA (Mowiol 28-99)	0.01	0.025	0.05	0.1	0.15
DI Water	0.2	0.2	0.2	0.2	0.2
Set 2	**Variables**				
	A	**B**	**C**	**D**	**E**
PEG (10kDa)	0.74	0.725	0.7	0.65	0.6
PVA (Mowiol 28-99)	0.01	0.025	0.05	0.1	0.15
DI Water	0.25	0.25	0.25	0.25	0.25
Set 3	**Variables**				
	A	**B**	**C**	**D**	**E**
PEG (10kDa)	0.69	0.675	0.65	0.6	0.55
PVA (Mowiol 28-99)	0.01	0.025	0.05	0.1	0.15
DI Water	0.3	0.3	0.3	0.3	0.3
Set 4	**Variables**				
	A	**B**	**C**	**D**	**E**
PEG (10kDa)	0.59	0.575	0.55	0.5	0.45
PVA (Mowiol 28-99)	0.01	0.025	0.05	0.1	0.15
DI Water	0.4	0.4	0.4	0.4	0.4
Set 5	**Variables**				
	A	**B**	**C**	**D**	**E**
PEG (10kDa)	0.49	0.475	0.45	0.4	0.35
PVA (Mowiol 28-99)	0.01	0.025	0.05	0.1	0.15
DI Water	0.5	0.5	0.5	0.5	0.5
Set 7	**Variables**				
	A	**B**	**C**	**D**	**E**
PEG (10kDa)	0.29	0.275	0.25	0.2	0.15
PVA (Mowiol 28-99)	0.01	0.025	0.05	0.1	0.15
DI Water	0.7	0.7	0.7	0.7	0.7
Set 8	**Variables**				
	A	**B**	**C**	**D**	**E**
PEG (10kDa)	0.19	0.175	0.15	0.1	0.05
PVA (Mowiol 28-99)	0.01	0.025	0.05	0.1	0.15
DI Water	0.8	0.8	0.8	0.8	0.8
Set 9	**Variables**				
	A	**B**	**C**	**D**	**E**
PEG (10kDa)	0.09	0.075	0.05	0.03	0.01
PVA (Mowiol 28-99)	0.01	0.025	0.05	0.07	0.09
DI Water	0.9	0.9	0.9	0.9	0.9

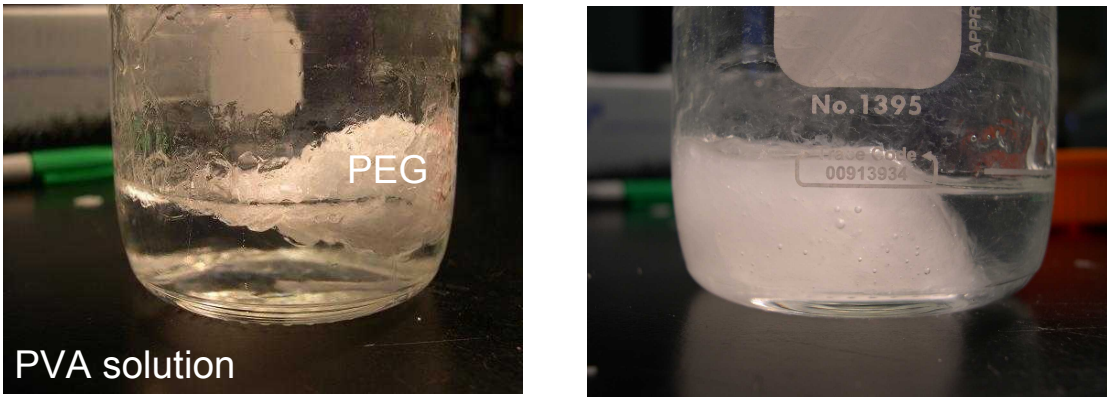

Figure 5.1 Formation of concentrated gel by phase separation

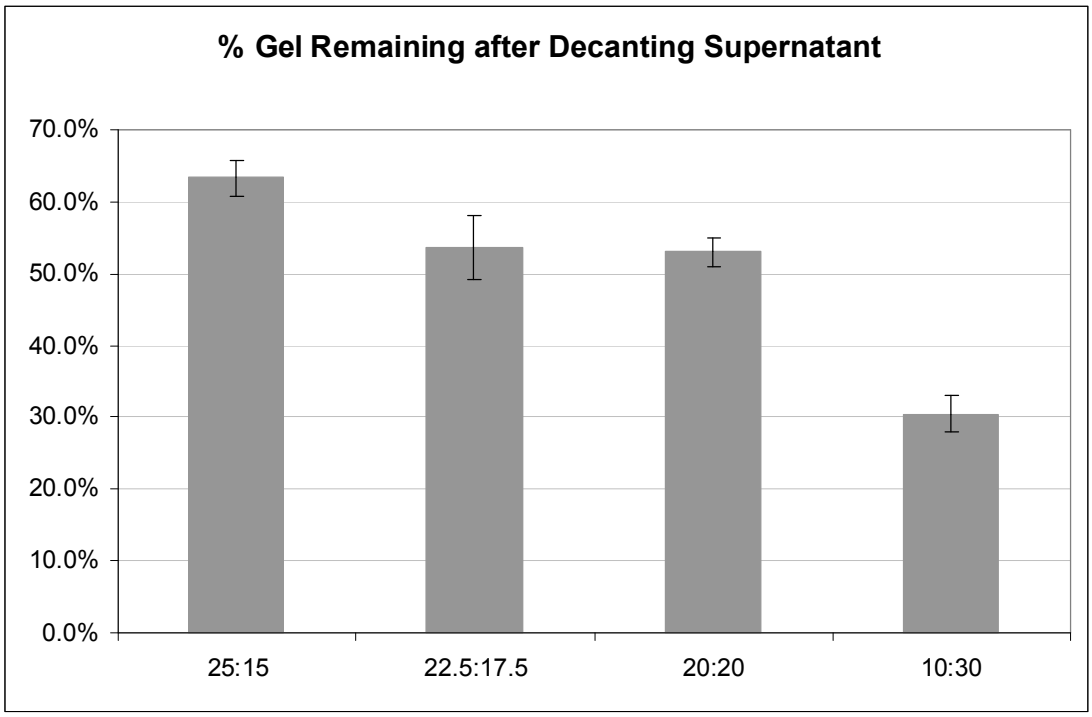

Figure 5.2 Shows the percentage of gel remaining, after supernatant is decanted from the equilibrated mixture.

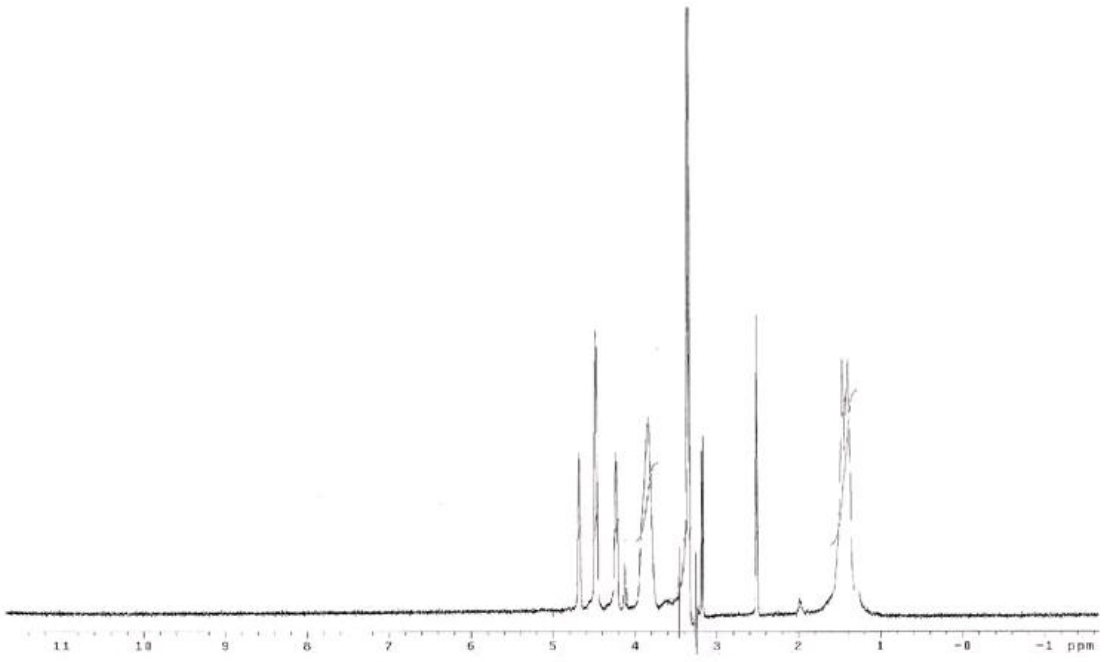

Figure 5.3 H-NMR spectra for poly(vinyl alcohol) [97].

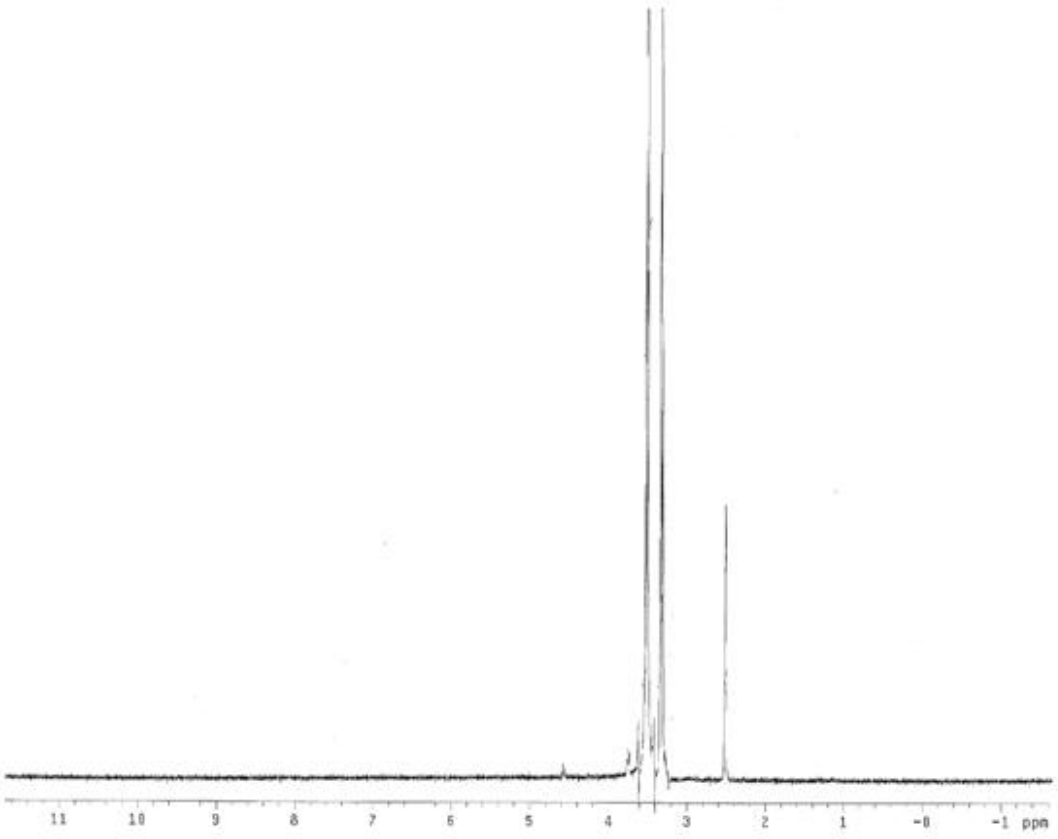

Figure 5.4 H-NMR spectra for poly(ethylene glycol).

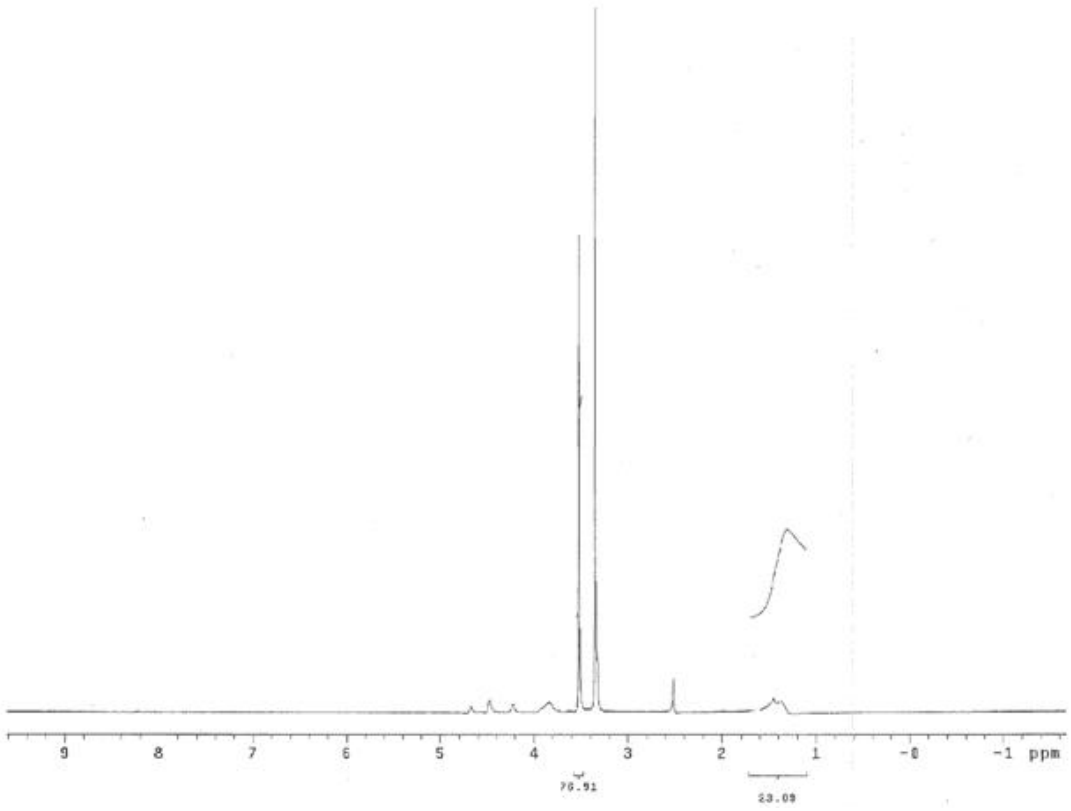

Figure 5.5 H-NMR spectra of PVA-PEG mixture showing peaks for both PVA and PEG

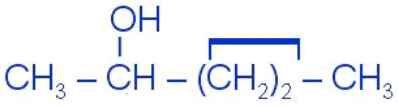

Figure 5.6 Reference for PVA from NMR Band Handbook [97]

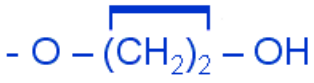

Figure 5.7 Reference for PEG from NMR Band Handbook [97]

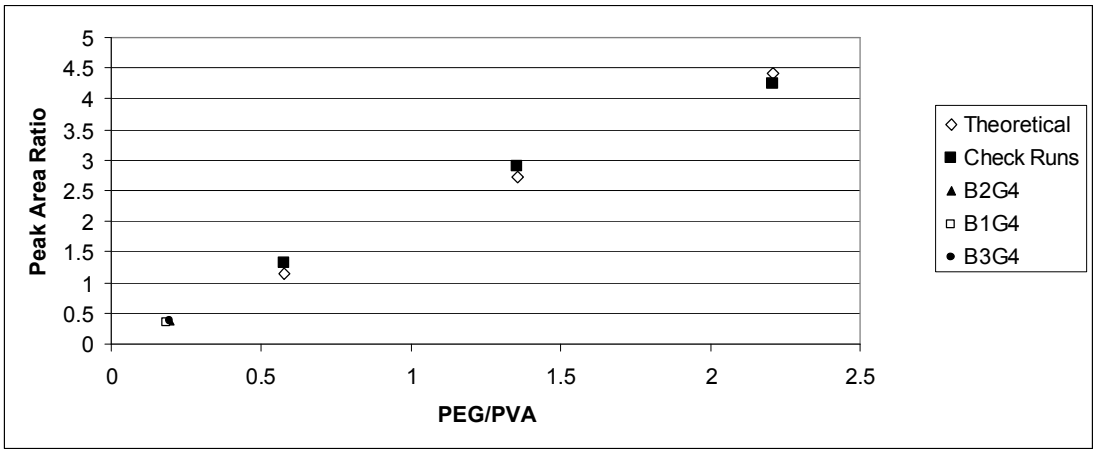

Figure 5.8 Comparison of check runs containing known amounts of PVA and PEG to the theoretical. Datapoints showing results for three identical independently prepared batches are shown to overlap at the left of the graph.

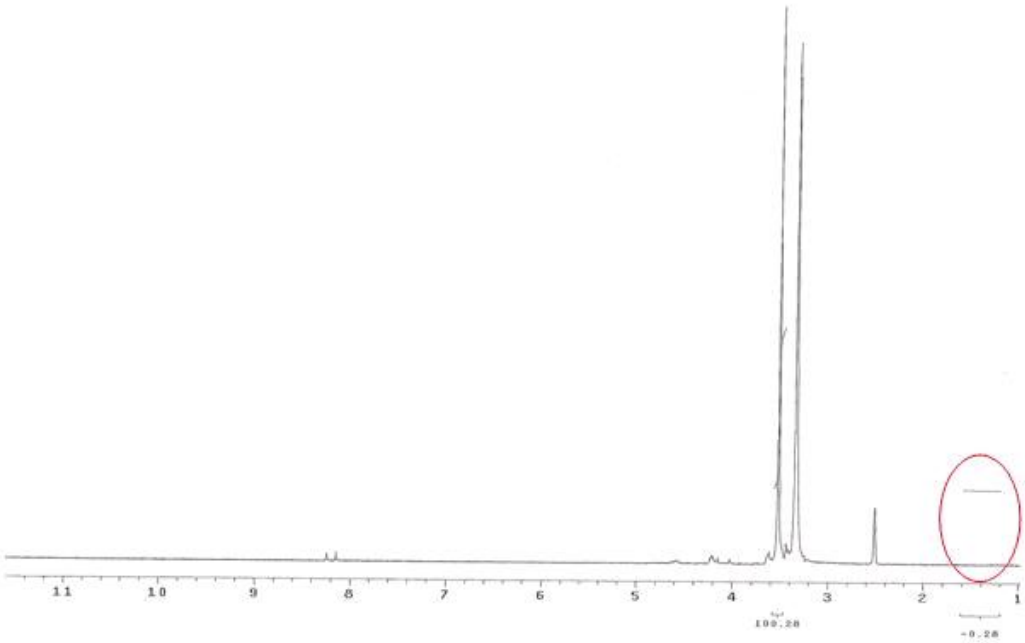

Figure 5.9 A representative H-NMR spectrum for supernatant eluting as a result of the equilibration process.

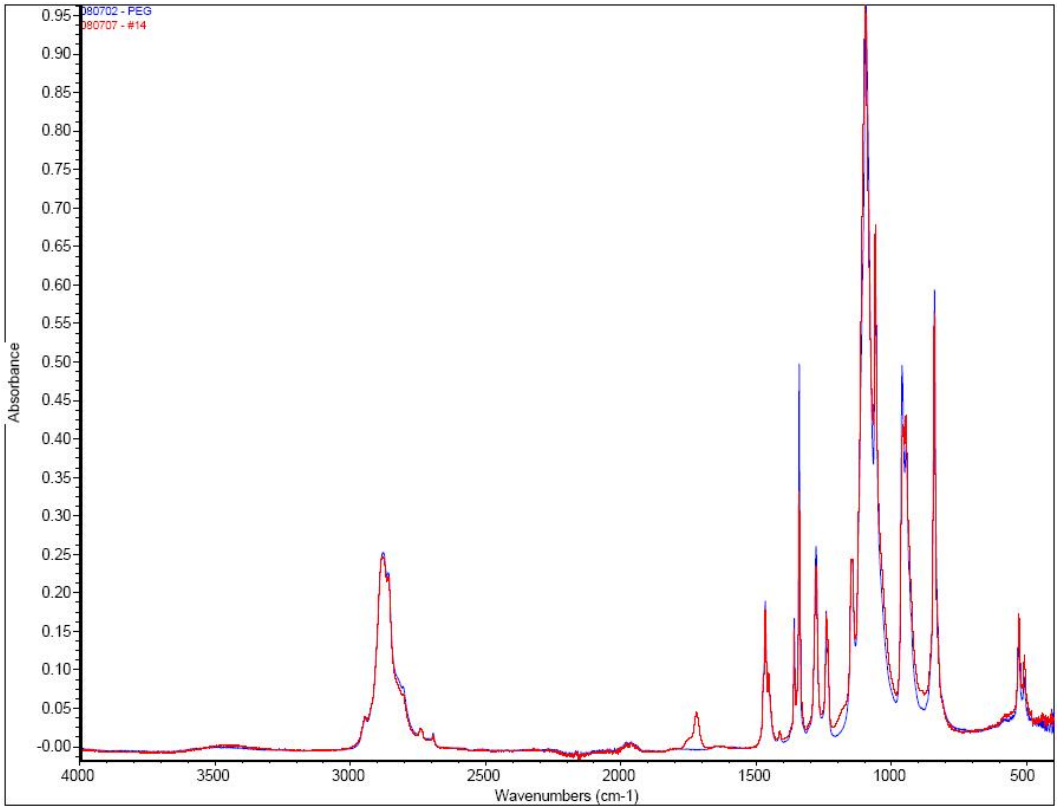

Figure 5.10 FTIR spectrum of PEG and dried supernatant. Supernatant shows an extra peak at 1730 cm^{-1} that is possibly due to degradation.

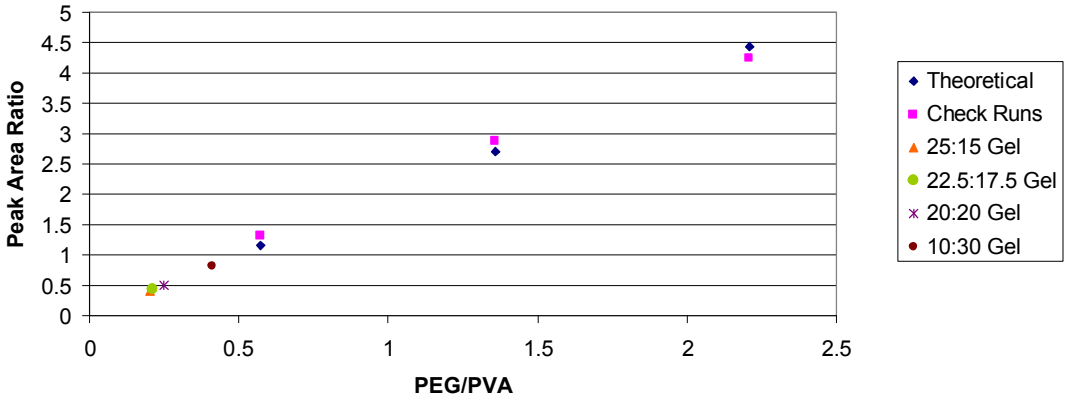

Figure 5.11 Peak area ratios of the four formulations as determined by NMR.

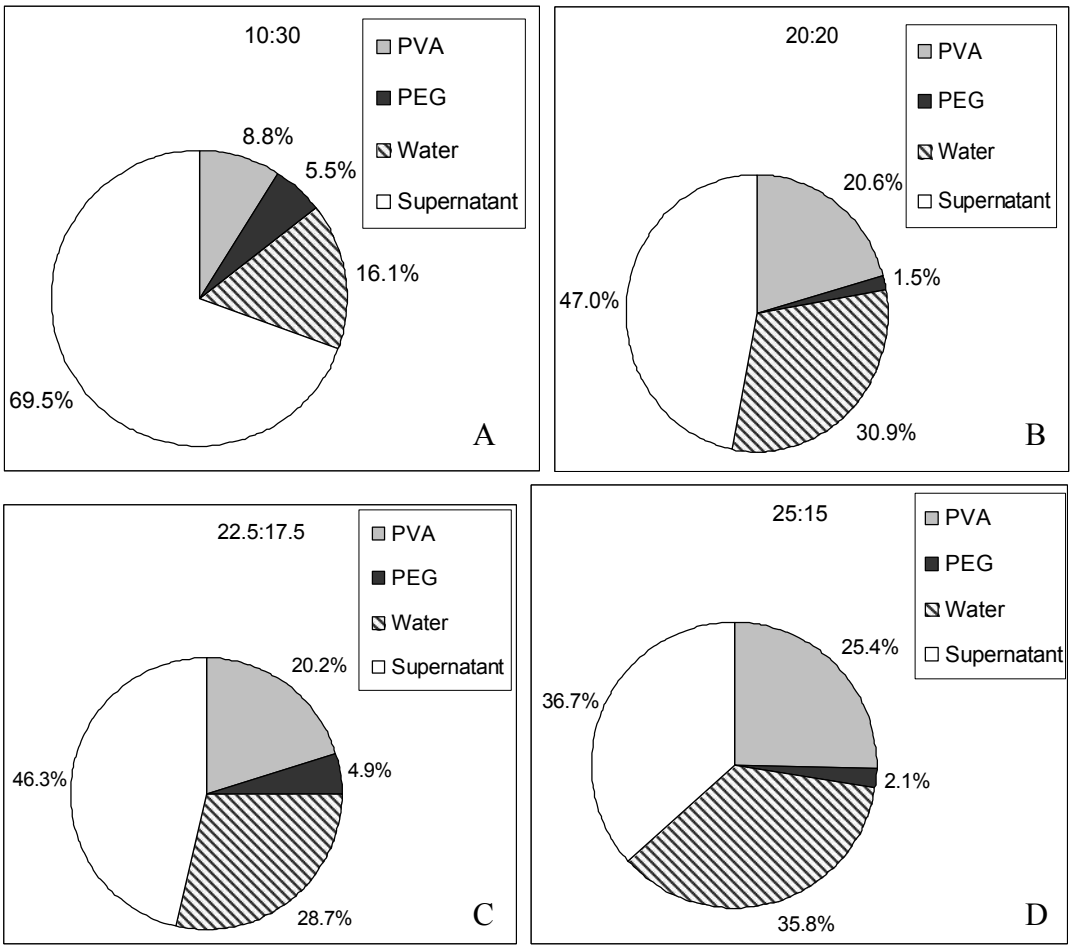

Figure 5.12 A – D show final composition for each of the four feed formulations described in section 4.5.1.

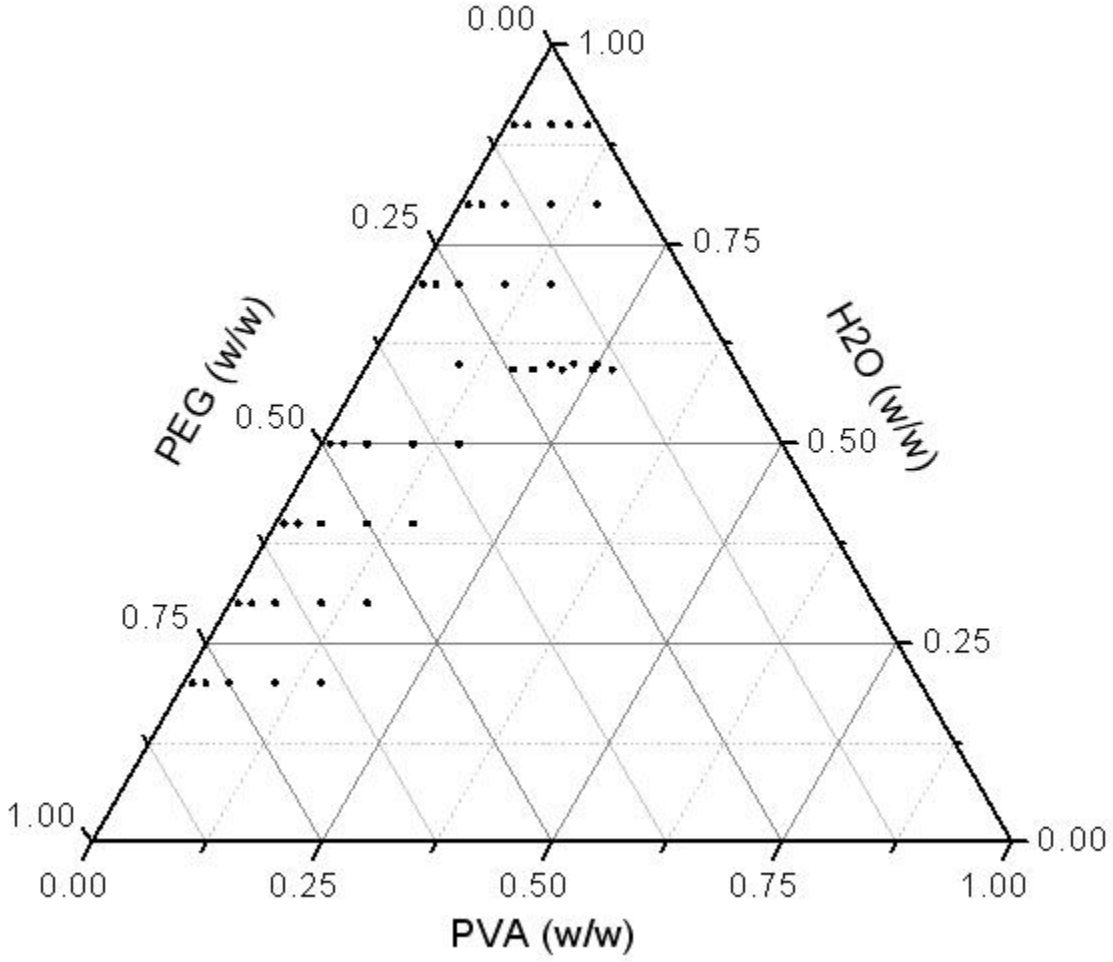

Figure 5.13 Formulations for determination of ternary diagram

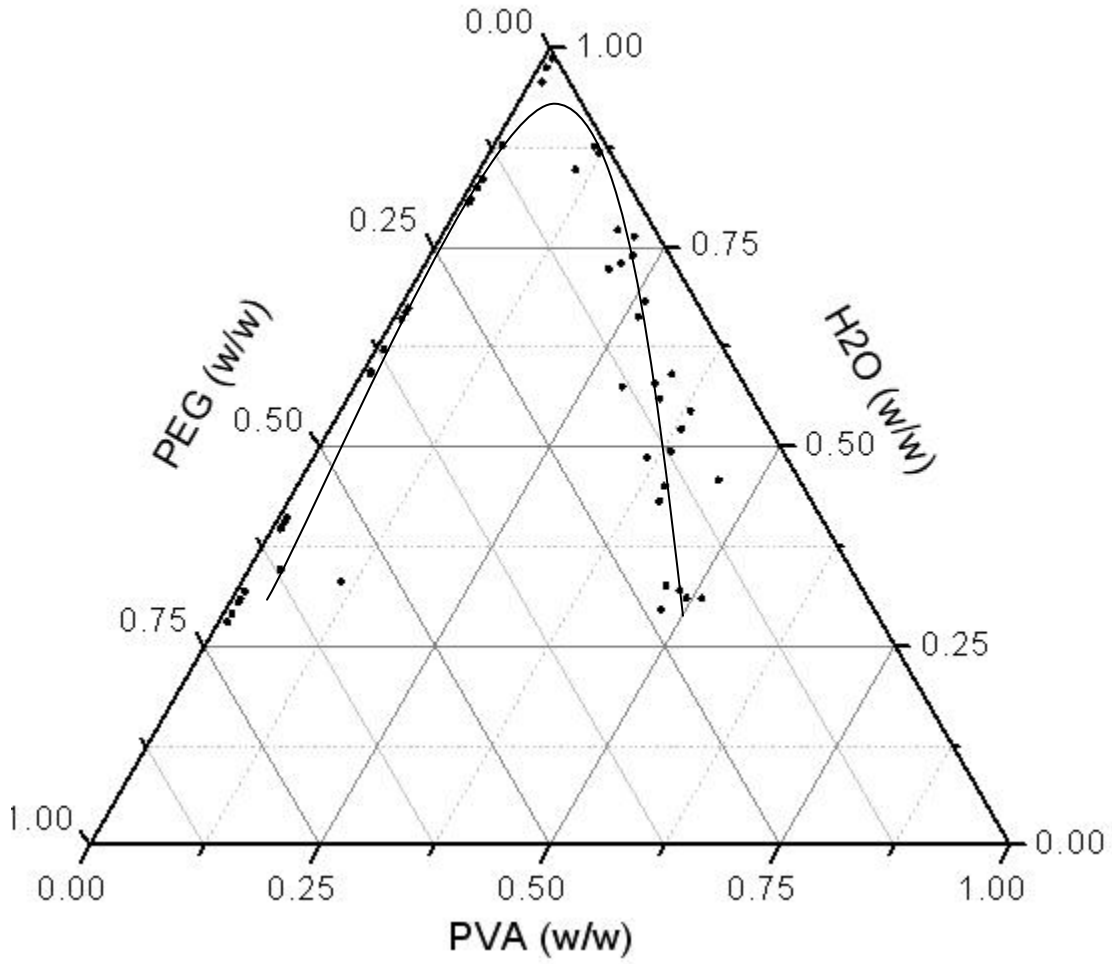

Figure 5.14 Ternary phase diagram for PVA 145kDa / PEG 10kDa / water system

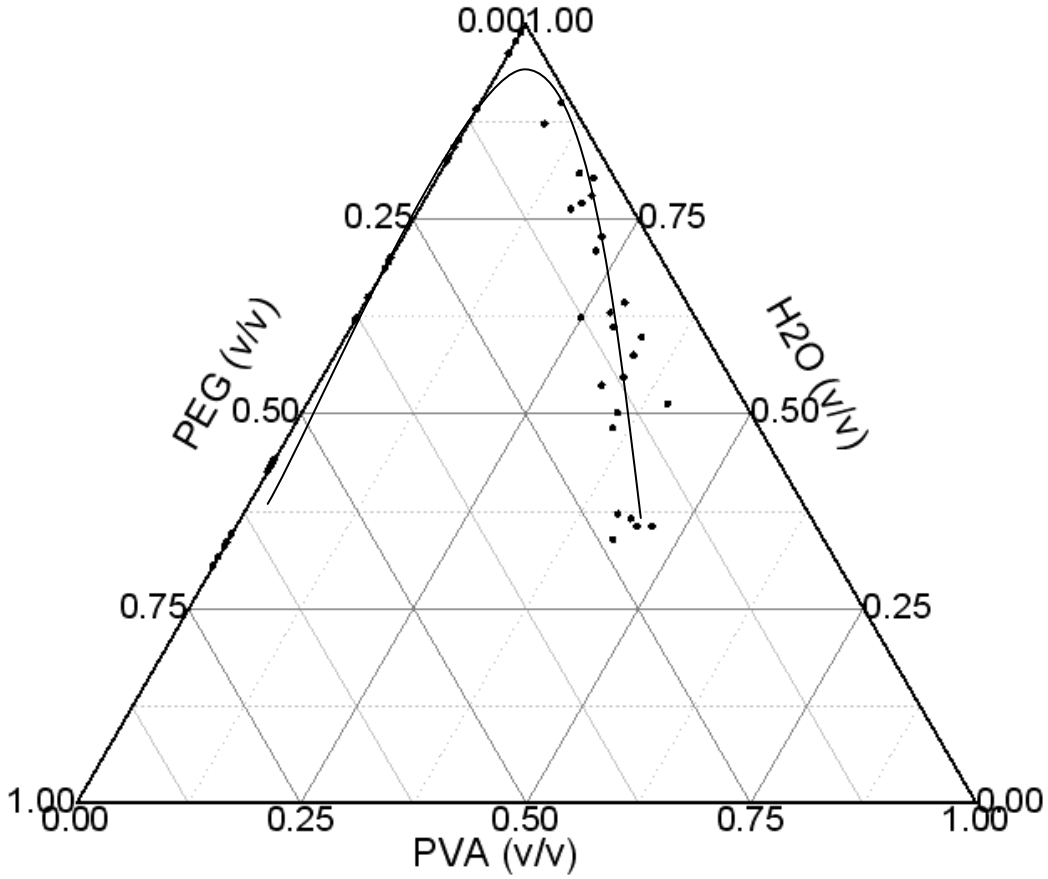

Figure 5.15 Ternary diagram adjusted for v/v

CHAPTER 6: SWELLING AND STABILITY OF PVA/PEG HYDROGELS

6.1 Introduction

To date, very little consideration has been given to the behavior of PVA/PEG gels with regards to swelling under varying osmotic conditions, such as the nucleus pulposus cavity. An understanding of the swelling behavior of the wide range of possible PVA/PEG formulations has yet to be obtained. For future development of a space-filling hydrogel implant, it is necessary to understand its interaction with the environment, in particular its volume change characteristics.

Whether swelling is preferable in a nucleus replacement device is dependent on applicaton and is a matter of debate. Moderate, controlled swelling may be acceptable depending on a number of conditions. Understanding of swelling equilibrium of any implanted gel is critical to careful design as a prosthetic tissue, in order to control the pressure on nearby structures, as well as the potential migration beyond the site of implantation. In order to ensure physical confinement of the implant, the method of delivery to the site (i.e. the size of the hole, or surgical defect), as well as the condition of the annulus, and presence of any fissures will determine whether the swelling material poses any risk to expulsion. Elasticity of swelling material will further affect the ability to resist migration, as elastic forces resist extrusion of the device through fissures or defects. Subsidence, or protrusion through the vertebral endplate, is also possible particularly for higher modulus implants, if swelling pressure is great enough.

Though phase separation for a given range of PVA/PEG formulations has been described previously [4, 76], the response of the gel portion of these formulations to an osmotic concentration has not yet been established in the literature. The response of the gel upon implantation in a physiologic osmotic environment has not yet been reported. Further, there is no understanding as to how the osmotic equilibrium condition will change as the gel is separated from the supernatant and subjected to an osmotic potential. This section addresses swelling as generated from immersion of the PVA/PEG gel phase in an osmotic medium. Based on a physiologic osmotic potential of 0.1-0.3MPa for nucleus pulposus tissue in the intervertebral disc, aqueous PEG solutions were prepared that simulate a 0.2MPa osmotic gradient [17, 18], and gels were subsequently immersed until equilibration, typically for 7 days, and change in volume was measured.

It has been well known that PVA/PEG formulations containing a PEG molecular weight below 0.6kDa do not produce supernatant. It is also known that the phase separation is dependent on the PEG molecular weight [4]. It is shown in this section that changing the PVA molecular weight has the ability to affect swelling behavior. It is also shown that PEG molecular weight affects the swelling behavior. The challenge presented in this section is finding a gel system that not only behaves correctly as an in situ forming hydrogel with the correct physical and mechanical properties, but a system where the gel phase is sufficiently at equilibrium with the osmotic pressure of the disc so as to not imbibe water upon implantation and

effectively dissolve or change density in the disc space, or to swell to create problems in the surrounding pain generating areas.

6.2 Current Material System

The first material system explored for swelling involves the formulation initially chosen for all early studies, where PVA M_w is 145kDa, and PEG M_w is 10kDa. PVA molecular weight was chosen to be high for elasticity and network formation. Previous experience with cryogels has shown us that gels produced using low molecular weights of PVA are prone to fracture, and lack the resilient nature of the tangled molecular network. Lower PEG molecular weights produced softer samples and PEG 0.4kDa did not provide the dehydration mechanism that was allowing the gels to be produced at such high concentrations.

Formulations were varied relative to a reference formulation that had properties that were considered acceptable (Control 1). Due to the ability of PEG to dehydrate PVA solution, gels having a range of PVA/PEG ratios in their feed formulations were prepared in order to scope this range in the first section (Formulations: Test 1-3). The following section deals with varying water content (Formulations: Test 4 & 5). These formulations are then related to their final gel formulations to determine a trend in swelling. A group of samples in the single phase region is then compared for swelling properties.

6.3 Effect of Varying PVA/PEG in Feed Formulation

6.3.1 Experimental

Swelling studies in 0.2MPa PEG_{aq} at 37°C were performed for three test formulations and one control over 14 days immersion, as described in Table 6.1. Formulations for this portion of the study were chosen within the two phase region (formulations are shown on a ternary diagram in Figure 6.1). PVA and PEG are varied to dehydrate the gel to different extents. The standard method of gel preparation was used: autoclaving at 121°C and equilibration at room temperature for 3 hours, as described previously.

Samples were heated to 95°C and molded into cylindrical molds (12mm dia. x 10mm height). After 30 minutes of molding, samples were de-molded and measured for density via immersion in heptane using the following equation:

$$\rho = \frac{(m_{air}\rho_{hept})}{(m_{air} - m_{hept})}$$

The density of heptane (ρ_{hept}) used in this equation is 0.69 g/ml. Masses were obtained in air or heptane for each using an analytical balance (Pinnacle Series, by Denver Instruments) fitted with a density determination kit. Day 0 volume was calculated via mass/density. Samples were then immersed separately in vials filled with 18g of de-ionized water that had been equilibrated to 37°C. Samples were allowed to freely swell over 7 days in these conditions. At the end of 7 days, samples were harvested and blotted to remove any excess water. Volume was measured using the technique described previously, and V/V_0 (Volume measured at post-swelling state divided by volume at pre-swelling state) was calculated. Water content was

performed in the usual manner of loss on drying in an oven at 105°C overnight for 16 hours. Water content was obtained for the isolated gel, as well as the gel equilibrated in osmotic solution.

6.3.2 Results/Discussion

Swelling reached equilibrium by 7 days (see Figure 6.2). Dehydrating the gel by increasing PEG content in the feed formulation resulted in a decrease in swelling. Swelling decreased with water content in gel (at pre-swelling state), as can be seen in Table 6.2. Equilibrium water content followed the same trend. When Test 1 was compared to the control, swelling was statistically similar. Test 3 could not be prepared because the gel lost its mechanical properties and came apart, seemingly due to high barium sulfate content.

Swelling is believed to be lower for more dehydrated gels, because the more concentrated gel forms a tighter network that resists the swelling pressure. These results follow the trend described by the Flory-Rehner relationship in Section 2.8 of this thesis, as the molecular weight between crosslinks is believed to increase and mesh size is believed to decrease with the increase in polymer content. The equation relating molecular weight between crosslinks and the swollen equilibrium polymer volume fraction tells us that as the polymer volume fraction increases, there is a corresponding precipitous drop in molecular weight between crosslinks, when other factors are viewed as being constant.

6.4 Effect of Varying Water Content

6.4.1 Experimental

Feed formulations having the same PVA/PEG ratio, but varying water contents as described in Figure 6.1 and Table 6.3 were evaluated for swelling. Feed water contents decrease in 5% increments. Swelling studies in 0.2MPa PEG_{aq} at 37°C were performed for three test formulations and one control over 14 days immersion. Formulations for this portion of the study are also within the two phase region. The standard method of gel preparation was used: autoclaving at 121°C and equilibration at room temperature for 3 hours, as described previously. Gel cylinders (12mm dia. x 10mm ht.) were heated to 95°C, then molded for 30 minutes at 37°C, demolded, then immersed in 18g of osmotic solution at 37°C. Swelling (V/V_0) was determined as described in the previous section. Water content was performed in the usual manner of loss on drying in an oven at 105°C overnight for 16 hours.

6.4.2 Results/Discussion

Water content in gels at pre-swelling state are seen to decrease along with swelling, as in Table 6.4 . This is attributed to the tighter network structure of the more concentrated gel, as seen through dehydration in the previous section. Test 6 formulation could not be made since the PVA solution could not be prepared due to it being extremely concentrated. On average for gels with varying water contents, Test 4 swelled to 3% less water and Test 5 swelled to 7% less water when compared with the control (see Figure 6.3). Differences in swelling for Test 4 and Control were not statistically significant, however.

The position of the gel is anticipated to fall along the binodal prepared in the previous section. When all samples are combined from the previous two sections, it can be seen in Figure 6.4 that there is a direct relation between swelling behavior and water content of the gel in the pre-equilibrated state for points along this binodal. Gels of lower water content swelled less.

These swelling results agree with the prediction from the Flory-Rehner relationship as described in the previous section. The results of decreased swelling for more concentrated formulations suggest that concentrating the gel phase has the effect of reducing the swelling, though to an extent that was considered to be too small (an 84% vs 100% swelling increase) in order to be considered as a means for control over swelling properties. The significance of these results is that the full reasonable scope of formulations is described to swell for this given PVA/PEG component system. Results further suggest that changes to polymer grade (possibly molecular weight or structure, as well as possibly degree of hydrolysis) are necessary in order to produce an implant that will not swell beyond the region of interest. Swelling is also a direct indication of stability of the implant, as will be described later in this thesis. Water imbibed from this process would also have deleterious affects on mechanical properties such as friability, modulus, wear resistance and fatigue life of the material.

6.5 Swelling and Stability within the Single Phase Region

6.5.1 Experimental

Three single phase compositions (see Table 6.5) also studied for gelation characteristics later in this thesis were tested for both swelling and dissolution in 0.2MPa at 37°C (n=3). Isolated gels at the pre-swelling state are expected to have water contents similar to that which are added in the initial feed formulations in order to clearly monitor equilibrium water changes. Formulations were prepared at similar PEG contents that would not produce supernatant. Other characteristics of sample preparation were kept the same. No supernatant was present to be decanted.

6.5.2 Results/Discussion

The gel with the lowest water content swelled less, similar to the previous study, however the highest water content swelled more (Formulations are shown in Figures 6.5a & b as datapoints on a ternary diagram, with corresponding swelling data annotated). When percent dry mass loss was obtained for these samples, the samples with a reduction in swelling similarly showed an increase in dry mass loss (Figure 6.5b). Based on the gel integrity as part of the study, it was determined that the anomalous decrease in swelling for high water content gels was in fact attributable to the loss of mass, and the observation that a decrease in water content increases the stability of the gels was maintained for the single phase samples.

With the exception of the high water content samples, results for samples prepared within the single phase region match the trend observed for varying water content. No observable difference in swelling character or magnitude was noticeable for samples prepared via dehydration/phase separation, as in the previous section, in comparison to those prepared for this study, as a single phase.

6.6 Effects of Setup on Swelling

6.6.1 Introduction

Identical formulations of F1-145/10 that had been allowed to sit at room temperature were swelled in comparison to identical samples that had been recently melted and cooled, in order to view differences in the uptake of water for gels still undergoing the process of gelation.

6.6.2 Experimental

Gels were used in the unmelted form, and had been allowed to set for five weeks at room temperature. The same sample was used that had sat the same length of time in the unmelted state, was melted to its flowable "as delivered" state, molded for 30 minutes at 37°C and allowed to swell. Samples were swollen in 0.2MPa PEG_{aq} osmotic solution at 37°C, in sink conditions, where 12mm dia. x 10mm height gels were molded for the "as delivered" samples. Cylinders of unmelted gels were cut to approximately the same size from longer cylinders and immersed in 18g of osmotic solution at 37°C.

6.6.3 Results/Discussion

Differences in swelling were seen to result from differences in time that gels have been allowed to set before immersion in an osmotic medium. See Figure 6.6. Significant differences in swelling can be seen between the two gel types. These results suggest that PVA network formation is more advanced for gels that have been allowed to age, and that there is a long-term time-dependent effect to network formation that is critical to resisting swelling. Results from this study are significant in that the implanted gel in the newly melted state cannot be viewed as having the same swelling properties as a gel that is prepared as a preformed device (i.e. the "unmelted" sample that had been allowed to gel for five weeks) and implanted. Swelling must be viewed in relation to the thermal history of the gel, and the time that has elapsed since cooling is critical to properly evaluating the swelling characteristics. For the purposes of this thesis, the gel is designed to be delivered in the melted state and subjected to the intervertebral disc swelling pressures immediately following delivery, at the time that the gel is still cooling to physiologic temperature.

6.7 Swelling at Varying PVA Molecular Weight

6.7.1 Introduction

Swelling affects at varying PVA molecular weight was determined. Preparation of samples of PVA gels with decreased molecular weight yielded samples that swelled a relatively smaller amount (volume increase of 55% in phosphate buffered saline

solution), however the material lacked structural integrity, was brittle and friable. This decreased swelling was in contrast to previous gels prepared from higher molecular weight PVA. Differential scanning calorimetry (DSC) is used to compare differences in thermal transition with swelling.

6.7.2 Experimental

6.7.2.1 Swelling

Concentrated PVA_{aq} gels (i.e. 50% w/w PVA in water) were prepared at varying PVA molecular weights (13-23kDa, 125kDa & 195kDa; the first PVA is a 98% hydrolyzed grade branded as Aldrich, and the second two are Mowiol 20-98 & 56-98 respectively; all are fully hydrolyzed PVA grades obtained through Sigma-Aldrich). In the test, aqueous solutions of PVA were prepared in an autoclave and injected into 11mm diameter x 100mm height stainless steel cylindrical molds. These cylinders were allowed to cool to room temperature for 16 hours, and then cut to 1mm height cylinders and immersed in 0.2MPa osmotic solution at 37°C for 7 days, in order to track swelling. Photos of the cylinders after 7 days of swelling are shown in Figure 6.7.

6.7.2.2 Differential Scanning Calorimetry (DSC)

A 50% aqueous solution of 12-23kDa PVA was prepared in an autoclave. The solution was allowed to stand at room temperature overnight for 16 hours, after which point the material was tested using the following method:

Step 1. Initial temperature = 25°C

Step 2. Temperature ramp: 5°C/min to 95°C

Step 3. Temperature ramp: 5°C/min to 25°C

Step 4. Temperature ramp: 5°C/min to 95°C

The same process was repeated for higher molecular weight material: A 50% w/w aqueous solution of 145kDa PVA was prepared in a similar manner, allowing it to cool by standing at room temperature overnight for 16 hours. Samples of high molecular weight were tested using the method described above.

6.7.3 Results/Discussion

Samples with high molecular weight PVA were observed to swell considerably. It can be seen in Figure 6.8 that swelling is dramatically lower for 13kDa samples (26.0% increase in volume), when compared with 125kDa and 195kDa samples (61.8% and 65.2%, increase in volume, respectively). Despite swelling reduction for the 13kDa samples, mechanical properties could be observed to decrease. Many 13kDa samples developed cracks as part of the swelling process. Samples of 125kDa and 195kDa were elastic and did not fragment easily.

DSC was performed for the low molecular weight material and compared with the high molecular weight, in order to show any network effects, such as an endotherm from crystallization that might indicate more physical crosslinking that would lead to a lower molecular weight between crosslinks, as anticipated by the Flory-Rehner

relationship. Two transitions were noticed for low molecular weight material (12-23kDa), the first at ~60°C and the second at 84°C (see Figure 6.9). The results of an evaluation using the same DSC method with 145kDa PVA are shown in Figure 6.10. None of the same transitions noticed for the low molecular weight were seen in the results for the test using high molecular weight. It is described by Muller et al, that there is an improved crystallizability of PVA at low molecular weights (<4.4kDa) due to the varying entropy and mobility of the smaller molecules [99]. It is understandable that due to these transitions and the observed brittle properties of samples that a secondary form of crystallization occurs with molecular weights below a certain value.

By decreasing the PVA molecular weight enough, swelling is believed to be mitigated. A balance must be obtained, between molecular weight swelling effects, (which favor low molecular weight PVA, see Figure 6.11), while avoiding the characteristic friability and brittle behavior of swelled low molecular weight PVA gels. The proposed solution is that samples with good structural integrity and swelling properties would be somewhere between the 13kDa and 125kDa samples, as described in the next section.

6.8 Optimization of PVA Molecular Weight for Minimal Swelling

6.8.1 Introduction

In order to best balance the friability observed in samples with low molecular weight PVA, and swelling observed in samples with high molecular weight PVA, swelling

studies were performed for formulations having intermediate molecular weights for PVA (27-61kDa range).

6.8.2 Experimental

A first study was performed where identical formulations were prepared using identical mixtures of the F1-x/10 formulation, where x = 61kDa PVA ("Test") for one formulation and x= 145kDa PVA ("Control"). Samples were evaluated for swelling. A second study was prepared comparing against even lower molecular weights of PVA (27kDa). Different formulations were prepared (F3 & F4 in Table 6.1), in order to reduce the water content for this gel. Swelling was performed using the methods previously described, in 0.2MPa PEG solution at 37°C.

6.8.3 Results/Discussion

Results in Figure 6.12 suggest that the same reduction in swelling that had been seen previously for low molecular weight PVA is not seen in 61kDa samples. 61kDa samples were also not brittle, suggesting the low molecular weight crystallization was not exhibited for these samples. When 61kDa was compared with 145kDa there was no difference in swelling (see Figure 6.12).

Lower water content formulations were prepared for even lower molecular weight PVA (Mowiol 4-98; 27kDa), in order to decrease swelling further, since swelling was seen in previous sections to be affected by water content, and low molecular weight

solutions formed noticeably weaker gels. PEG grade is 10kDa, and all other components are same. Lower water content formulations F3 and F4 were chosen in order to increase viscosity for lower molecular weight material. As shown in Figure 6.13, swelling for F3 and F4 was similar for both at ~30-33%. Samples prepared using 27kDa PVA retained their general shape (Figures 6.14a & b) and had a relatively high modulus. Sample modulus was measured at 1.8MPa. Samples were inelastic and brittle, however. When tested in compression, the sample fractured (Figure 6.14c), which is an unacceptable mode of failure for a nucleus replacement. More elastic samples with a higher elongation at break are necessary. Final sample compositions were not determined due to the brittle behavior and unacceptable nature of the samples.

It should be noted that samples of lower molecular weight PVA were observed to have a difference in melting characteristics. Samples did not melt to a smooth texture when being injected into the mold, suggesting that the melting temperature was higher and the flow was limited to melt fracture. The incomplete melting possibly had an affect on the ability of the gel to form up correctly. If melted to a greater extent the material may seem less brittle and display better mechanical properties, however it was outside of this study to increase the injection temperature, as the gel must be designed to have a delivery temperature low enough for implantation.

6.9 Swelling at Varying PEG Molecular Weight

As mentioned above, phase equilibrium exhibited by the gel/supernatant system is affected by the molecular weight of PEG that is chosen [4]. It is reasonable to assume that since the equilibrium of the gel with the supernatant is affected by changing PEG molecular weight, so would the equilibrium of the gel in other environments, namely in an osmotic environment such as the disc, or the 0.2MPa PEG solution that it being tested. This is at least in part due to the presence of the molecular weight term in the osmotic virial equation.

6.9.1 Experimental

A swelling study was performed, where the F3 formulation, as described in Table 4.1 and the previous section was prepared using three different PEG molecular weights. The PVA molecular weight was fixed at 61kDa, and the PEG molecular weight in each formulation was 0.4, 1 or 10kDa. Samples were molded into cylinders over 30 minutes then immersed in 0.2 MPa osmotic solution at 37°C for 7 days and swelling (V/V_0) was tracked as in the previous studies.

6.9.2 Results/Discussion

Results from the 7-day swelling study (see Figure 6.15) showed that lower molecular weight PEG resulted in a lower degree of swelling. The 0.4kDa PEG produced no swelling at this formulation (V/V_0=0.98), whereas 1kDa PEG samples produced a V/V_0 of 1.31, and 10kDa PEG had a V/V0 of 1.90, which was close to our F1-145/10

control (V/V_0=1.97). Previous data has shown that swelling decreases with an increase in water content. Pre-swelling water contents for 0.4kDa and 1kDa respectively had been 46.4±0.9% and 40.4±2.1% which is opposite to the direct correlation of water content and swelling. This further supports the effect of a strong direct correlation between PEG molecular weight and swelling.

Mass loss was similarly measured for these samples. 0.4kDa PEG had a 36±0.3% dry mass loss, though integrity of samples was good after swelling. It is likely that the majority of mass lost due to swelling was 0.4kDa eluting from the sample during equilibration. Samples with 1kDa PEG exhibited only a 9.4±3.0% dry mass loss. As will be seen in the next section, this trend is opposite to what is observed when swelled in de-ionized water for formulations and is attributed to the presence of the osmotic environment, which swells the material less, trapping higher molecular weight in the gel phase.

6.10 Effect of PEG on Swelling and Stability within the Single Phase Region

6.10.1 Experimental

Swelling studies were performed for single phase "G" in Table 6.5 at varying molecular weights of PEG (0.4, 1, 10, 20 & 35 kDa). Samples were each prepared by the standard method of heating in an autoclave at 121°C, and cooling to room temperature afterward. No supernatant was present to be poured off. Swelling and dry mass loss were obtained, as previously described, with the exception that samples were swollen in de-ionized water at 37°C for 7 days. Water was dried at the end of

the study to look for signs of eluting PEG via FTIR. Mass loss studies for three formulations in 0.2MPa osmotic solution were also prepared separately and are used for comparison.

6.10.2 Results/Discussion

An increase in molecular weight was seen to produce an increase in swelling, with a maximum at 10kDa (see Figure 6.16). Dry mass loss at 7 days immersion was seen to increase with PEG molecular weight, which is understandable due to the greater amount of swelling exhibited by gels with higher molecular weight PEG. It is possible that the effect observed in this case for de-ionized water was not previously observed for dry mass loss in osmotic solution because the network was not able to expand as much in the osmotic environment, effectively keeping in more material that would otherwise elute out. Mass loss for formulations prepared in 0.2MPa solution (see Figure 6.17) shows a trend where higher molecular weight PEG is retained after swelling.

6.11 Statistical Treatment of Swelling Data

Available data for formulations under consideration was evaluated statistically in order to properly define resulting trends from the available input factors, in particular, those of component percentage, as well as component grade (i.e. molecular weight). F1, F3 & F6 from Table 4.1 are prepared and Table 6.6 shows the swelling data generated across the range of formulations, and molecular weights of materials.

Figure 6.18 shows the main effects plot resulting from that data. Other than the affect of PEG molecular weight, no other major factor was shown to contribute to swelling. Feed composition was shown to not be as significant a variable in the formulation range of interest. In ruling out very low PVA molecular weights because of brittleness, there was little affect varying between 61kDa and 145kDa PVA.

A main effects plot was generated for swelling data using the available factors for composition. A one way ANOVA was performed to determine significant factors to swelling. With the exception of PEG molecular weight (P(2Tail) = 0.002), each of the factors (H_2O, PVA, PEG, PVA-molecular weight, PEG-molecular weight) showed little or no affect on swelling.

Main effects plot data regarding PEG molecular weight showed the same result as had been highlighted in previous sections, where the incorporation of lower molecular weight leads to a lower degree of swelling. The resulting effects of a greater molecular weight polymer, such as PEG, that is both very flexible, and hydrophilic to the extent of being able to bind large quantities of water and swell considerably [6, 71, 72]. Larger molecular weight PEG will result in a larger hydrodynamic radius for the swollen polymer. In other words, a shorter linear polymer of the same chemistry will result in a smaller radius when in its swollen state. Larger polymers generate a swelling pressure that follows from their hydration and expansion.

Table 6.1 Initial feed formulations for samples with varying PVA vs. PEG ratio

	Ctrl-1 (F1-145/10)	**Test-1 (0.75PVA/PVP)**	**Test-2 (0.5PVA/PVP)**	**Test-3 (0.25PVA/PVP)**
PVA	20.1%	15.0%	10.0%	5.0%
PVP	0.2%	0.2%	0.1%	0.1%
PEG	17.7%	22.8%	27.9%	32.9%
$BaSO_4$	7.0%	7.0%	7.0%	7.0%
Water	55.0%	55.0%	55.0%	55.0%

Table 6.2 Swelling for varying PVA vs. PEG samples.

	Ctrl-1		Test-1		Test-2		Test-3	
	Average	**Std. Dev.**	**Average**	**Std. Dev.**	**Average**	**Std. Dev.**	**Average**	**Std. Dev.**
Water Content in Gel (Pre-Swelling)	50.4%	0.6%	45.4%	1.0%	40.8%	0.5%	N/A	N/A
Equilibrium Water Content (14days)	74.5%	0.3%	71.0%	0.1%	67.2%	2.3%	N/A	N/A
Swelling	201.6%	5.7%	197.6%	1.9%	184.3%	6.4%	N/A	N/A

Table 6.3 Initial feed formulations for samples with varying water content.

	Control-1 (F1-145/10)	**Test-4 (-5% Water)**	**Test-5 (-10% Water)**	**Test-6 (-15% Water)**
PVA	20.1%	22.3%	24.6%	26.8%
PVP	0.2%	0.2%	0.2%	0.3%
PEG	17.7%	19.7%	21.6%	23.6%
$BaSO_4$	7.0%	7.8%	8.6%	9.3%
Water	55.0%	50.0%	45.0%	40.0%

Table 6.4 Swelling for varying water content samples.

	Control-1		**Test-4**		**Test-5**		**Test-6**	
	Average	**Std. Dev.**	**Average**	**Std. Dev.**	**Average**	**Std. Dev.**	**Average**	**Std. Dev.**
Water Content in Gel (Pre-Swelling)	50.4%	0.6%	46.4%	1.0%	44.1%	0.9%	N/A	N/A
Equilibrium Water Content (14days)	74.5%	0.3%	72.1%	1.1%	68.3%	3.5%	N/A	N/A
Swelling	201.6%	5.7%	200.6%	2.3%	193.8%	6.5%	N/A	N/A

Table 6.5 Three initial feed formulations prepared within the single phase region.

	Variables					
	F		G		H	
Composition variables	**Mmol**	**%**	**Mmol**	**%**	**mmol**	**%**
PEG (10kDa)	0.625	6.25	0.625	6.25	0.555	5.55
PVA (Mowiol 28-99)	0.221	32.01	0.267	38.75	0.314	45.56
DI Water	3427.1	61.74	3052.9	55	2713.8	48.9

Table 6.6 Data set for main effects plot

FormIn	PVA-MW (kDa)	PEG-MW (kDa)	H2O (wt.%)	PVA (wt.%)	PEG (wt.%)	Swelling (V/V_0)
F1	61	10	59.20	21.71	19.09	1.90
F1	145	1	59.20	21.71	19.09	1.26
F1	145	10	59.20	21.71	19.09	2.00
F6	61	0.4	53.27	21.49	25.25	0.94
F6	145	0.4	53.27	21.49	25.25	1.08
F6	145	1	53.27	21.49	25.25	1.40
F3	61	0.4	48.44	21.74	29.82	1.00
F3	61	1	48.44	21.74	29.82	1.30
F3	61	10	48.44	21.74	29.82	1.55

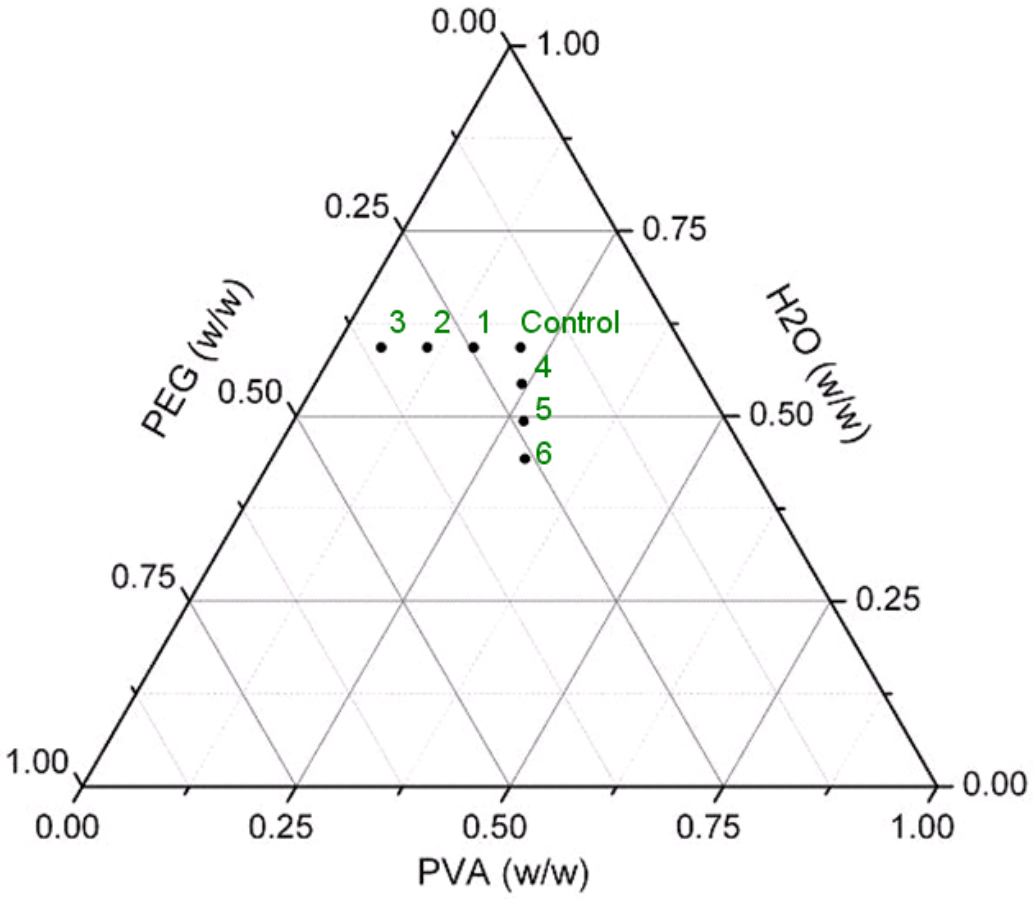

Figure 6.1 Feed formulations from Tables 6.1 & 6.3, as depicted on a ternary diagram.

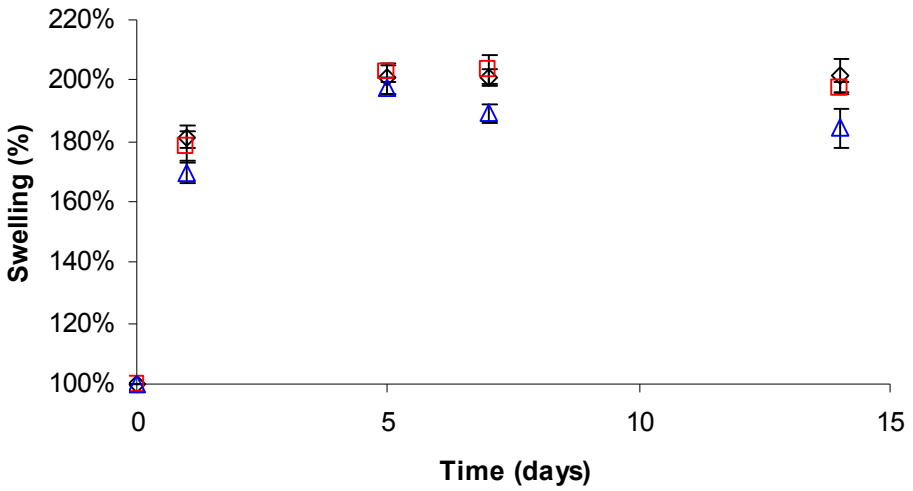

Figure 6.2 Volume change (expressed as final volume over initial volume) for swelling in 0.2 MPa osmotic solution (◇ Control, □ Test 1, & △ Test 2).

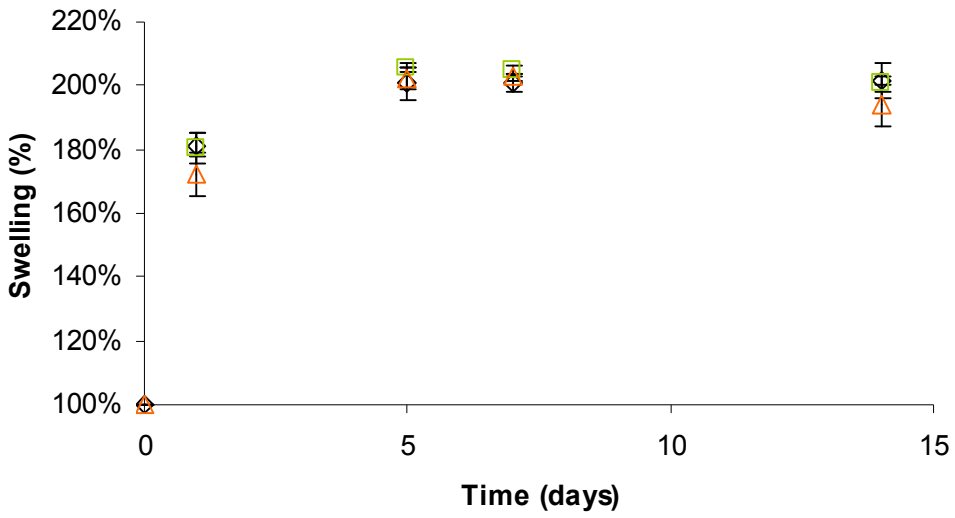

Figure 6.3 Swelling for formulations with varying water content (◇ Control, □ Test 4 & △ Test 5)

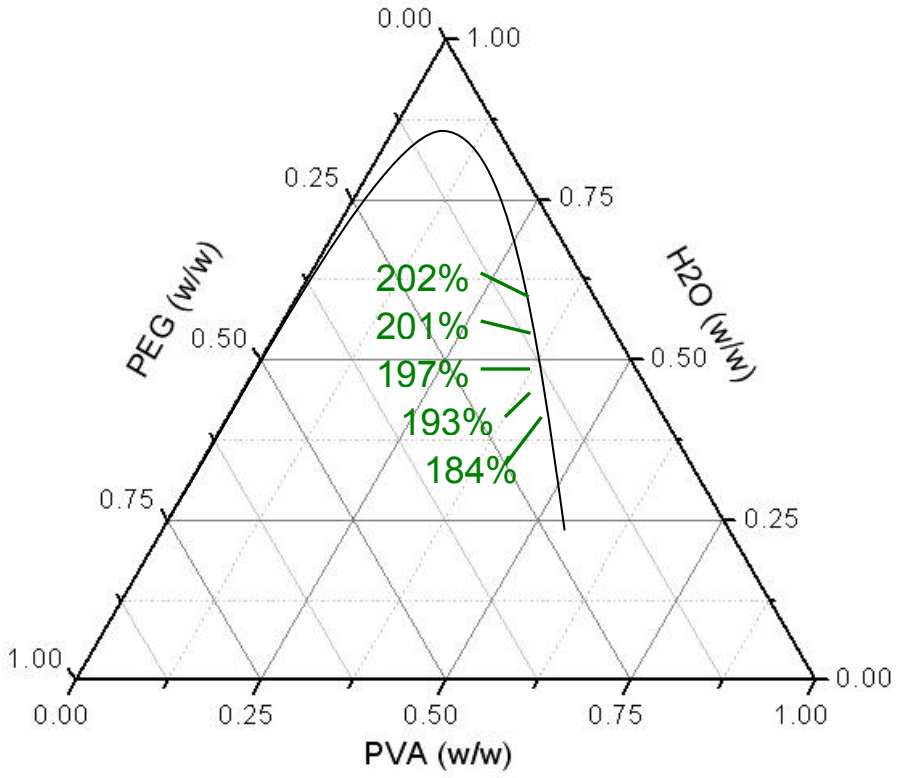

Figure 6.4 Ternary diagram showing swelling (% of initial volume) at varying water content on diagram.

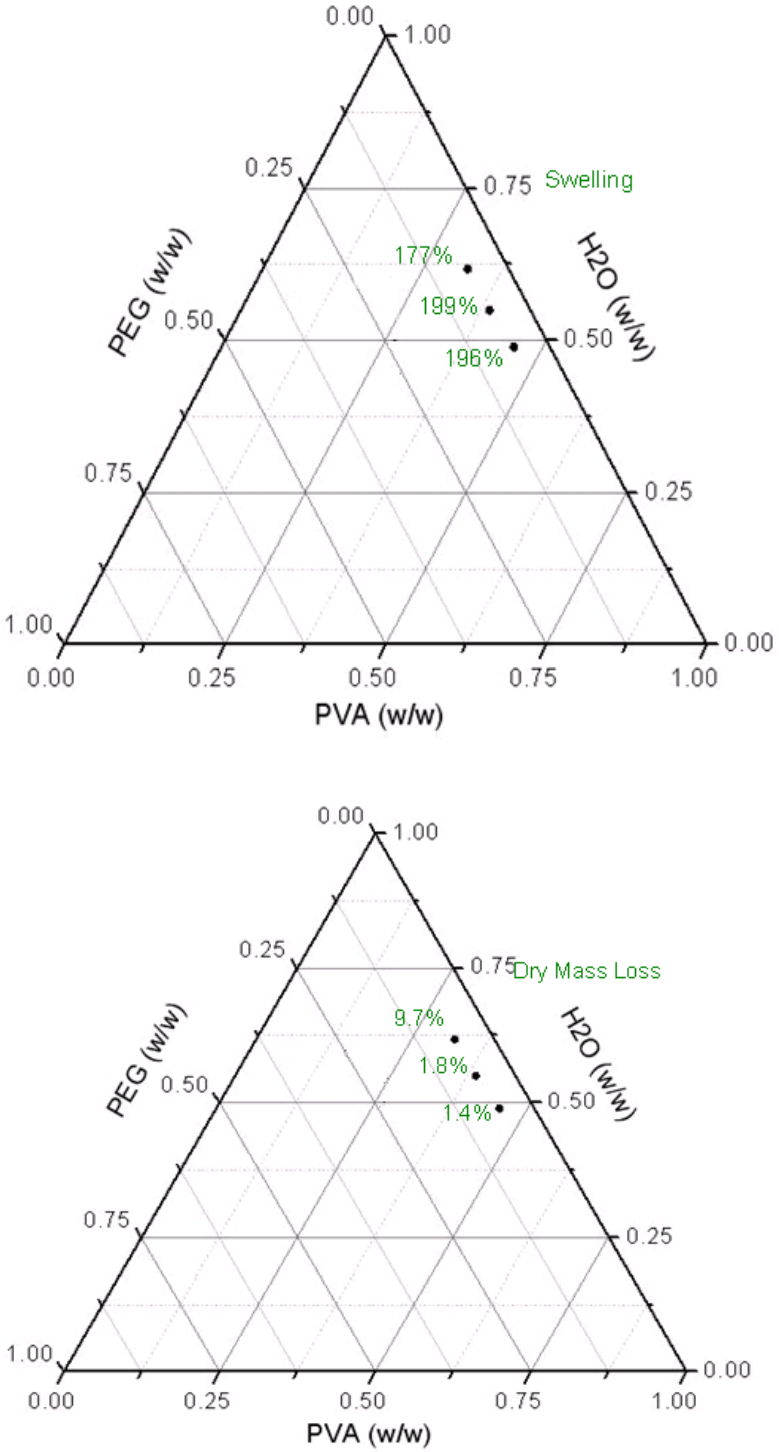

Figure 6.5 a) Swelling for formulations that were prepared to result in a single phase (compositions F, G, & H). and b) Percent dry mass loss for formulations prepared to result in a single phase. Previous formulations are included for reference.

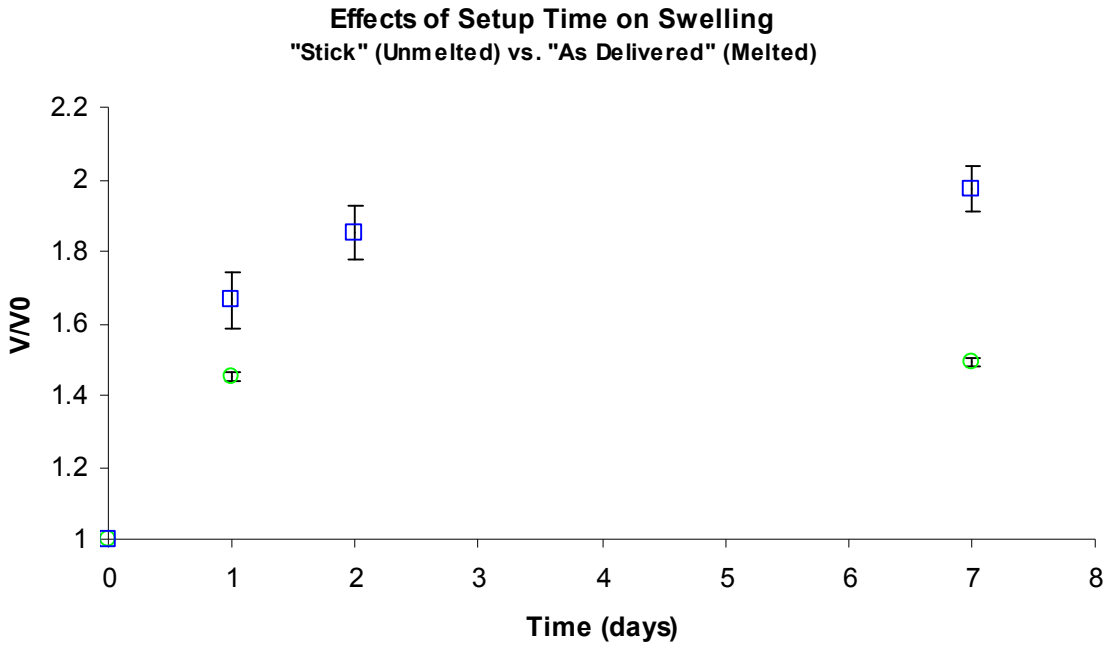

Figure 6.6 Effects of gel setup time on 7 days of swelling in 0.2 MPa solution. Gels melted from the stick at 95°C for delivery were compared against unmelted sticks stored for 5 weeks(○ unmelted & □ melted).

Figure 6.7 Photos of 50% PVA gels at 7 days swelling at varying molecular weights. From left to right: 13kDa, 125kDa and 195kDa samples.

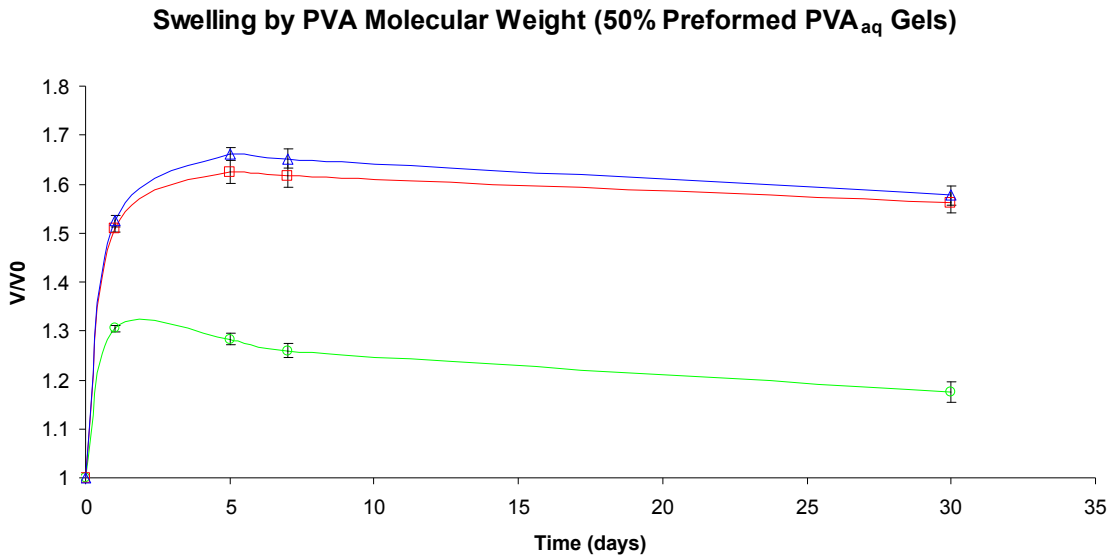

Figure 6.8 Swelling of 50% PVA_{aq} gels (13kDa, 125kDa & 195kDa)

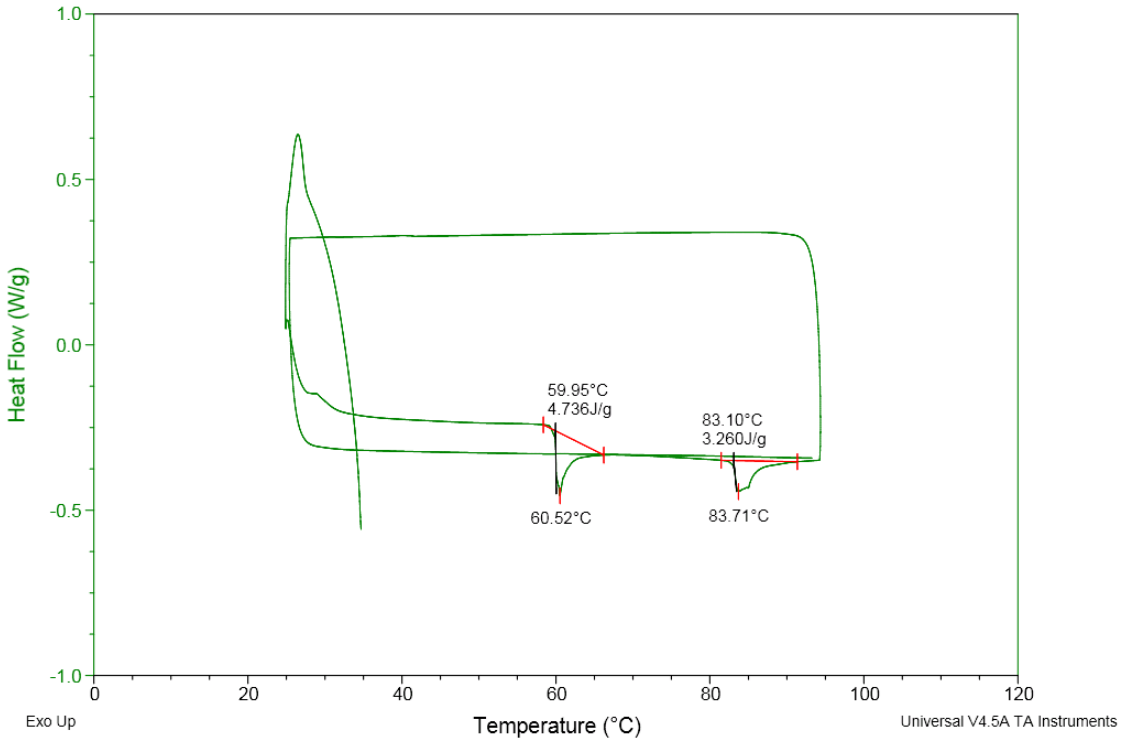

Figure 6.9 DSC of low molecular weight PVA (50% aq.) after being allowed to stand at room temperature for 16 hours. Two transitions are visible.

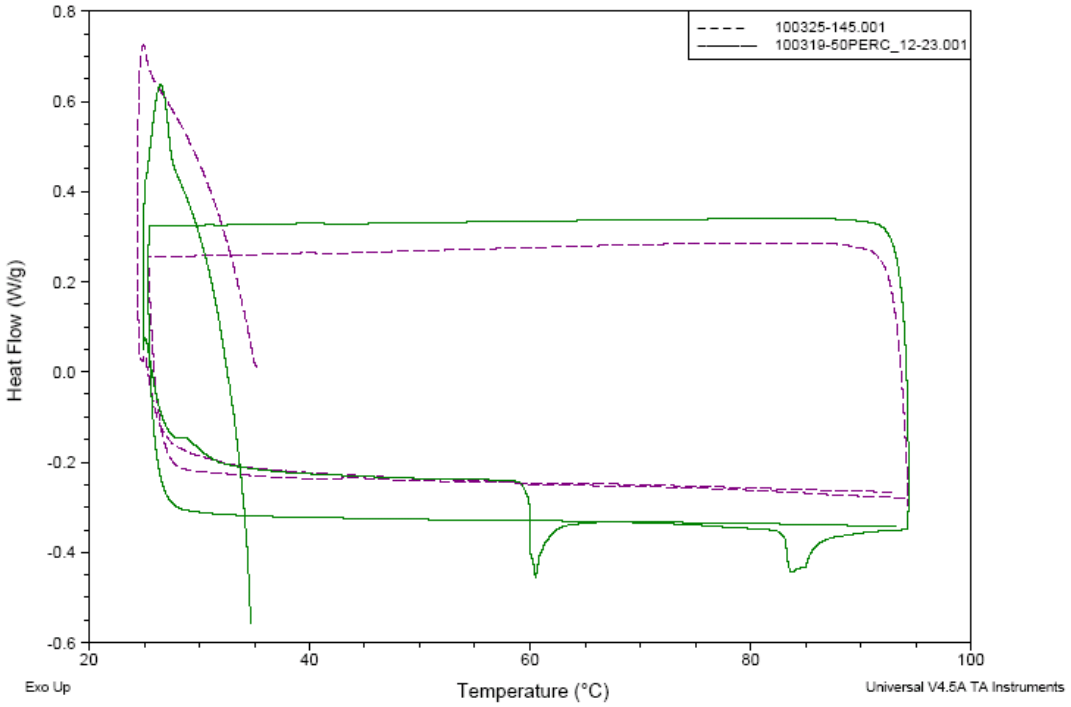

Figure 6.10 DSC Results for neat 50% aqueous gels of 145kDa PVA (dashed line). Results for neat 50% aqueous 12-23kDa PVA are included for comparison.

Figure 6.11 Low molecular weight (at left) vs. high molecular weight (at right) 50% PVA_{aq} gels at 7 days of swelling. The low molecular weight PVA sample has retained its shape but is brittle whereas the higher molecular weight is elastic, but has swelled.

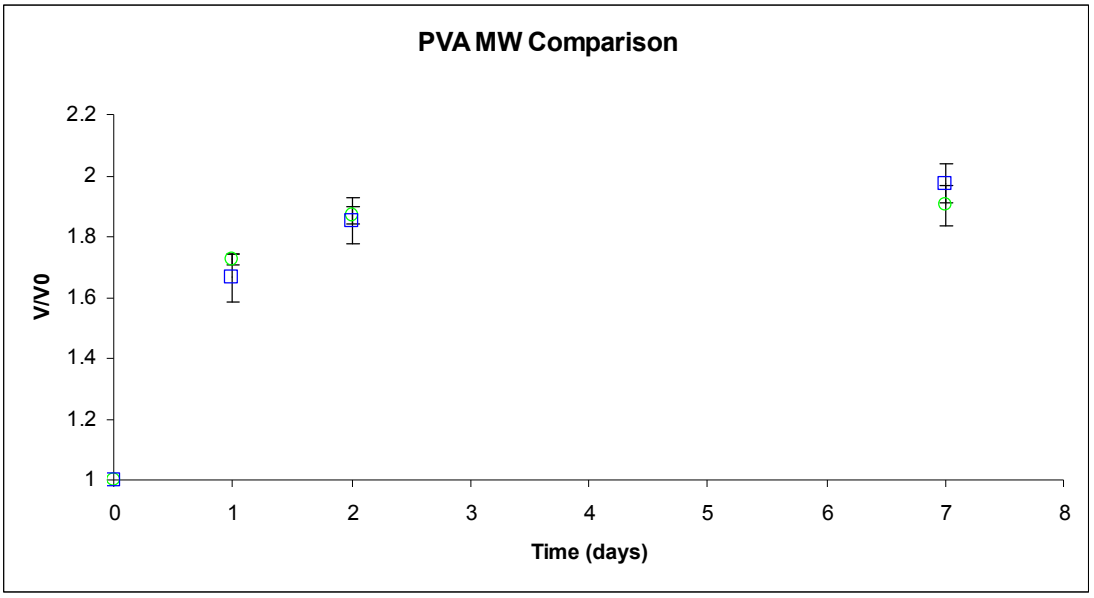

Figure 6.12 Swelling with varying PVA molecular weights gels (○ 61kDa & □ 145kDa)

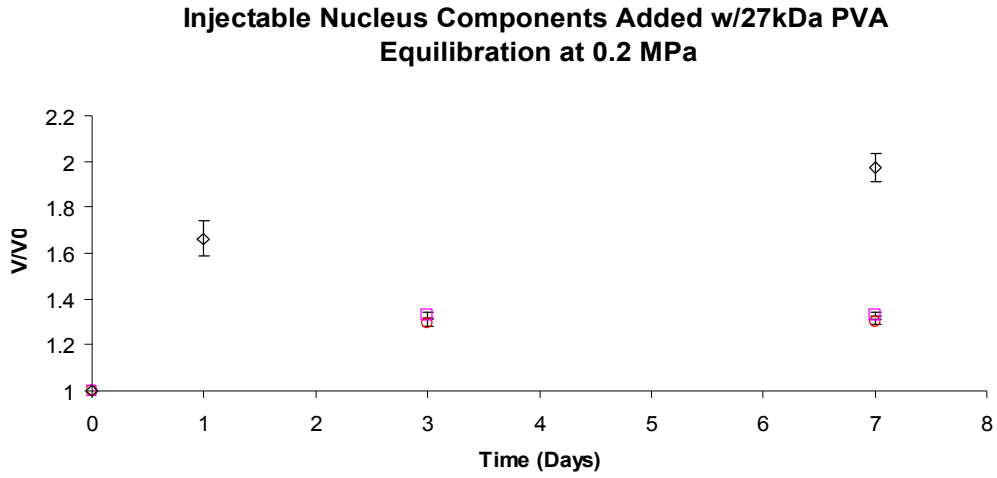

Figure 6.13 Swelling in 0.2MPa PEG solution prepared using 27kDa PVA (○F3-27/10, □F4-27/10, ◇F1-145/10)

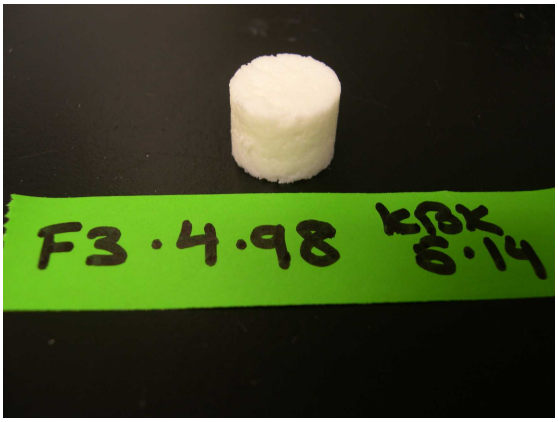

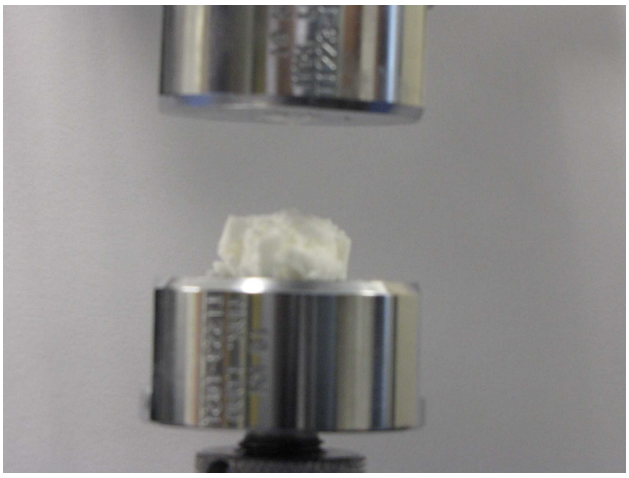

Figure 6.14 a) showing a 27kDa-PVA sample (Formulation is F3-27/10) at Day 0; and b) Day 3; Figure c) shows the sample fractured after compression testing.

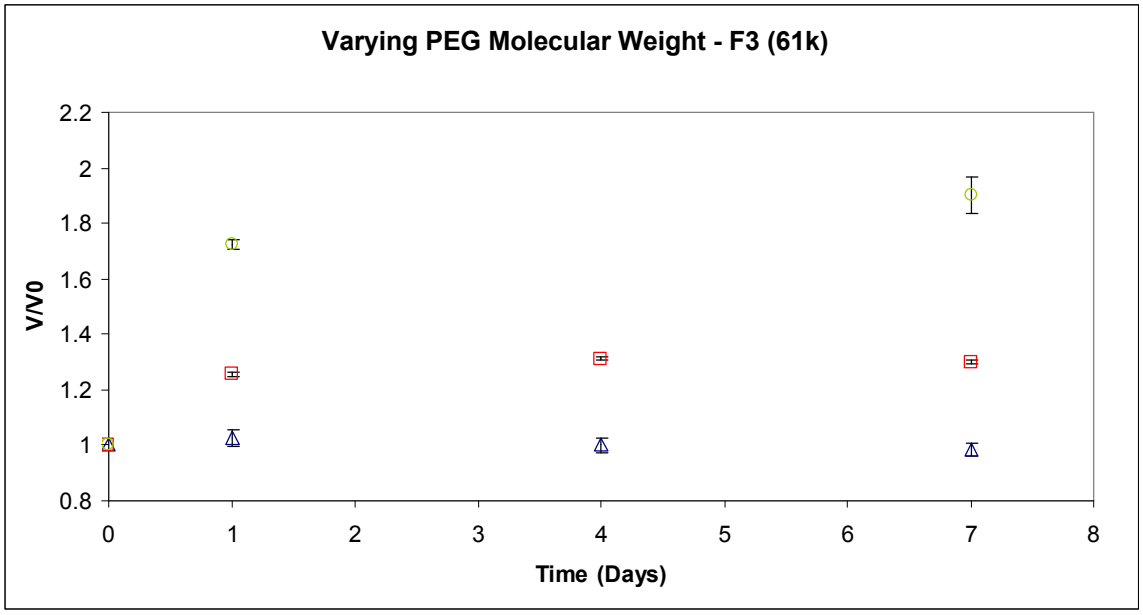

Figure 6.15 Swelling for the F3-61/x formulation prepared using three different molecular weights of PEG: x = △PEG-0.4kDa; □ PEG-1kDa; and ○ PEG-10kDa

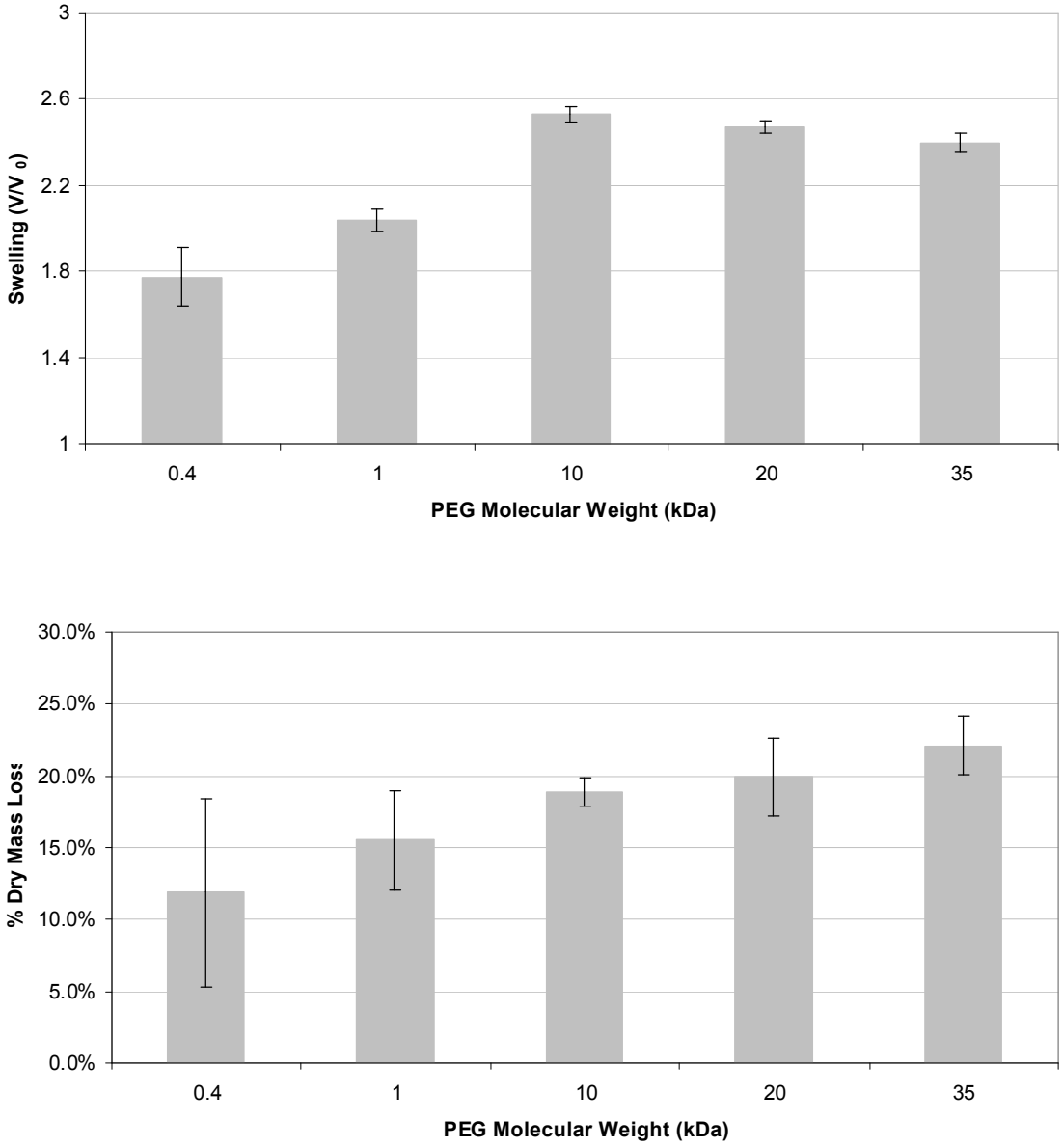

Figure 6.16 Single phase formulation "G" a) swelling upon immersion and b) dry mass loss upon immersion (both at 7 days in de-ionized water) with a range of PEG molecular weights

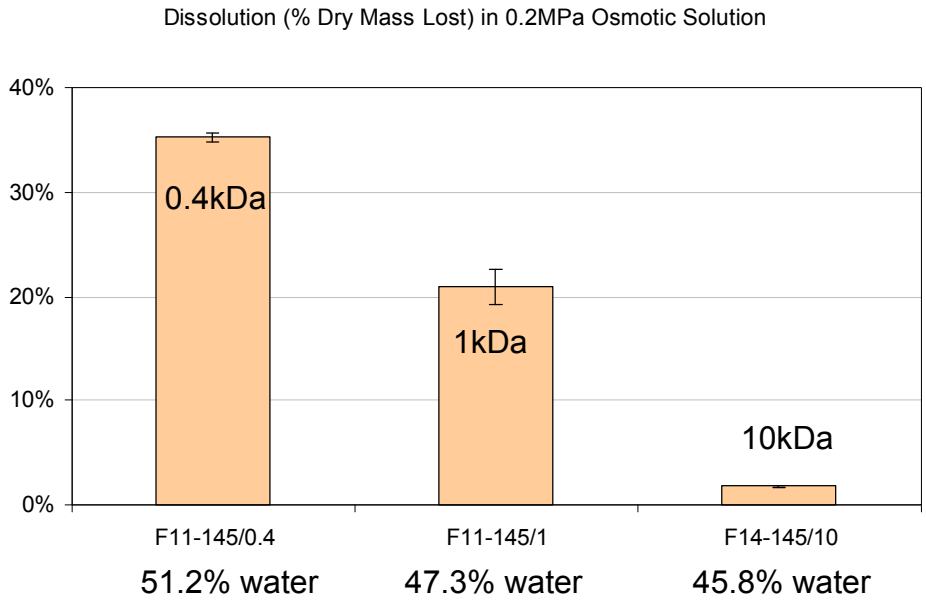

Figure 6.17 Percent dry mass loss in 0.2 MPa osmotic solution

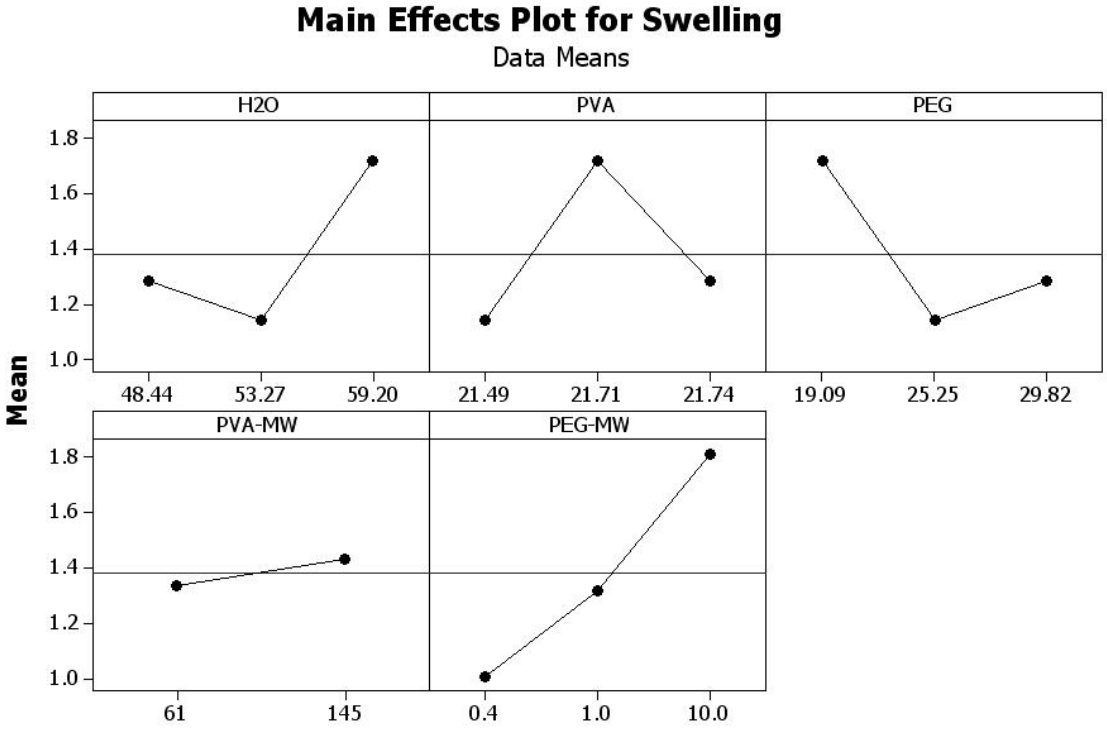

Figure 6.18 Main affects plot showing factors (composition, as well as PVA & PEG molecular weight and response (swelling)

CHAPTER 7: GELATION

7.1 Introduction

As described earlier, cooling of the concentrated aqueous PVA/PEG system from the sol produces a gelation mechanism with a rheology that has yet to be appropriately characterized. Differences between neat aqueous PVA solutions and the PVA/PEG system, with regard to the transitional state from sol to gel are defined in the following sections. Based on the results generated, comparisons for viscosity transitions for pre- and post- gelation are able to be made. Quantifications of the relative size of transitions are also able to be made with respect to formulations. The temperatures of the transitional state, as well as the factors affecting it are able to be defined, enabling tailoring of setting profiles to material application. Gelation data are collected at the point of implantation. It is important to note that gelation concerns implants in the newly delivered, or pre-swelled state. As described earlier in the swelling section of this thesis, there is an effect of time the material is allowed to gel on the resultant swelling properties.

7.2 Gel Point

7.2.1 Experimental

An AR2000 rheometer (TA Instruments) with 40mm diameter crosshatched parallel plates was used to test samples in oscillatory shear (0.5% strain/s) (see Figure 7.1). Cross-hatching was used to fix samples into position for the oscillatory strain setup.

The gap between plates was set at 750µm. Temperature was controlled using a Peltier plate heating system. Gel could not be easily cut at the edges of the testing apparatus, since it was very elastic. Gels within this section are prepared with 145kDa PVA (Mowiol 28-99, purchased from Kuraray, Inc) and 10kDa PEG purchased from Sigma-Aldrich. Gel point was determined using a temperature ramp from 95 to 37°C over 20 minutes (2.9°C/min), with an initial 5 minute equilibration at 95°C. The crossover point of the storage and loss modulus is defined in ASTM 4473 as the "gel point"[100].

7.2.2 Results/Discussion

As shown in Figure 7.2, setting behavior of PVA/PEG gels shows an increase in storage modulus with a decrease in temperature. Secondary effects become noticeable in the region below 42°C as the storage modulus increase becomes much more dramatic. Due to similarities between the storage and loss modulus at higher temperatures, the crossover point had showed variability (65-84°C was the range for measured crossover points when four identical samples were evaluated), and it is shown that due to the close nature of the two curves, that differences between storage and loss modulus at higher temperatures were not significant. Storage modulus dominated below this temperature, indicating gelation for samples cooled past this point. For averaged samples (n=5; Figure 7.2), storage and loss modulus were within one standard deviation at temperatures above 61°C. Below 61°C, storage modulus becomes the dominant term contributing to total complex modulus. Gelation can be seen to undergo the steep incline in modulus at ~45°C, for both storage modulus, and

loss modulus to a lesser extent. The source of the transition will be described in the following sections with respect to the combined viscoelastic term of complex viscosity. The chemical and physical basis for the shape of this transition will be further described in the following sections, as it relates to viscosity measurements in the literature describing similar transitions, such as the viscosity drop and interference of PVA hydrogen bonding for the PVA systems observed by Briscoe et al (see Section 2.9 of this thesis) [6]. In this work, Briscoe et al describes a solubility transition where apparent viscosity in the high temperature state decreases due to a decrease in the hydrogen bonding interaction between PVA and water, as a result of the incorporation of a second component such as PEG which is a known plasticizer that competes for water affinity in the system [5].

7.3 Temperature Effects on Viscosity

7.3.1 Experimental

Complex viscosity was calculated from dynamic rheometry data as $\eta^* = \eta` + i\eta``$, $\eta`$ is dynamic viscosity, and $\eta``$ is the remaining imaginary term [101]. $\eta`$ is defined as the loss component divided by angular frequency G"/ω; and similarly $\eta``$ is defined as G`/ω. Complex viscosity is used to combine both viscous and elastic effects during gelation.

In a first test to evaluate the effects of temperature on complex viscosity, a temperature ramp was performed using the same method and experimental setup as in the previous section (crosshatched parallel plates, 0.5% Strain; 1 Hz; 0.75mm plate

gap. The method used was 95°C for 5 minutes and a ramp over 20 minutes from 95°C-37°C). A sample of PVA gel of the same PVA/water ratio (equal to 43% w/w) was included as a control.

In a second test, complex viscosity was plotted for the same formulation at a range of temperatures, over time. Again, this experiment was performed using a parallel plate rheometer in oscillatory shear in a setup similar to above. Methods were changed however to include rapid temperature jumps, cooling to each of four temperatures: 37, 45 & 70°C. A sample was also held at 95°C as a control. Each was then followed by 30-minute temperature equilibration steps where viscosity was monitored. As part of this test, viscosities for multiple replicates were also obtained for samples after they had equilibrated to one of three temperatures of interest (37, 45 and 70°C; see Figure 7.6). The substantial increase in viscosity experienced after temperature equilibration for samples at 45°C could once again be seen between the initial and five minute timepoints.

7.3.2 Results/Discussion

For the first test (results are shown in Figure 7.3), the temperature response for viscosity is evaluated over a controlled cool. The gel (F1-145/10) can be seen to undergo a transition at 45°C that results in a decreased apparent viscosity at high temperatures (Figure 7.14) reminiscent of that described previously in this thesis in data from Briscoe [6]. At this higher concentration this effect corresponds to a setting transition for this component system. This data is compared with the viscosity

profiles of aqueous PVA solutions as shown in Figure 7.4. The current PVA/PEG formulation (F1-145/10; shown as hollow circles) is compared with that same final formulation without PEG (solid circles). This PVA gel corresponds to the same PVA/water ratio, or 43% w/w. The high temperature (or "delivery") viscosity (viscosity at T>42°C) is seen to be dramatically lower for samples containing PEG, as compared to those without. The PVA control can be seen to exhibit a steady viscosity increase without transition, as predicted by the literature for high degree of hydrolysis material [6].

For the second test, viscosities were held at varying temperatures over short time intervals (as shown in Figure 7.5). In most cases, the viscosity can be observed to undergo two types of behavior, the first type, which is largely temperature dependent, and the second type, which is time dependent. The graphs in the figure were observed to reach their respective temperatures at the instant in which the viscosity changes to a much shallower slope and begins to only slowly creep upward with time. An exception to the temperature behavior described can be seen for 45°C samples, where the viscosity does not immediately reach a steady value (as indicated in the circle in Figure 7.5). The lag in viscosity experienced for 45°C samples can be seen to be at the location of the transition described in the accompanying study. It is not clear why viscosity does not immediately stabilize at this given temperature; however it may be due to instability from the gelation transition region at which temperature it is located. Figure 7.6 shows averaged data for gels equilibrated at varying

temperatures. It is useful to note the fact that little viscosity change occurs over short times at 95°C allows for maintaining the flowability of the gel prior to testing.

7.4 Relationship of Phase Behavior to Gelation

7.4.1 Introduction

The following sections will describe the temperature dependent viscosity transition observed in the previous section, with respect to changes in components and formulation. Gels are prepared with the intention of tracing across a range of formulations in order to determine the setting transition with respect to composition, for a given system of component materials. The following studies explore the change from a PVA/PEG phase separating system exhibiting the transition previously described, to the PVA gel without PEG exhibiting no transition, similar to that described in Figure 7.4.

7.4.2 Experimental

7.4.2.1 Comparison between PVA and PVA/PEG Transitions

Samples were prepared as described previously in the sample preparation section with little deviation (145kDa PVA, 10kDa PEG). Formulations are as shown in "A" through "E" in Table 7.1, in varying millimolar quantities of PEG. Formulations were varied with respect to a given "reference" formulation. This is described as the

PEG 1.0 formulation. A sample containing no PEG is also included ("Control") for comparison. The control consists solely of aqueous PVA solution.

Rheometry measurements were performed using an AR2000 rheometer (TA Instruments) with 40mm diameter crosshatched parallel plates which tested samples in oscillatory shear (0.5%strain; 1 Hz) using the method as previously described (95°C to 37°C / 2.9°C.min). Cross-hatching was used to fix samples for the oscillatory strain setup. Gap between plates was set at 750µm. Temperature was controlled using a Peltier plate heating system.

7.4.2.2 Affect of Water Content on Setting Transition

In a second study, three more formulations were prepared within the region determined by the position of the binodal to be single phase. Water content in the gels was varied. PEG content was similar for each formulation. Table 6.5 describes the formulations. Figure 7.7 shows the formulations along with the first set on a ternary diagram, along with the approximate position of the binodal.

7.4.3 Results/Discussion

7.4.3.1 Comparison between PVA and PVA/PEG Transitions

Formulations range on either side of the point where supernatant begins to form. In Table 7.1, formulations with PEG concentrations for sample group D and E form supernatant, whereas formulations with PEG concentrations less than this do not.

Figure 7.8 shows gels within the single phase region, with less PEG than will produce supernatant. The gels are observed to undergo a decrease in viscosity as PEG is added in increasing amounts. The resultant effect is a lower viscosity for a higher polymer content due to the plasticization created by the presence of small amounts of PEG. This reduction in viscosity for small PEG additions is to be expected when the results of Lim et al are taken into consideration [5], where an interference occurs in the ability of PVA and water to hydrogen bond. This reduction in hydrogen bonding produces the observable decrease in apparent viscosity with PEG addition.

Figure 7.9 shows the samples as the PEG content is increased further into the two phase region. The samples exhibit an increasing transition, as the PEG dehydrates to successively lower water contents for the gels.

7.4.3.2 Affect of Water Content on Setting Transition

Figure 7.10 shows samples prepared in the single phase region. Setting transition is seen to increase, as water decreases. Based on this brief study, gels prepared as a single phase were observed to exhibit similar gelation profiles to phase separated ones. Setting transition increased with a decrease in water content in the single phase region.

For increasingly concentrated gels the viscosity transition becomes visible. These results match those described in Briscoe et al, in that the transition is a concentration

dependent effect. This behavior describes a setting transition (sol to gel) in the concentrated systems described in this thesis, as opposed to the dilute solution behavior described in Briscoe et al [6]. The temperature-related increase in viscosity can be seen to have a greater affect when there is a greater polymer concentration in the system, suggesting a tighter network for both PVA and PEG components.

7.5 Setting Behavior at a Range of Compositions

7.5.1 Introduction

In order to correlate gel viscosity with final composition of samples, formulations previously described for composition (Table 5.4) were subjected to viscosity vs. temperature testing on the AR2000 rheometer. Results in the following section compare gel composition with setting characteristics, with the objective of minimizing pre-setting viscosity and maximizing the viscosity of the post-setting state.

7.5.2 Experimental

Temperature ramps from 95°C to 37°C were performed over 20 minutes using the same methods as described above (samples were tested using parallel crosshatched plates in oscillatory shear at 0.5% strain/s). Formulations are F1-145/10, as well as ±3% and ±5% PEG, as described in Table 5.4. Initial and final formulations are shown in a ternary diagram in Figure 7.11. Viscosity curves were obtained, data was averaged and compared for viscosities at the pre- and post-setting states.

7.5.3 Results/Discussion

Viscosity-temperature relationships for varying compositions are shown in Figure 7.12. Increasing PEG content showed an increase in setting transition. Figure 7.13 shows the relationship between PEG in feed and the pre- and post-setting viscosities. There is a generally increasing trend in viscosity for all formulations. The deviation from the trend for "minus 5%" samples is due to a slightly higher PVA content in the initial formulation as well as the gel (see Table 7.2). The viscous contribution of PVA begins to dominate at these low PEG concentrations.

The difference between post-setting and pre-setting viscosity is greatest for samples with larger amounts of PEG in the feed solution. As post-setting viscosity increases, however, so does pre-setting viscosity, so a balance must be obtained between the desired post-set viscosity and a pre-set viscosity that allows for adequate workability. Based on preliminary injection testing, 8000Pa*s was chosen as a point where the solution becomes unworkable. Approximate temperatures where each formulation crosses this point are listed in Table 7.3.

For a low %PEG in the feed, the water content in the gel is high, which decreases the post-setting viscosity. Pre-setting viscosity for these samples is high due to increased PVA content. An ideal setting formulation would have a low pre-setting viscosity and a high post-setting viscosity, such as is exhibited by formulations "F1-145/10" and

"+3% PEG". +5% PEG also produced favorable results, though high pre-setting viscosities may be prohibitive for delivery.

7.6 PEG Molecular Weight Affect on Gelation

7.6.1 Introduction

It was shown by Lim [5] that PEG molecular weight has an affect on the plasticization and general rheological properties of PVA solutions. Higher degrees of plasticization were exhibited by lower molecular weight PEG (0.4kDa, when compared with 1.5kDa). The reasoning provided was a reduction in hydrogen bonding between vinyl alcohol units (the polymer tested for the study by Lim was polyvinyl butyral). FT-IR was used for characterization of this behavior. It was found that the suspension viscosity decreased with decreasing PEG molecular weight. Glass transition temperature, as identified by DSC, was lower for lower PEG molecular weight, as well. Samples were reported to also have become more ductile for low molecular weights. An objective of the following study is to define the setting response of the PVA gel network that results from the incorporation of a range of PEG molecular weights. A further objective is to test the Lim hypothesis of interference of hydrogen bonding in vinyl alcohol units in the case of the nucleus replacement system being evaluated.

7.6.2 Experimental

A single phase formulation (i.e. initial and final compositions are same) is prepared (Formulation "G", as described in Table 5.5) for formulations having an identical PVA molecular weight, but each sample type having different PEG molecular weights (0.4, 1, 10, & 20kDa). This is the identical sample set as previously described in the swelling and stability section. Standard sample preparation techniques were used, and rheometry testing was performed in the standard manner:

Samples had been autoclaved prior to testing, and allowed to sit for 5 minutes in a 75°C bath prior to testing. Samples were tested on an AR2000 rheometer, and were equilibrated at 95°C for 5 minutes on the rheometer platen (Peltier plate, with 40mm stainless steel crosshatched platens) before testing. Testing was performed via oscillatory shear at 0.5% strain. For analysis, temperature was ramped from 95 to 37°C over 20 minutes to simulate implant cooling to physiologic temperature from the temperature at which it was made flowable.

7.6.3 Results/Discussion

Formulation G was prepared with five different molecular weights of PEG. Molecular weights 0.4, 1, 10 and 20 kDa are shown in Figure 7.14. 35kDa values were also tested and proved to be close to 20kDa, suggesting the effect of molecular size had reached a maximum. Data represents average complex viscosity (n=4). Figure 7.14 also shows the reduction in viscosity at high temperatures, in samples containing the higher molecular weight PEG. Both 1 and 10kDa can be seen to have

lower viscosities in the sol, when compared with 0.4 kDa. An incline is clearly visible in the graph for 10kDa, at below 42°C, where the material transitions from the low viscosity high temperature state, to the high viscosity, low temperature state. When greater molecular weights of PEG are incorporated (see Figure 7.14), the transition in viscosity is seen to grow, as greater molecular weights of PEG increase the strength of the PVA/PEG network. Results for incorporation of both 20kDa and 35kDa were very close and it is possible that the effect of molecular size has reached a maximum at 20kDa. When compared with the results of Briscoe [6], the corresponding greater transition of the PVA/PEG system with higher molecular weight PEG results from a greater incompatibility between the polymers, as was described for polymers having lower degree of hydrolysis or greater amounts of hydrophobic material. The resulting effect in production of an increasing transition size is related to both the incorporation of a greater molecular weight polymer to the structure, which dictates how high the low temperature viscosity will extend, as well as the decreased interaction of PVA and water via the PEG in solution, which dictates the extent of plasticization and high temperature viscosity reduction.

The change in equilibrium water content of the gels upon implantation must be considered in conjunction with the setting characteristics observed here, as greater water contents will result in weaker gels. In other words, a greater setting transition alone will not provide a stronger gel if there is a significant change in water content upon equilibration with the implantation site. Increased swelling of the PEG results in a less stable gel when samples are immersed in de-ionized water. This is not a

clear indication of behavior in an environment such as the intervertebral disc, however.

Using the same rheometry testing method, setting for the F1 formulation with 0.4kDa PEG was also determined. Samples with 0.4kDa PEG could be seen to have a steady increase in viscosity similar to samples not containing PEG (see Figure 7.15). Both lacked the setting transition displayed by samples having 10kDa PEG.

It was also observed that samples containing lower molecular weights of PEG had a greater loss in polymer mass (see Chapter 6 for general stability and mass loss trends). Samples containing PEG molecular weights at 0.4kDa were observed to elute greater than 35% of their polymer mass which suggests that the PEG may be eluting with the supernatant. It is likely that any plasticization effect brought about by PEG as seen in Lim et al, is lessened by this elution. Conversely, higher molecular weight PEG (10kDa) has been observed to be retained within gels, as evidenced by the NMR data for the ternary phase diagram prepared in this thesis. The presence of PEG in gels is suggested as the source of the high temperature viscosity reduction in the higher molecular weight PEG formulations.

7.7 Calorimetric Studies for the Identification of Gel Point

7.7.1 Experimental

DSC was performed in order to locate gel point, corresponding to the presence of physical crosslinking in gels of the F1-145/10 formulation. A descending

temperature ramp is designed to mimic the behavior of samples cooling from the melt as a result of injection from the ratchet gun delivery device. Test method steps are as follows:

1. Equilibrate at 25°C
2. Temperature jump: 25°C to 95°C.
3. Temperature ramp 5°C/min to 37°C
4. Temperature ramp to 95°C.

7.7.2 Results/Discussion

Test runs showed no peaks. No transition was observed in either descending or ascending ramp (see Figure 7.16) within the region described as the gel point. These results suggest that the formation of any physical crosslinks in gels is not through a uniform crystallization. The absence of a uniform peak suggests that physical crosslinking from uniform crystallinity that melts and reforms as a result of phase separation and spinodal decomposition as described in Ruberti et al is unlikely[77]. Results from physically crosslinked PVA gels, such as those prepared via freeze-thaw methods show an endotherm peak that is produced from the melting out of crystallites. DSC results suggest that a non-uniform physical hydrogen bonded association is responsible for the network and resulting high viscosity. In other words, at low temperatures, once the viscosity reduction is no longer occurring, the effects of PVA concentration are again able to manifest in high viscosities.

Table 7.1 Feed formulations prepared at a range of PEG contents (quantities are in mmol).

	Variables					
	Control	**A**	**B**	**C**	**D**	**E**
Composition variables	**PEG (0.0)**	**PEG (1.0)**	**PEG (0.80)**	**PEG (0.40)**	**PEG (0.09)**	**PEG (0.045)**
PEG (10kDa)	0	0.080	0.16	0.71	1.42	1.77
PVA (Mowiol 28-99)	0.138	0.138	0.138	0.138	0.138	0.138
DI Water	3050	3050	3050	3050	3050	3050

Table 7.2 Viscosity relationships, pre- and post-setting.

	Sample Type (% PEG in Feed)				
	-5% PEG	**-3% PEG**	**F1-145/10**	**+3% PEG**	**+5% PEG**
Viscosity Pre-Set (Pa*s@45C)	7880	5040	6040	7330	10770
Viscosity Post-Set (Pa*s@37C)	18920	13950	21620	23690	31240
Δ|η*| (Post minus Pre Setting Viscosities) (Pa*s)	11040	8910	15580	16360	20470

Table 7.3 Approximate temperatures at which viscosity crosses 8000 Pa*s.

	Sample Type (% in Feed)				
	-5% PEG	**-3% PEG**	**F1-145/10**	**+3% PEG**	**+5% PEG**
Injection Limit Temperature (°C)	45.0	40.0	42.5	45.0	47.5

Figure 7.1 Closeup of a gel between two parallel plates on rheometer, crosshatching is visible at lower right.

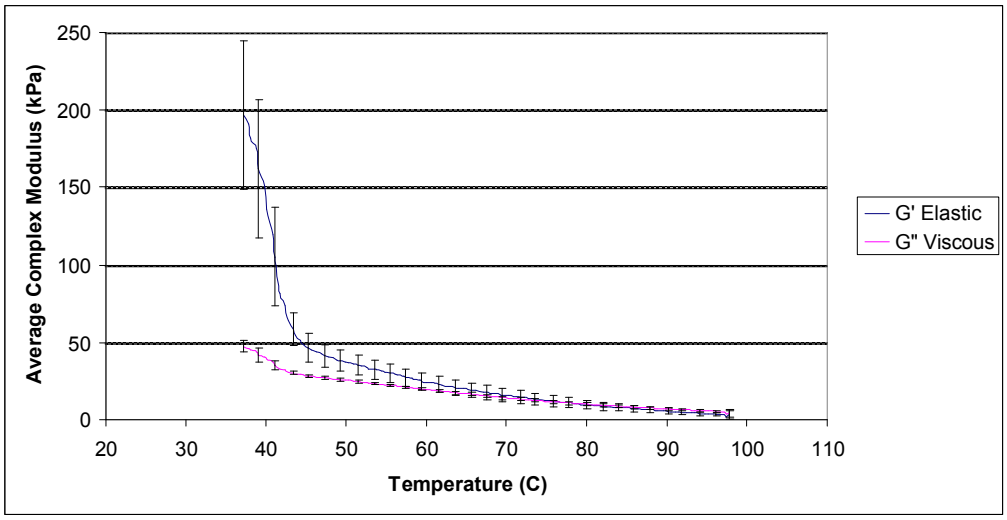

Figure 7.2 A curve representing average of modulus data (n=5) for F1-145/10.

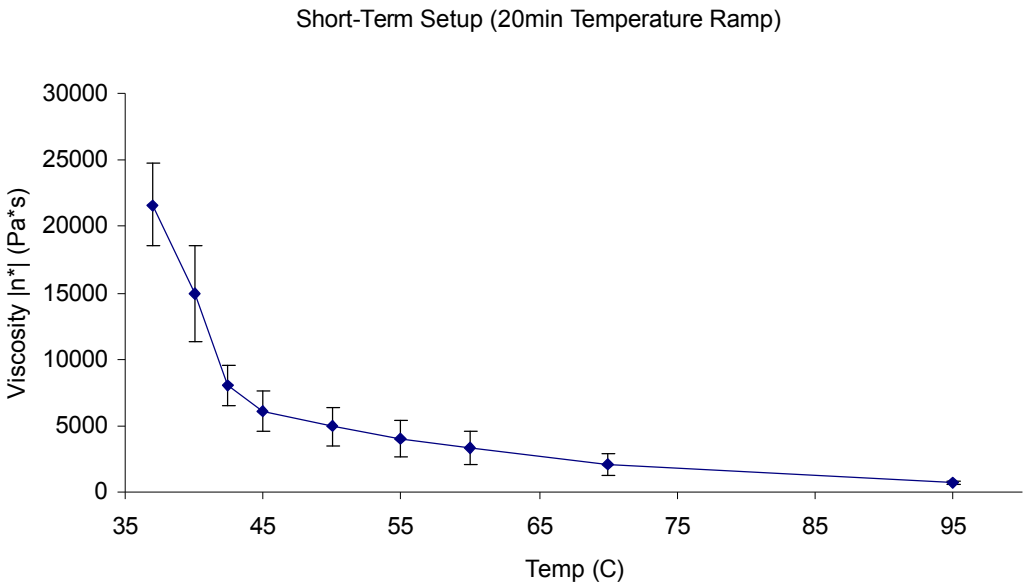

Figure 7.3 Temperature response of viscosity when samples are subjected to a controlled cool from the sol (samples contain PEG; n=4)

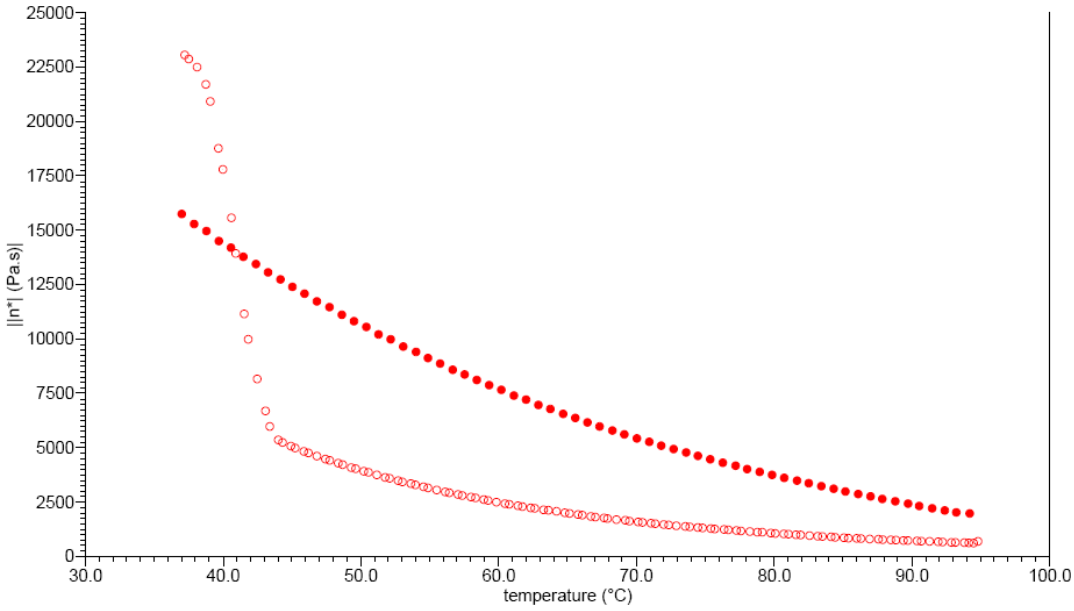

Figure 7.4 Complex viscosity vs. temperature for the F1-145/10 formulation (hollow circles) in comparison to that same formulation without the PEG plasticizer (solid circles).

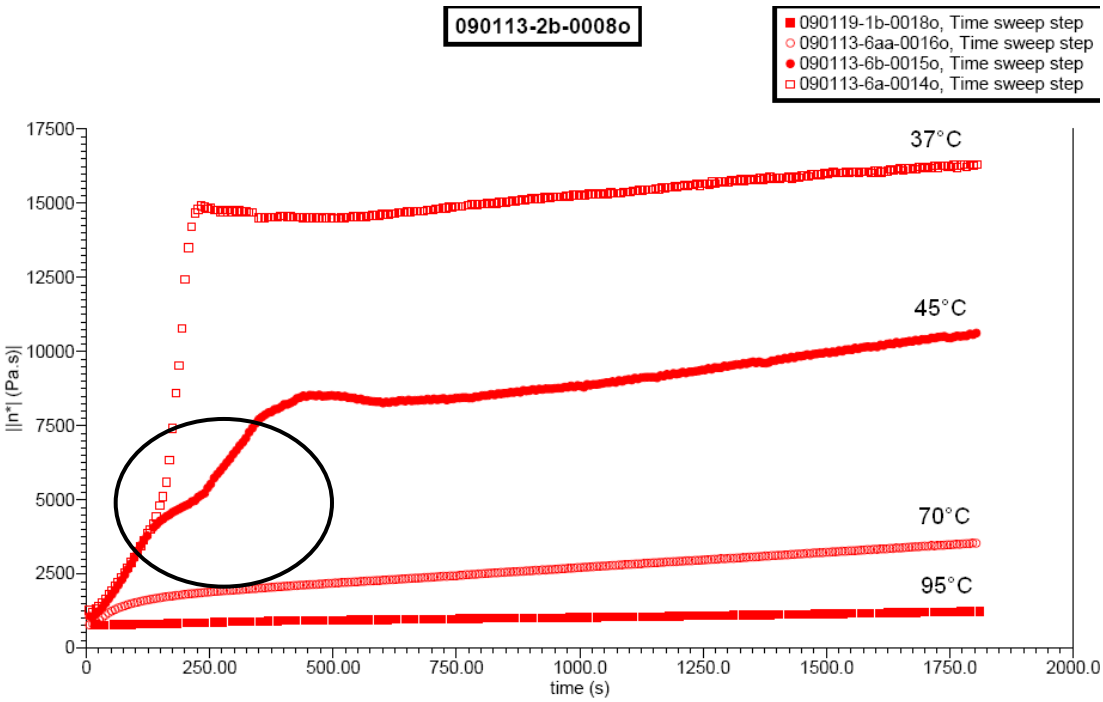

Figure 7.5 Curves showing viscosity change with time at varying hold temperatures.

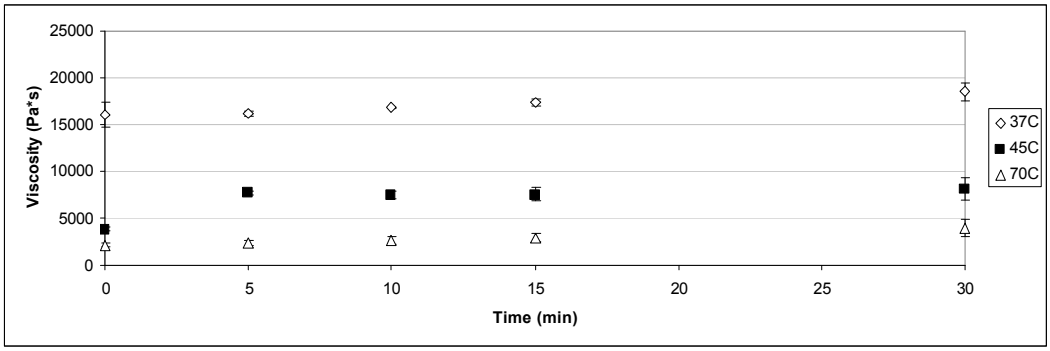

Figure 7.6 Viscosity vs. time data for three constant temperature steps (n=2).

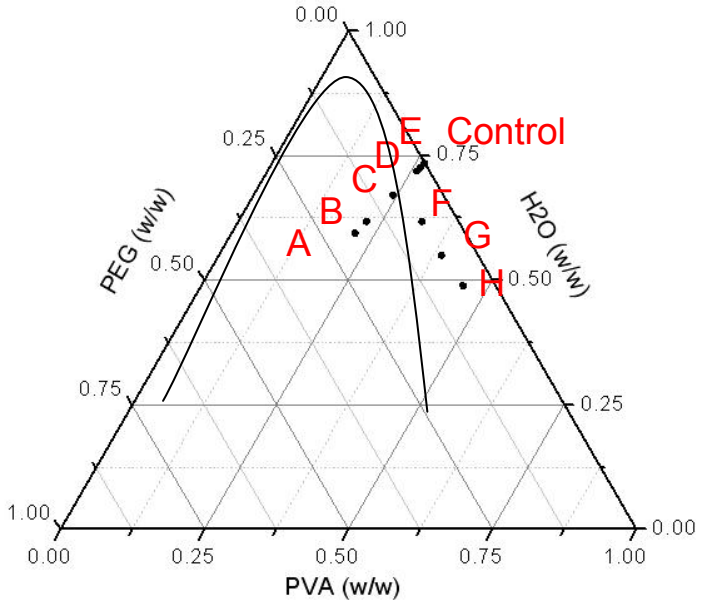

Figure 7.7 The feed formulations referenced in Table 7.1 trace a line across the binodal as shown above. Three formulations prepared in the single phase region are also included (F-H, Table 5.5)

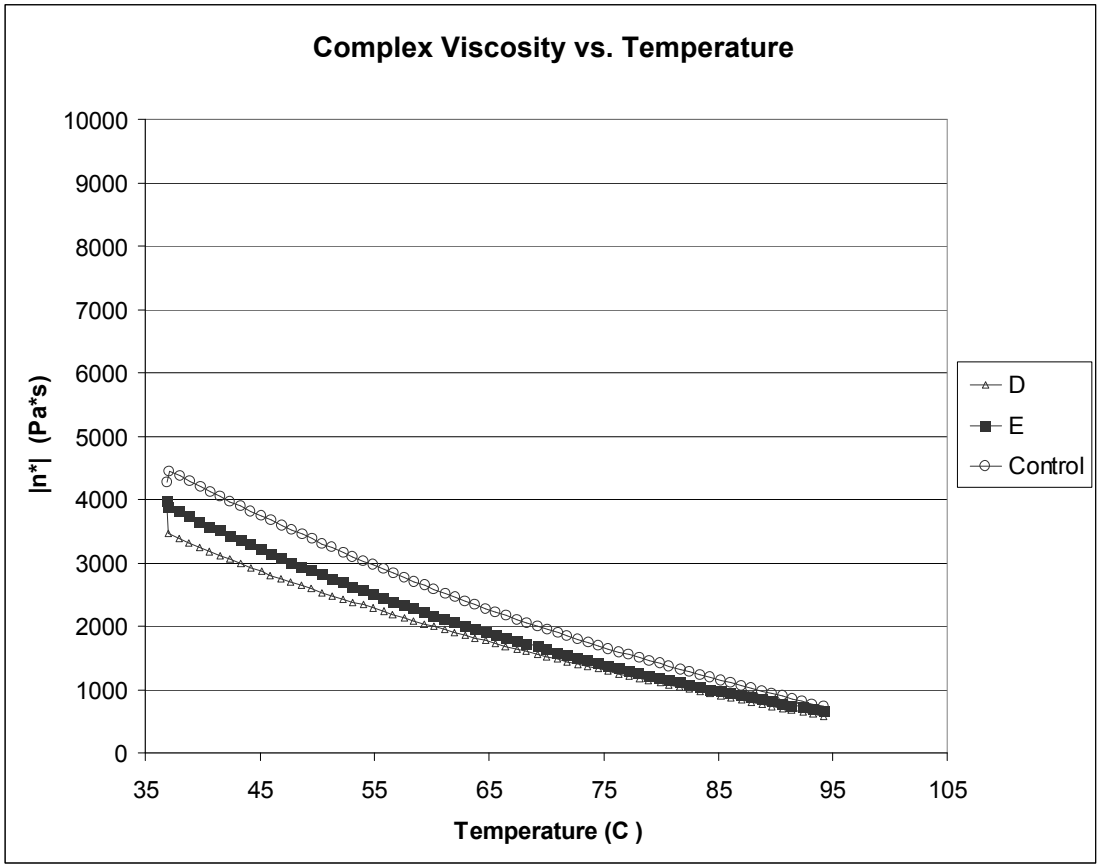

Figure 7.8 Plasticization from small amounts of added PEG. Data presented are averages (n=3).

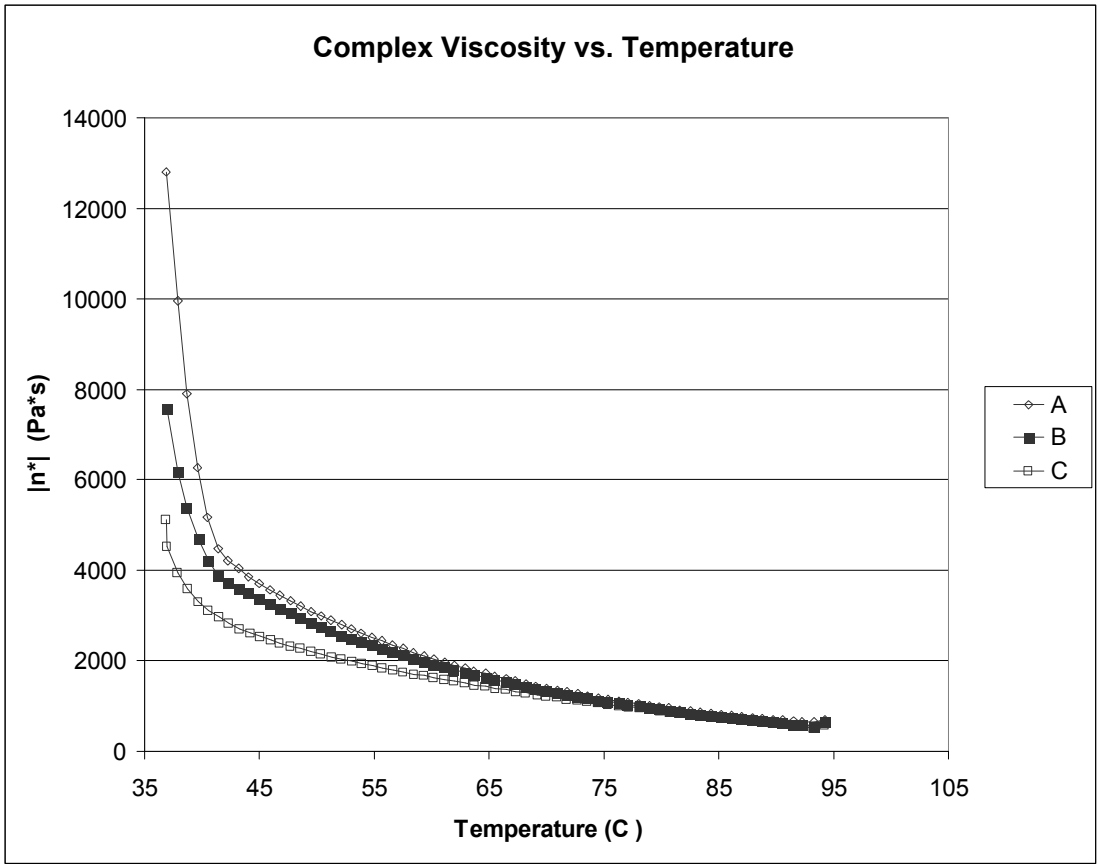

Figure 7.9 Gels after phase separation. A steep transition in viscosity can be seen for these samples at low temperatures. This is in comparison to samples below the point of supernatant formation (Figure 7.8). |n*| is average complex viscosity in all cases (n=3).

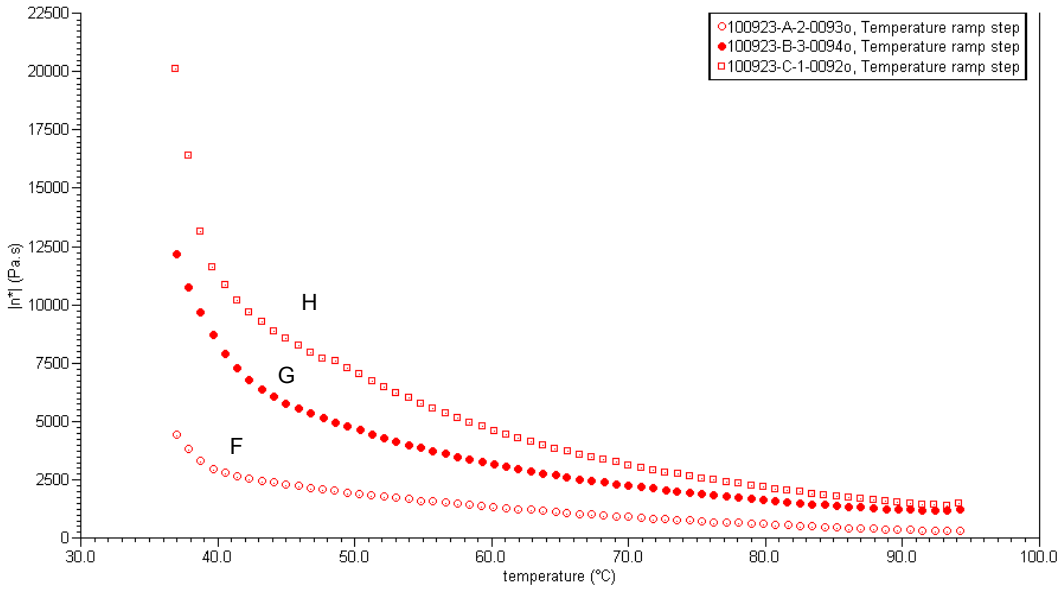

Figure 7.10 Single phase gels. |n*| is average complex viscosity in all cases (n=1).

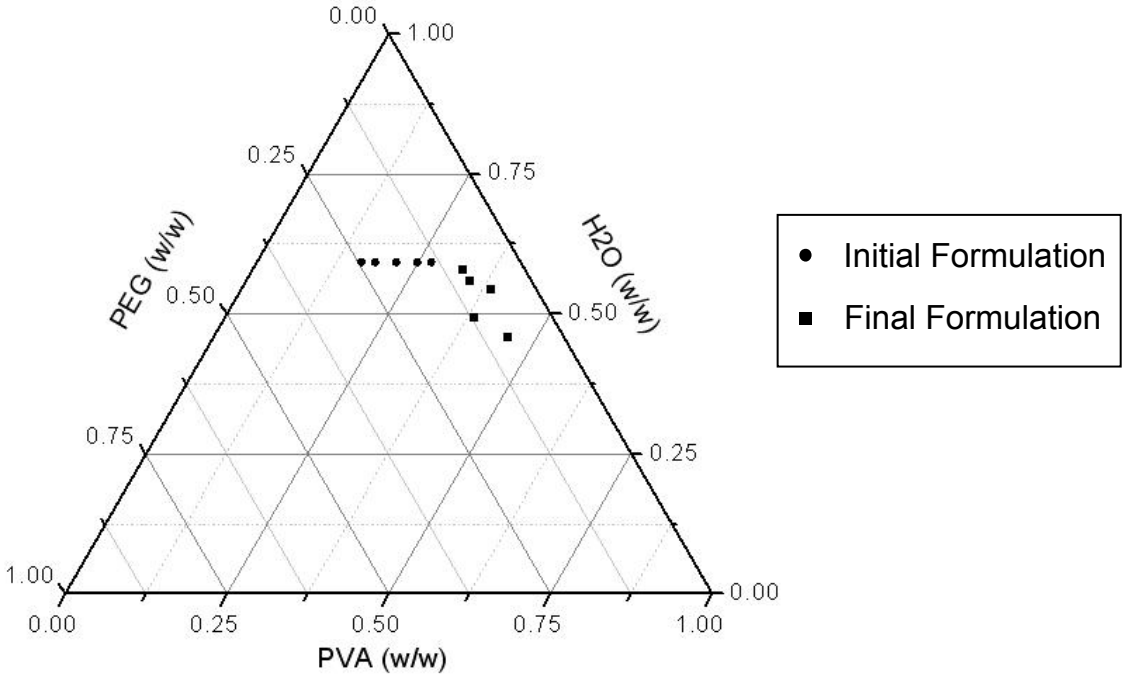

Figure 7.11 Feed compositions and Final compositions on a ternary diagram. Dehydration produces lower water contents for greater PEG in the feed.

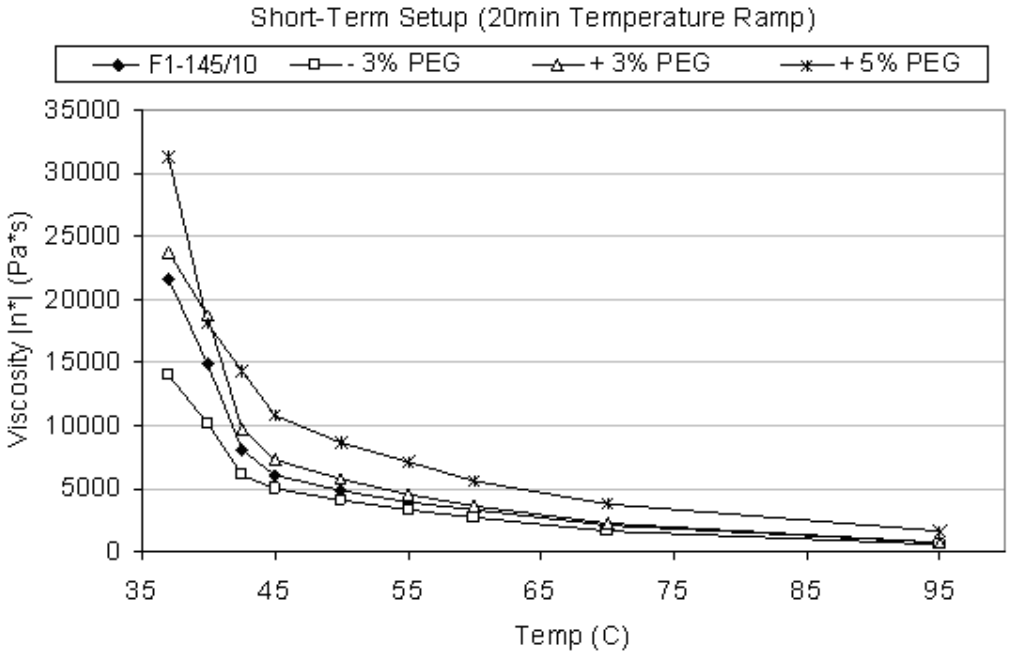

Figure 7.12 Viscosity for varying PEG concentrations in the feed. The -5% PEG sample set is omitted for simplicity

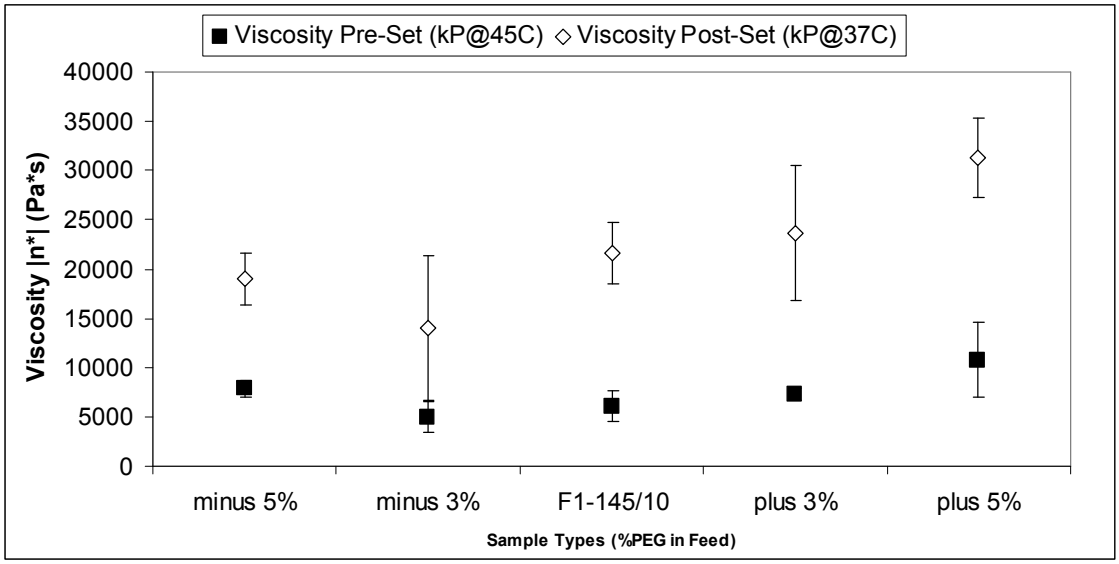

Figure 7.13 Pre and post-setting viscosities

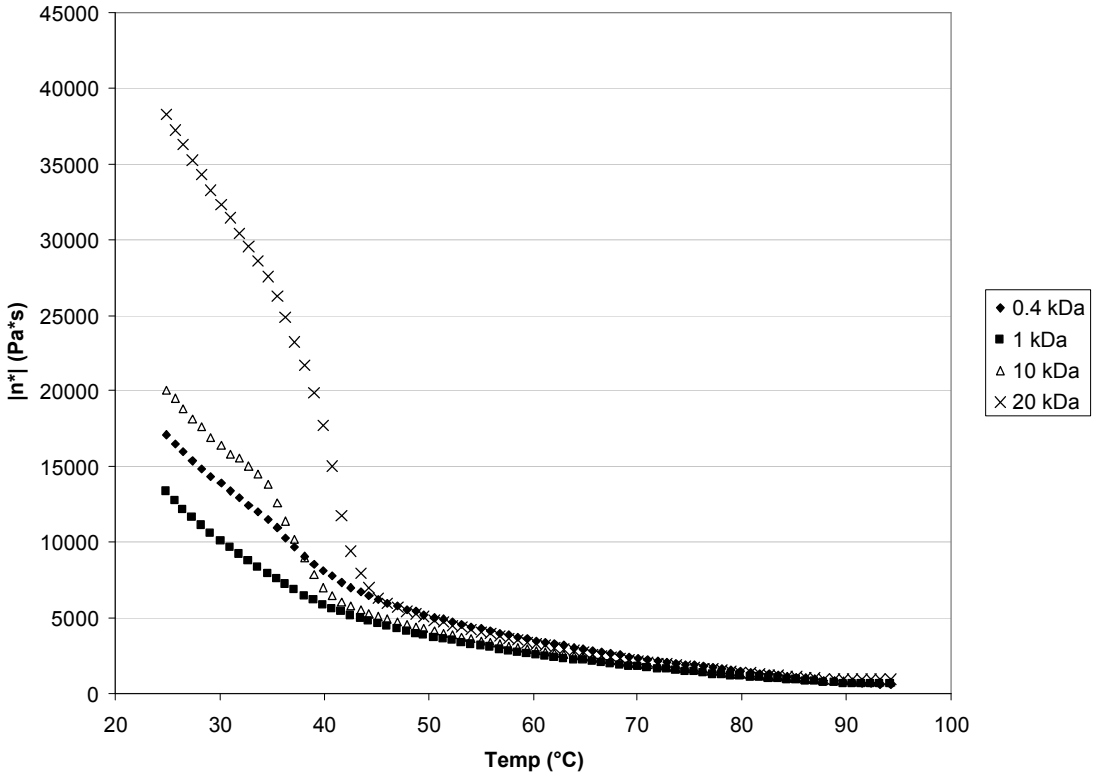

Figure 7.14 Single phase gel composition G for varying PEG molecular weight 0.4, 1, 10 and 20 kDa (n=4).

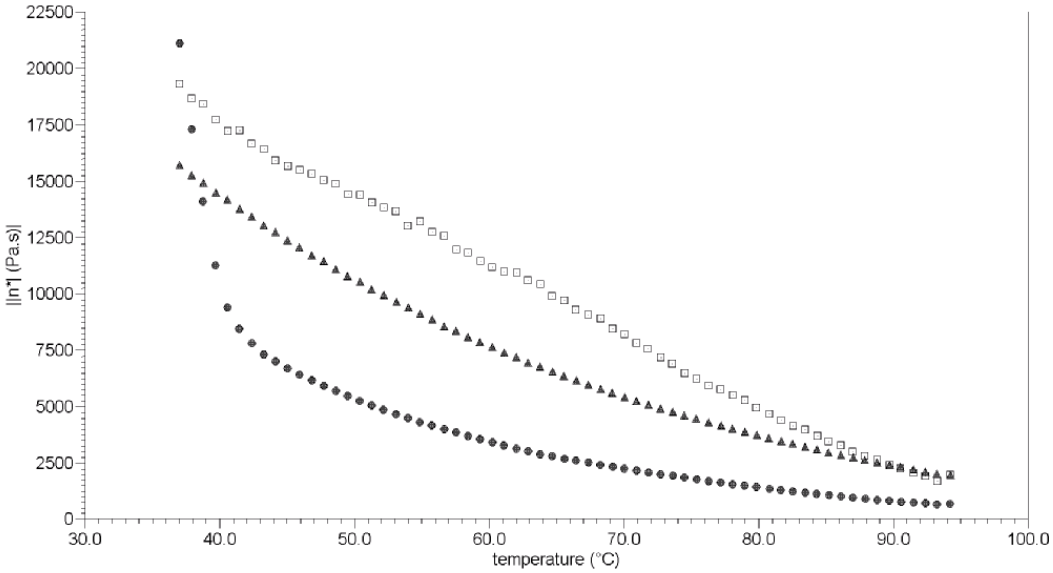

Figure 7.15 Setting transitions for the F1 formulation with 0.4kDa (□) and 10kDa (⬟) PEG. Also included is the PVA gel without PEG (▲) for comparison

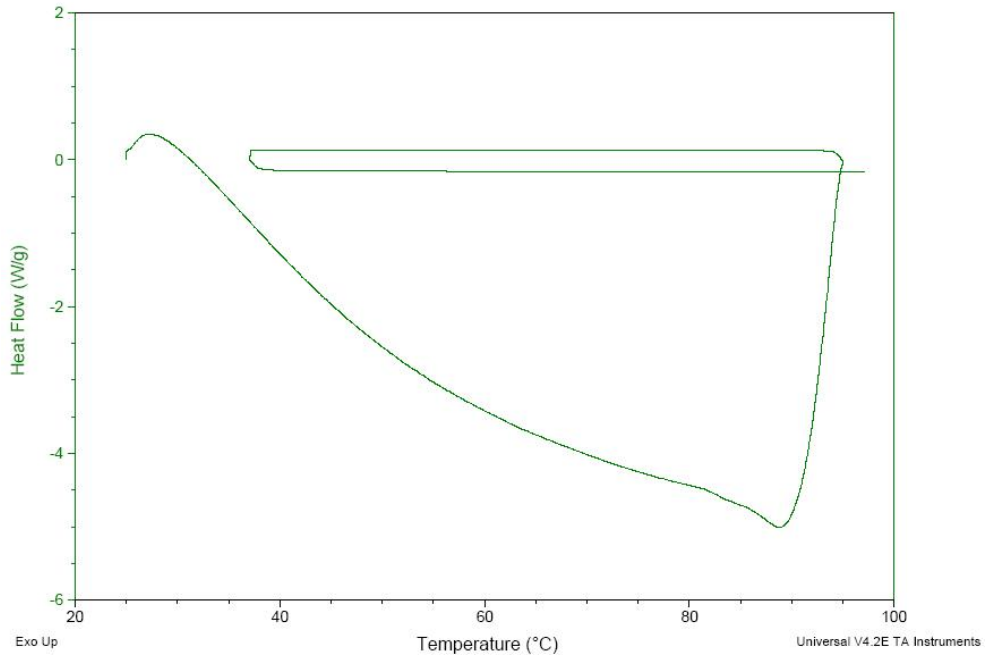

Figure 7.16 DSC analysis used to mimic gel delivery system: 1. Temperature jump to 95°C; 2. descending ramp and 3. an added ascending ramp (5°C/min).

LIST OF REFERENCES

1. Coventry, M.B.e.a., *The intervertebral disc: it's microscopic anatomy and pathology. Part II. Changes in the intervertebral disc concomitant with age.* J. Bone Joint Surg., 1945. **27**(227-247).

2. Goins, M.L., et al., *Nucleus pulposus replacement: an emerging technology.* Spine J, 2005. **5**(6 Suppl): p. 317S-324S.

3. Darwis, D., et al., *Characterization of poly(vinyl alcohol) hydrogel for prosthetic intervertebral disc nucleus.* Radiation Physics and Chemistry, 2002. **63**: p. 539-542.

4. Inamura, I., *Liquid-liquid phase separation and gelation in the poly(vinyl alcohol)-poly(ethylene glycol)-water system. Dependence on molecular weight of poly(ethylene glycol).* Polymer Journal, 1986. **18**(3): p. 269-272.

5. Lim, L.Y.e.a., *The Effect of Plasticizers on the Properties of Polyvinyl Alcohol Films.* Drug Development and Industrial Pharmacy, 1994. **20**(6): p. 1007-1020.

6. Briscoe, B.e.a., *The effects of hydrogen bonding upon the viscosity of aqueous poly(vinyl alcohol) solutions.* Polymer, 1999. **41**(3851-3860).

7. Gray, H., F.R.S., *Anatomy, Descriptive and Surgical*, ed. T.P.a.H. Pick, R. 1901: Running Press.

8. White, A.A. and M.M. Panjabi, *Clinical Biomechanics of the Spine*. 2nd ed. 1990, Philadelphia, PA: Lippincott Williams & Wilkins.

9. Keaveny, T.M.a.B., J M, *Chapter 4. Biomechanics of Vertebral Bone*, in *Spine Technology Handbook*, K.S.M.a.E.A. A, Editor. 2006, Elsevier.

10. Diwan, A.D.e.a., *Current Concepts in Intervertebral Disk Restoration.* Tissue Engineering in Orthopedic Surgery, 2000. **31**(3): p. 453-464.

11. Nachemson, A. and J.M. Morris, *In Vivo Measurements of Intradiscal Pressure. Discometry, a Method for the Determination of Pressure in the Lower Lumbar Discs.* J Bone Joint Surg Am, 1964. **46**: p. 1077-92.

12. Eyre, D.R., *Biochemistry of the Intervertebral Disc.* Int. Rev. Connect. Tissue Res., 1979. **8**: p. 227-291.

13. Guerin, H.A.a.E., DM, *Chapter 3 - Structure and Properties of Soft Tissues in the Spine*, in *Spine Technology Handbook*, K.S.M.a.E.A. A, Editor. 2006, Elsevier. p. 37.

14. Sieber, A.N.e.a., *Concepts in Nuclear Replacement.* The Spine Journal, 2004. **4**(2004): p. 322S-324S.

15. Martinez, J., V. Oloyede, and N. Broom, *Biomechanics of load-bearing of the intervertebral disc: an experimental and finite element model.* Medical engineering & physics, 1997. **19**: p. 145-56.

16. Urban, J.P., *The role of the physicochemical environment in determining disc cell behaviour.* Biochem Soc Trans, 2002. **30**(Pt 6): p. 858-64.

17. Urban, J.P. and A. Maroudas, *Swelling of the intervertebral disc in vitro.* Connect Tissue Res, 1981. **9**(1): p. 1-10.

18. Urban, J.P., et al., *Swelling pressures of proteoglycans at the concentrations found in cartilaginous tissues.* Biorheology, 1979. **16**(6): p. 447-64.

19. Urban, J., S. Roberts, and J.R. Ralphs, *The nucleus of the Intervertebral disc from development to degeneration.* American Zoologist, 2000. **40**: p. 53-61.

20. Shiradzi-Adl, A.a.D., G, *Load bearing role of facets in a segment under sagittal plane loadings.* J. Biomech. Eng, 1987. **20**(6): p. 601.

21. Wilke, H., et al., *Intradiscal pressure together with anthropometric data--a data set for the validation of models.* Clin Biomech (Bristol, Avon), 2001. **16 Suppl 1**: p. S111-26.

22. Simunic, D.I., N.D. Broom, and P.A. Robertson, *Biomechanical factors influencing nuclear disruption of the intervertebral disc.* Spine, 2001. **26**(11): p. 1223-30.

23. Allen, M.J., et al., *Preclinical Evaluation of a Poly (Vinyl Alcohol) Hydrogel Implant as a Replacement for the Nucleus Pulposus.* Spine, 2004. **29**(5): p. 515-523.

24. Thomas, J., et al., *The effect of dehydration history on PVA/PVP hydrogels for nucleus pulposus replacement.* J Biomed Mater Res B Appl Biomater, 2004. **69B**(2): p. 135-40.

25. Bibby, S.R., et al., *The pathophysiology of the intervertebral disc.* Joint Bone Spine, 2001. **68**(6): p. 537-42.

26. Adams, M.A. and P. Dolan, *Recent advances in lumbar spinal mechanics and their clinical significance.* Clin Biomech (Bristol, Avon), 1995. **10**(1): p. 3-19.

27. Bertagnoli, R., et al., *Mechanical testing of a novel hydrogel nucleus replacement implant.* Spine J, 2005. **5**(6): p. 672-81.

28. Jin, D., et al., *Prosthetic disc nucleus (PDN) replacement for lumbar disc herniation: preliminary report with six months' follow-up.* J Spinal Disord Tech, 2003. **16**(4): p. 331-7.

29. Frei, H., et al., *The effect of nucleotomy on lumbar spine mechanics in compression and shear loading.* Spine, 2001. **26**(19): p. 2080-9.

30. Adams, M.A. and W.C. Hutton, *Gradual disc prolapse.* Spine, 1985. **10**(6): p. 524-31.

31. Adams, M.A., P. Dolan, and W.C. Hutton, *The stages of disc degeneration as revealed by discograms.* J Bone Joint Surg Br, 1986. **68**(1): p. 36-41.

32. White, A.A.a.G., S L, *Synopsis: Workshop on idiopathic low back pain.* Spine, 1982. **7**: p. 141.

33. Wyke, B., *The neurological basis of thoracic spine pain.* Rheumatol. Phys. Med., 1970. **10**: p. 356.

34. Sagi, H.C., Q.B. Bao, and H.A. Yuan, *Nuclear replacement strategies.* Orthop Clin North Am, 2003. **34**(2): p. 263-7.

35. Bao, Q.B., et al., *The artificial disc: theory, design and materials.* Biomaterials, 1996. **17**(12): p. 1157-67.

36. Falagas, M.E. and S.K. Kasiakou, *Mesh-related infections after hernia repair surgery.* Clin Microbiol Infect, 2005. **11**(1): p. 3-8.

37. Bao, Q.B. and H.A. Yuan, *Prosthetic disc replacement: the future?* Clin Orthop, 2002(394): p. 139-45.

38. Pope, M., V. Boel, and D. Sumner, *Biomechanics of Fusion and Stabilization.* Spine, 1995. **20**(24): p. S85-S99.

39. Davis, G.W. and G. Onik, *Clinical experience with automated percutaneous lumbar discectomy.* Clin Orthop Relat Res, 1989(238): p. 98-103.

40. Meakin, J.R. and D.W. Hukins, *Effect of removing the nucleus pulposus on the deformation of the annulus fibrosus during compression of the intervertebral disc.* J Biomech, 2000. **33**(5): p. 575-80.

41. Eysel, P., et al., *Biomechanical behaviour of a prosthetic lumbar nucleus.* Acta Neurochir (Wien), 1999. **141**(10): p. 1083-7.

42. Villarraga, M., *Chapter 7. Historical Review of Spinal Instrumentation for Fusion*. Spine Technology Handbook, ed. S.M.a.E.A.A. Kurtz. 2006: Elsevier.

43. McKay, B.e.a., *Chapter 9. Biologics to Promote Spinal Fusion*. Spine Technology Handbook, ed. S.M.a.E.A.A. Kurtz. 2006: Elsevier.

44. Zigler, J.E., *Lumbar spine arthroplasty using the ProDisc II.* Spine J, 2004. **4**(6 Suppl): p. 260S-267S.

45. Nachemson, A., *Lumbar intradiscal pressure. Experimental studies on post-mortem material.* Acta Orthop Scand, 1960. **Suppl 43**: p. 1-104.

46. Carl, A., et al., *New developments in nucleus pulposus replacement technology.* Spine J, 2004. **4**(6 Suppl): p. 325S-329S.

47. Boyd, L.M. and A.J. Carter, *Injectable biomaterials and vertebral endplate treatment for repair and regeneration of the intervertebral disc.* Eur Spine J, 2006. **15 Suppl 15**: p. 414-21.

48. *A Prospective, Multicenter Pilot Study of the Disc Dynamics DASCOR™ Disc Arthroplasty System in the Treatment of Degenerative Disc Disease*. [website] [cited 2007 25 Jul]; Available from: http://www.discdyn.com/pdf/US-101.pdf.

49. Ahrens, M., et al., *Nucleus Replacement with an in situ Curable Balloon Contained Polymer and Restoration of Segmental Kinematics.* European cells & materials, 2005. **10**(Suppl. 3).

50. Ray, C.D., *The artificial disc: Introduction, history, and socioeconomics*, in *Clinical Efficacy and Outcome in the Diagnosis and Treatment of Low Back Pain*, J.N. Weinstein, Editor. 1992, Raven Press, Ltd.: New York. p. 205-225.

51. Klara, P.M. and C.D. Ray, *Artificial nucleus replacement: clinical experience.* Spine, 2002. **27**(12): p. 1374-7.

52. Ramseyer, P.e.a., *Polyacrylonitrile-based hydrogel as a therapeutic bulking agent in urology.* Biomaterials, 2007. **28**(6): p. 1185-1190.

53. Lemaire, J.P.e.a., *Intervertebral Disc Prosthesis - Results and Prospects for the Year 2000.* Clinical Orthopaedics and Related Research, 1997. **337**: p. 64-76.

54. Saunders, K.J., *Organic Polymer Chemistry - 2nd ed.* 1988: Blackie Academic.

55. Wade, L.G., *Organic Chemistry 5th ed.* 2003, Upper Saddle River, NJ: Prentice Hall.

56. Lee, E.J.e.a., *Rheological Properties of Solutions of General Purpose Poly(vinyl alcohol) in Dimethyl Sulfoxide.* Journal of Polymer Science Part B: Polymer Physics, 2003. **42**(8): p. 1451-1456.

57. Peppas, N.A. and E.W. Merrill, *Poly(vinyl alcohol) hydrogels: Reinforcement of radiation-crosslinked networks by crystallization.* Journal of polymer science - Polymer chemistry edition, 1976. **14**: p. 441-457.

58. Peppas, N.A. and N.K. Mongia, *Ultrapure poly(vinyl alcohol) hydrogels with mucoadhesive drug delivery characteristics.* Eur J Pharm Biopharm, 1997. **43**: p. 51-58.

59. Peppas, N.A., *Infrared spectroscopy of semicrystalline poly(vinyl alcohol) networks.* Die Makromolekulare Chemie, 1977. **178**: p. 595-601.

60. Onogi, S.e.a., *Time-Humidity Superposition in Some Crystalline Polymers* Journal of Polymer Science, 1962. **58**: p. 1-17.

61. Hyon, S.-H.e.a., *US Pat. 4,663,358 - Porous and Transparent Poly(vinyl alcohol) Gel and Method of Manufacturing the Same*. 1987.

62. Hoffman, A., *Hydrogels for biomedical applications.* Advanced Drug Delivery Reviews, 2002. **43**: p. 3-12.

63. Odian, G., *Principles of Polymerization.* p. 574, 748.

64. Hermanson, G.T., *Bioconjugate Techniques 2nd ed.* 2008: Elsevier.

65. Peppas, N.A.a.M.E.W., *Crosslinked Poly(vinyl alcohol) Hydrogels as Swollen Elastic Networks.* Journal of Applied Polymer Science, 1977. **21**: p. 1763-1770.

66. Zhang, X.e.a., *Double network hydrogel with high mechanical strength prepared from two biocompatible polymers.* Journal of Applied Polymer Science, 2009. **112**: p. 3063-3070.

67. Lozinsky, V., *Cryotropic gelation of poly(vinyl alcohol) solutions.* Russian Chemical Reviews, 1998. **67**(7): p. 573-586.

68. Stammen, J.A., et al., *Mechanical properties of a novel PVA hydrogel in shear and unconfined compression.* Biomaterials, 2001. **22**(8): p. 799-806.

69. Fabula, A.G., *Proc. Fourth Intern Congr. Rheol., Part 3*. 1965. p. 189.

70. Rodriquez, F., *Principles of Polymer Systems, 4th ed.*, ed. T.a. Francis. 1989.

71. Ratner, B.D.e.a., *Biomaterials Science*. 1996: Elsevier.

72. Gregonis, D.e.a., *Poly(ethylene glycol) surfaces to minimize protein absorption.* . Trans. Sec. World Conr. Biomater. , 1984 **7:**: p. 266.

73. Flory, P.J., *Principles of Polymer Chemistry*, ed. Cornell. 1953.

74. Borzacchiello, A.a.A., L., *Structure Property Relationships in Hydrogels*. Hydrogels - Biological Properties and Applications, ed. R. Barbucci. 2009, Milan: Springer.

75. Toyoshima, K., *Poly(vinyl alcohol)*, ed. C.A. Finch. 1973: Wiley Interscience. 535.

76. Inamura, I.e.a., *Effects of Molecular Weight on the Phase Equilibrium of a Poly(vinyl alcohol)-Poly(ethylene glycol)-Water System.* Polymer Journal, 1984. **16**(8): p. 657-660.

77. Ruberti, J.e.a., *Systems and Methods for Controlling and Forming Polymer Gels*. 2009.

78. Oral, E.e.a., *Vitamin C hinders radiation crosslinking in aqueous poly(vinyl alcohol) solutions.* Nuclear Instruments and Methods in Physics Research B, 2007(265): p. 92-97.

79. Llanos, G.R.a.S., M.V., *Immobilization of Poly(ethylene Glycol onto a Poly(vinyl alcohol) Hydrogel. 1. Synthesis and Characterization.* Macromolecules, 1991. **24**: p. 6065-6072.

80. Chang, J.Y.e.a., *Biopolymers/PVA Hydrogels/Anionic Polymerisation/Nanocomposites*: Springer.

81. Tanaka, Y.e.a., Prog. Polym. Sci., 2005. **30**: p. 1.

82. TsingHua, *Toxicity and healing effect of PEO/PVA hydrogels as wound dressings.* Journal of Radiation Research and Radiation Processing, 2000.

83. Yoshii, F.e.a., *Electron beam crosslinked PEO and PEO/PVA hydrogels for wound dressing.* Radiation Physics and Chemistry, 1999. **55**(2): p. 133-138.

84. Cruise, e.al United States Patent Application 20090028945.

85. Ash, *Handbook of Fillers, Extenders, Diluents*.

86. Harris, J.M., *Poly(ethylene Glycol) Chemistry: Biotechnical and Biomedical Applications*.

87. Chiropractors, D. 2010; Available from: http://www.mountainviewpaincenter.com/wp-content/uploads/2010/02/lumbar_disc_herniation2.jpg.

88. Chiu, J.e.a., *Posterolateral endoscopic thoracic microcompressive discectomy.* The internet journal of minimally invasive spinal technology.

89. Assocs., B.N. *Lumbar Fusion*. 2010; Available from: http://www.bnasurg.com/patient-resources-back-pain.php.

90. USSynthesProdisc.com, *Prodisc Lumbar Total Disc Replacement.*

91. SpineUniverse.com. *Acroflex Total Disc*. 2010; Available from: spineuniverse.com.

92. An, H.S. *Artificial Disc Replacement*.

93. Tompa, H., Trans. Faraday Soc., 1949. **45**: p. 1142.

94. Bamford, C.H.a.T., H. , Trans. Faraday Soc., 1950. **46**: p. 310.

95. Lozinsky, V.I., et al., *Study of cryostructuration of polymer systems. XII. Poly(vinyl alcohol) cryogels: Influence of low-molecular electrolytes.* Journal of Applied Polymer Science, 1996. **61**: p. 1991-1998.

96. Thomas, J., A. Lowman, and M. Marcolongo, *Novel associated hydrogels for nucleus pulposus replacement.* J Biomed Mater Res, 2003. **67A**(4): p. 1329-37.

97. Szymanski, H.A.a.Y., R E, *NMR Band Handbook*, ed. IFI/Plenum. 1968, New York.

98. Painter, P.a.C., M., *Fundamentals of Polymer Science: An Introductory Text, First Edition*. 1996: Wiley Interscience.

99. Muller, R.e.a., *POLYMER NETWORKS*. 2006.

100. ASTM, *Standard Test Method for Plastics: Dynamic Mechanical Properties: Cure Behavior*, in *4473*

101. Dealy, J.a.W., K, *Melt Rheology and Its Role in Plastics Processing*. 1995, London: Chapman and Hall.

VITA

Kristin Benjamin Kita was born in Doylestown, Pennsylvania on December 15, 1974. He was introduced to the science of polymers while enrolled at the Pennsylvania State University by Dr. Paul Painter, who became his advisor in the program. His undergraduate research pertained to hydrogen bonding and crystallization of polyamides. In 1998 he completed his B.S. in Materials Engineering with an option in Polymer Science. After graduation, he worked with both the development of pharmaceutical suspensions at McNeil Consumer Healthcare, as well as pharmaceutical product release at Cardinal Healthcare, both in southeastern Pennsylvania. He was enrolled in graduate school for Materials Engineering at Drexel University in 2003 to study implantable biomaterials, and funded his education through employment at Gelifex, Inc., a startup company founded by local entrepreneurs, Drexel professors, and a spine surgeon. In this position he developed poly(vinyl alcohol) and poly(n-isopropylacrylamide) hydrogel nucleus replacement technologies. The company was sold to Synthes Spine, Inc. where Kristin assisted in bringing the major Gelifex nucleus replacement product to clinical trials. During his Synthes employment, Kristin authored several patent applications ranging from bioadhesive hydrogels to hydrogels crosslinked via novel methods. He spent years as a scientist at Synthes developing in-situ curing poly(vinyl alcohol) hydrogels by both chemical and physical crosslinking techniques. In 2008, Kristin was awarded the Synthes Spine innovation award for his work in nucleus replacement. Kristin defended his Ph.D. on December 9, 2010.